Impact of vapor-phase contaminants on microbial growth and chemotaxis

1 author:

Joanna Hanzel
Friedrich Schiller University Jena
8 PUBLICATIONS **43** CITATIONS

HELMHOLTZ
CENTRE FOR
ENVIRONMENTAL
RESEARCH – UFZ

PhD Dissertation 04/2012

Impact of vapor-phase contaminants on microbial growth and chemotaxis

Joanna Hanzel

ISSN 1860-0387

Impact of vapor-phase contaminants on microbial growth and chemotaxis

Der Fakultät für Biowissenschaften, Pharmazie und Psychologie

der Universität Leipzig

eingereichte

D I S S E R T A T I O N

zur Erlangung des akademischen Grades

doctor rerum naturalium

Dr. rer. nat

vorgelegt von

Master of Science Joanna Hanzel

geboren am 25. Mai 1982 in Cieszyn, Polen

Leipzig, den 20.07.2011

Impact of vapor-phase contaminants on microbial growth and chemotaxis

Faculty of Biology, Pharmacy and Psychology

University Leipzig

submitted

D I S S E R T A T I O N

to obtain academic grade

doctor rerum naturalium

Dr. rer. nat

presented by

Master of Science Joanna Hanzel

born on 25. May 1982 in Cieszyn, Poland

Leipzig, 20.07.2011

BIBLIOGRAPHISCHE DARSTELLUNG

Joanna Hanzel

Impact of vapor-phase contaminants on microbial growth and chemotaxis

Fakultät für Biowissenschaften, Pharmazie und Psychologie

Universität Leipzig

Dissertation

102 Seiten, 84 Literaturangaben, 5 Abbildungen, 2 Tabellen

Der wasserungesättigte Boden (Vadose-Zone) ist ein mikrobiologisch hochaktiver Teil des Boden-Ökosystems. Neben seiner Bedeutung für die Bodenfruchtbarkeit trägt die Vadose-Zone auch wesentlich zum mikrobiellen Abbau anthropogener Schadstoffe bei. Während die mikrobielle Populationsdichte und Diversität oft beschrieben wurde, ist das Wissen um die mikrobielle Aktivität unter dem Einfluss flüchtiger Schadstoffe im Luftraum des Bodens noch sehr gering. Dies ist umso erstaunlicher, da sich viele Bakterien an der Luft-Wasser-Grenzschicht ansammeln und diese für den mikrobiellen Umsatz flüchtiger Stoff im Boden sehr wichtig sind.

Ziel der vorliegenden Promotionsarbeit war es daher, das Wachstum und die Chemotaxie schadstoffabbauender Bakterien unter dem Einfluss gasphasengetragener Schadstoffe zu analysieren und zu quantifizieren. In kontrollierten Labormodellsystemen wurde dabei die räumliche und zeitliche Dynamik des bakteriellen Wachstums und Mobilitätsverhaltens unter dem Einfluss gasphasengetragener Schadstoff-Gradienten quantifiziert und mittels qualitativer Modelle allgemeingültig beschrieben. Dabei wurden der flüchtige polycyclische aromatische Kohlenwasserstoff Naphthalin (NAPH) und das NAPH-abbauende Bakterium *Pseudomonas putida* (NAH7) G7 als Modellsysteme verwendet. Mittels hypothesengetriebener Ansätze wurde dabei getestet (1) ob und wie sich der luftgetragene, diffusive NAPH-Transport und das räumlich-zeitliche Wachstum von *P.putida* G7 gegenseitig beeinflussen und bedingen, (2) ob und wie *P.putida* G7 Bakterien an Luft-Wasser-Grenzschichten chemotaktisch auf luftgetragene NAPH-Gradienten reagieren und, (3) ob und wie der Abbau von NAPH durch *P.putida* G7 Gemeinschaften in unterschiedlicher Populationsstärke als effektiver Entgiftungsmechanismus agiert, um den potenziell toxischen NAPH Einfluss zu reduzieren und ein optimales Wachstum zu erlangen.

Die Resultate der Promotionsarbeit zeigen, dass *P. putida* G7 luftgetragenes NAPH effektiv und in hohen Raten abbaut und dass eine nur wenige Zentimeter dicke, mikrobiell aktive Vadose-Zone prinzipiell als effektiver Bio-Filter für flüchtige Schadstoffe agieren und somit das Ausgasen flüchtiger Grundwasser-Schadstoffe in die Atmosphäre verhindern könnte. Die Ergebnisse weisen gleichzeitig darauf hin, dass die hohe Bioverfügbarkeit von luftgetragenem NAPH (und dies bei Absolutkonzentrationen, die in der wässrigen Phase keine toxische Wirkung zeigen) zu wachstumshemmenden Effekten und einem unerwarteten, chemotaktischen Verhalten von Bakterien an der Luft-Wasser-Grenzschicht führen kann. Dies unterstreicht die Wichtigkeit der konzeptuellen Differenzierung zwischen der Absolutkonzentration und der Bioverfügbarkeit bei der Voraussage des Abbaus und der Toxizität von Schadstoffen in der Umwelt.

Abstract

A view of the vadose zone as a sterile or barley populated region of soil has dominated until 1970s, picturing the subsurface microbial communities as not very important to the ecology or fertility of soil system. Since then, the vadose zone is seen as highly active part of terrestrial ecosystem, where, e.g., active biodegradation of various soil contaminants takes place. So far, microbiological research in the water-unsaturated zone has mostly been restricted to documenting the presence, abundance and diversity of microbes inhabiting such environments. Hence, it still remains a fairly unknown compartment of soil system. Limited information exists on bacterial activity in the vadose zone, and on the influence of soil air on the diffusive transport of contaminants. Whereas under conditions typical for the unsaturated subsurface the mobility of bacteria is restricted by the discontinuity of water pockets and the tendency of microbes to accumulate at the air-water interfaces, the diffusion of volatile contaminants is more efficient than in the water-saturated soils, resulting in their higher bioavilability in the air-filled pores of the vadose zone environments. The enhanced availability of oxygen points at the higher degradation potentials in the unsaturated subsurface, relative to oxygen-limited aquifers. As the air-water interfaces contain the highest density of microbial populations, they are of a special interest for biodegradation of volatile compounds present in the unsaturated subsurface.

Microbial degradation of environmental contaminants may serve different functions for a degrading organism including assimilative biodegradation and/or intracellular detoxification of potentially toxic impacts. It is clear that degradation may reduce the extent of the microbes' exposure to the chemical and, therefore, influence the dynamics and activity of the entire microbial biomass. Such complex interactions are often overlooked in bioremediation studies, possibly due to erroneous assumption that contaminant-degrading bacteria are tolerant even to high concentrations of substrates. Hence, poor knowledge exists on the influence of enhanced bioavailability of vapor-phase contaminants on the spatio-temporal

growth of surface-associated bacteria. Information of how and where microbial populations develop in vapor-phase substrate gradients is of a great importance for a better understanding of the degradation of volatile contaminants which are found for instance in the vadose zone of terrestrial environments.

In this thesis the naphthalene-degrading bacterium *Pseudomonas putida* (NAH7) G7 and the semi-volatile polycyclic aromatic hydrocarbon naphthalene (NAPH) were used as a model system to study the interplay between the diffusive transport of volatile contaminant and the activity of the bacteria. Three different hypotheses tested were: (1) if the diffusive transport of NAPH determines the spatio-temporal growth of NAPH-degrading bacteria *P.putida* G7, (2) how the enhanced effective diffusivity of potentially inhibitory substrate shapes microbial growth, and to which extent the competition between degrading organisms influences NAPH degradation, (3) to what extent surface-associated bacteria react chemotactically to vapor-phase contaminant gradients, and whether substrate consumption may be used as a detoxification mechanism reducing its potentially inhibitory effects to *P.putida* G7. These issues are of a great importance for the dynamics of microbial ecosystems and the ecology of contaminant biodegradation.

Obtained results demonstrated that vapor-phase gradients of naphthalene influenced the spatio-temporal growth of the planktonic bacteria. Despite high gas-phase naphthalene diffusivity microbial growth was strongly depended on the distance to the naphthalene spot source, and for a given distance on the numbers of bacteria competing for the gas-phase substrate. Mass transfer limitation of the bacteria was more apparent at longer distances from the source, and in the presence of an elevated microbial consumption potential, particularly when the competing microbes were located closer to the source. Furthermore, by using growth data the spatial distribution of headspace NAPH concentrations were estimated. Vapor-phase naphthalene concentrations and corresponding degradation rates sharply dropped within a few centimetres, and changes in the headspace NAPH concentrations and

degradation rates heavily depended on the amount of biomass and its spatial distribution. The competition experiment has demonstrated that bacteria located close to the source strongly suppressed the growth of remoter cells. This indicates at high bacterial efficiency to influence vapor-phase naphthalene concentration gradients at the centimetre-scale.

When studying the spatio-temporal microbial growth under the influence of enhanced bioavilability of vapor-phase naphthalene obtained results were in agreement with the previous study only at larger distances from the source. At these locations bacterial growth was inversely correlated to the distance from the naphthalene, and an increased competition between bacterial cells at different locations led to decreased growth rates. For shorter distances the results were contrary to previous study, and negative correlation between growth, and distance to the vapor-phase substrate and bacterial cell numbers were found. In addition, competition at this immediate distance to the source promoted growth of surface-associated cells. Different observed growth kinetics of *P.putida* G7 on potentially inhibitory vapor-phase naphthalene at low and high cell densities were further explained by an integrated Best-equation describing microbial growth influenced by substrate availability and inhibition.

When exposing chemotactic bacteria to vapor-phase contaminant gradients clear movement away from the substrate source (negative chemotaxis) was observed, with cells being repelled at a distance representing a compromise of acceptable toxicity and sufficient substrate supply. Interestingly, after prolonged period of time the bacteria alleviated potential naphthalene stress by, e.g., 'diving' into the agar, where they were chemotactically attracted by its aqueous gradients formed in response to the vapor-phase gradients (positive chemotaxis). Furthermore, by allowing bacteria to grow on potentially inhibitory substrate cells changed the location of initial settlement and moved towards the naphthalene source. Thus, substrate consumption was shown to be an effective detoxification mechanism reducing potentially inhibitory effects of vapor-phase contaminant to degrader organism.

Results from these studies show that contaminated and rich in microbes the vadose zone may be an effective natural bio-filter for volatile contaminants emanating from groundwater and soil. Because of their high vapor pressure volatile compounds can effectively 'travel' large distances through the air-filled pores of the unsaturated soil system and, thus, may be easily transported to other soil compartments. Whereas chemotactic dispersal along vapor-phase gradients may allow motile bacteria to approach contaminant source, microbial growth may prevent long-distance subsurface transport of such contaminants through the vadose zone.

Zusammenfassung

Bis in die 1970er Jahre überwog die Meinung, dass der Bodenbereich über dem Grundwasserspiegel, die so genannte ungesättigte oder Vadose Zone, wenig mit Bakterien durchsetzt und kaum mikrobiologisch aktiv ist. Als Konsequenz wurden deren mikrobielle Gemeinschaften als nicht sonderlich wichtig für die Ökologie und Fruchtbarkeit des Erdbodens angesehen. Heute ist die Vadose Zone jedoch als hochaktiver Teil des Boden-Ökosystems anerkannt, in dem ein signifikanter biologischer Abbau verschiedenster Schadstoffe stattfinden kann. Trotz dieser Erkenntnis hat sich die mikrobielle Forschung bisher hauptsächlich darauf beschränkt, die Präsenz, Populationsdichte und Diversität der Bakterien in der ungesättigten Zone zu dokumentieren. Zur bakteriellen Aktivität, insbesondere unter dem Einfluss flüchtiger Schadstoffe im luftgefüllten Porenraum, existieren hingegen nur wenige Informationen. In ungesättigten Systemen ist die Mobilität von Bakterien beschränkt. Diese haften entweder an Bodenpartikeln oder akkumulieren an der Luft-Wasser-Grenzschicht im Porenraum. Flüchtige Schadstoffe hingegen besitzen, anders als im Bodenwasser gelöste oder an Bodenpartikel sorbierte Stoffe, eine hohe Mobilität im luftgefüllten Porenraum des Bodens. Für den Abbau der Schadstoffe ist die Luft-Wasser-Grenzschicht von speziellem Interesse, da sie die höchste Dichte mikrobieller Population aufweist.

Bakterien bedienen sich unterschiedlicher Strategien für den Schadstoffabbau, wie die die innerzelluläre Entgiftung oder den assimilativen Abbau potentiell toxischer Chemikalien. Werden Schadstoffe durch Bakterien abgebaut, sind diese dadurch sukzessive immer weniger Chemikalien ausgesetzt, was die Dynamik und Aktivität der gesamten mikrobiellen Biomasse beeinflusst. Solche komplexen Interaktionen werden oft in Bioremediations-Studien übersehen, vermutlich wegen der irrtümlichen Annahme, dass Bakterien auch hohen Schadstoff-Konzentrationen gegenüber tolerant sind. Dementsprechend ist auch wenig über

den Einfluss der erhöhten Bioverfügbarkeit von flüchtigen Schadstoffen auf das räumliche und zeitliche Wachstum der Bakterien an der Luft-Wasser-Schnittstelle bekannt.

In dieser Promotionsarbeit wurden der flüchtige polycyclische aromatische Kohlenwasserstoff Naphthalin (NAPH) und das NAPH-abbauende Bakterium *Pseudomonas putida* (NAH7) G7 als Modellsysteme verwendet. Mittels hypothesengetriebener Ansätze wurde dabei getestet (1) ob und wie sich der luftgetragene, diffusive NAPH-Transport und das räumlich-zeitliche Wachstum von *P. putida* G7 gegenseitig beeinflussen und bedingen, (2) ob und wie *P. putida* G7 Bakterien an Luft-Wasser-Grenzschichten chemotaktisch auf luftgetragene NAPH-Gradienten reagieren und (3), ob und wie der Abbau von NAPH durch *P. putida* G7 Gemeinschaften in unterschiedlicher Populationsstärke als effektiver Entgiftungsmechanismus agiert, um den potenziell toxischen Einfluss von zu reduzieren. Dies ist besonders wichtig, um die Dynamik des mikrobiellen Ökosystems und die Ökologie des biologischen Abbaus von Schadstoffen zu verstehen.

Trotz der hohen Diffusivität des Naphthalins in der Luft, war das mikrobielle Wachstum stark abhängig von der Distanz zur NAPH-Quelle. So gab es bei größeren Entfernungen von der Quelle ein erhöhtes mikrobielles Konsumptionspotential und ein messbar geringeres Naphthalinvorkommen, um dass die Bakterien konkurrierten. Das Wachstum der Bakterien ist somit nicht nur zeitlich, sondern auch räumlich beeinflusst. Weiterhin konnte durch die Analyse der Wachstumsraten eine räumliche Streuung von mehr und weniger großen NAPH-Konzentrationen beobachtet werden, die sich innerhalb weniger Zentimeter stark verändern konnte und insbesondere von der jeweiligen Menge der Biomasse (und deren Streuung) abhängig war. Ein „Konkurrenzversuch“ zeigte, dass nahe der NAPH-Quelle lokalisierte Bakterien das Wachstum weiter entfernter Zellen behinderte. Die Bakterien waren auch hier in der Lage die NAPH-Gradienten in der Gasphase effizient und bereits im Zentimeterbereich zu beeinflussen.

Bei der Untersuchung des Einflusses der erhöhten Bioverfügbarkeit von Naphthalin auf das räumliche und zeitliche Wachstum, konnten zu einer vorrangegangenen Studie analoge Resultate erzielt werden, solang lediglich weiter von der NAPH-Quelle entfernte Bakterien betrachtet wurden. Die Wachstumsraten waren dort umgekehrt proportional zur Entfernung von der Naphthalinquelle und aufgrund der Konkurrenz um das verfügbare Naphthalin beschränkt. In kurzen Entfernungen zur Quelle hindert also eine hohe Bioverfügbarkeit des flüchtigen Schadstoffes die mikrobielle Entwicklung, und eine erhöhte katabolische Aktivität schwächt inhibitorische Effekte ab, indem Schadstoffkonzentrationen in der Gasphase auf ein Niveau reduziert werden, dass ein optimales Wachstum erlaubt. Darüber hinaus wurden in einem „Gleichgewichts-Versuch“ verschiedene Beobachtungen zur Wachstumskinetik von *P. putida* G7 auf potentiell hemmendes Naphthalin in der Gasphase bei hohen und niedrigen Zellendichten angestellt, der das mikrobielle Wachstum bei unterschiedlicher Substratverfügbarkeit beschrieb.

Werden chemotaktische Bakterien Schadstoffgradienten der Gasphase ausgesetzt, ist eine eindeutige Bewegung weg von der Naphthalinquelle zu beobachten (negative Chemotaxis), bei der sich die Zellen von der Substratquelle zu Stellen mit gerade genügend Substratangebot bewegen, um die Toxizität zu ertragen. Interessanterweise kehrte sich dieser Effekt nach einer längeren Zeitspanne um und die Bakterien bewegten sich wieder auf die Naphthalinquelle zu (positive Chemotaxis). Dieser Effekt lässt sich möglicherweise so erklären, dass sich als Reaktion auf die luftgetragenen NAPH-Gradienten wässrige NAPH-Gradienten im Agar bildeten, von welchem die Bakterien angezogen wurden, nachdem sie in das Agar abtauchten, um der Belastung durch den luftgetragenen NAPH-Gradienten zu entgehen.

Die Ergebnisse der durchgeführten Studien zeigen, dass eine mikrobiell angereicherte ungesättigte Zone ein effektiver natürlicher Bio-Filter für flüchtige Schadstoffe sein könnte, die aus dem Grundwasser und der gesättigten Zone entstammen. Auf Grund des hohen

Dampfdrucks der flüchtigen Chemikalien können diese große Entfernungen durch die luftgefüllten Porenräume der ungesättigten Zone zurücklegen und in andere Bodenteile oder die Atmosphäre gelangen.

Table of contents

Chapter 1
Introduction

1.1 Outline of the thesis

Limited information exists on the influence of diffusive transport of volatile contaminants on the activity of the bacteria present in the vadose zone. For instance, little is known about the role of microbial growth and chemotactic dispersal on the bioremediation of such contaminants. Whereas air-filled pores of the vadose zone restrict the mobility of the bacteria, the diffusivity of volatile chemicals is highly enhanced. As many bacteria accumulate at air-water interfaces, such boundary layers are of a special interest for biodegradation of vapor-phase contaminants present in the vadose zone.

The concept of microbial degradation under conditions typical for the unsaturated soil systems is introduced in **Chapter 1**. The vadose zone environment is briefly described, and the influence of enhanced bioavailability of volatile contaminants on the activity of the bacteria is further discussed. Special emphasis is given to chemotactic dispersal along contaminant concentration gradients, seen as an important adaptation strategy allowing microbial cells to position themselves with respect to contaminant bioavilability.

In **Chapter 2,** a study demonstrating the interplay between the spatio-temporal distribution of the bacteria, and the diffusive transport of vapor-phase contaminant is presented. Whereas in the first part growth of planktonic bacteria is taken as a quantitative indicator of the vapor-phase substrate transport, in the second part microbial growth under the conditions of enhanced bioavilability of volatile contaminants is discussed. In the latter case, an extended Best equation is developed and proposed as relevant description of microbial growth on potentially inhibitory substrate.

Chemotactic dispersal along vapor-phase contaminant gradients is addressed in **Chapter 3.** The first part focuses on the chemotactic response of the bacteria, while the second part studies bacterial chemotaxis and growth on potentially inhibitory substrate. In the latter case, the role of substrate consumption on the degradation of the vapor-phase contaminant is further examined.

In **Chapter 4,** the practical significance of obtained results in natural attenuation of soils and aquifers contaminated with volatile contaminants is evaluated and an outlook for further research needs is given.

1.2 Aim of the thesis

The naphthalene-degrading bacterium *Pseudomonas putida* (NAH7) G7 and the semi-volatile aromatic hydrocarbon naphthalene (NAPH) were used as a model system to study the influence of vapor-phase contaminant gradients on bacterial growth and chemotaxis. The hypotheses tested were:

(1) if the diffusive NAPH transport determines the spatio-temporal growth of *P.putida* G7 (section 2.1),

(2) how the enhanced effective diffusivity of potentially inhibitory NAPH shapes the spatio-temporal growth of the bacteria, and to which extent the competition between degrading organisms influences NAPH biodegradation (section 2.2),

(3) to what extent surface-associated bacteria react chemotactically to vapor-phase NAPH gradients (section 3.1), and whether substrate consumption may be used as a detoxification mechanism reducing its potentially inhibitory effects to *P.putida* G7 cells (section 3.2).

1.3 Soil as a habitat of microbial life

Soil is a product of long-term weathering processes, where changes in temperature, water availability, and biological activity alter its parent materials, resulting in a great variability of inorganic and organic components (1). Soils plays an important role in all terrestrial ecosystems, as it provides mechanical support for higher plants, supplies soil-inhabiting organisms with essential nutrients and water, and provides a suitable environment for many microorganisms, such as bacteria, fungi, algae and protozoa (2). Great abundance and

diversity of microbial populations highly exceed the presence of eukaryotic ones, as one gram of soil contains up to 10 billion of microorganisms representing thousands of different species (3). Among soil microorganisms bacteria are particularly prevalent, and typical genera found in most soils are represented by *Agrobacterium*, *Arthrobacter*, *Bacillus*, *Clostridium* and *Pseudomonas.* Bacteria assigned to the latter genus are of a special ecological relevance (4), as they are known to metabolize different organic compounds and, hence, play an important role in contaminants degradation (1).

Soil bacterial communities are heterogeneously distributed within soil. One important factor often controlling their spatial organization is the content of organic matter. As the amount of organic matter decreases with an increasing soil depth, the total microbial biomass normally follows this tendency (1, 5). The availability of water, soil temperature, oxidation-reducing potential and soil pH are the physicochemical soil properties which are of a great significance, as they strongly influence the activity of microbial communities (1). Furthermore, due to the fact that microbes normally live in associations with other organisms, the type of such interactions is an important factor determining their biodiversity (6). For instance, bacterial associations with plant roots are of a special ecological relevance, as they satisfy important nutritional microbial requirements and have positive effects on plants. Hence, the zones immediately adjacent to their roots, so-called *rhizosphere*, normally contain high numbers of bacteria. They are also known to have higher degradation potential, relative to non-rhizosphere ones and, therefore, are of a special interest for contaminant degradation (7, 8). Bacteria inhabiting soil system play a crucial role in the biogeochemical cycles of many bioelements, such as carbon, nitrogen, phosphorus, sulphur. In addition, they tend to degrade many different organic contaminants, i.e. hydrocarbons. For these reasons, the presence of microbial hot-spots with enhanced biological activity play a fundamental role in the ecology of terrestrial ecosystems (1, 9).

1.3.1 The vadose zone as an important soil compartment

The vadose zone can be defined as a distinct layer beneath land surface, separated from the water-saturated zone by the capillary fringe (CF), an important and an integral part of its environment. CF is a region immediately above the water table which acts as a transition zone between the both layers (10, 11). The thickness of the vadose zone may vary significantly, and in arid or semi-arid areas may reach hundreds of meters, whereas, e.g., in wetlands may be even absent (12). What distinguishes the unsaturated subsurface from the water-saturated zone is the aquatic habitat, as it is highly fragmented and restricted to thin films adsorbed on solid soil particles (13). Discontinuous nature of such water pockets could lead to erroneous assumption that microbial processes taking place in the vadose zone are insignificant, e.g., for soil bioremediation. However, since many environmental contaminants were shown to be degraded within this zone, it is recognized as highly active part of terrestrial ecosystem (14, 15). Furthermore, typically in the vadose zone the abundance of the gas-phase highly exceeds the presence of the aqueous-phase and results in enhanced bioavilability of soil gases (i.e. oxygen) and volatile contaminants, relative to water-saturated soils. This is caused by approximately 10,000 higher diffusion coefficients of gas molecules in the air, relative to aqueous media (12, 13). The indicated dominance of the gas-phase consequently increases the surface area of the air-water interfaces (16), and as an increased presence of air influences transport processes of volatile contaminants, it may results in higher microbial activity (17, 18). Schematic view of the main soil constitutes within the unsaturated and the saturated soil are shown on Figure 1.1.

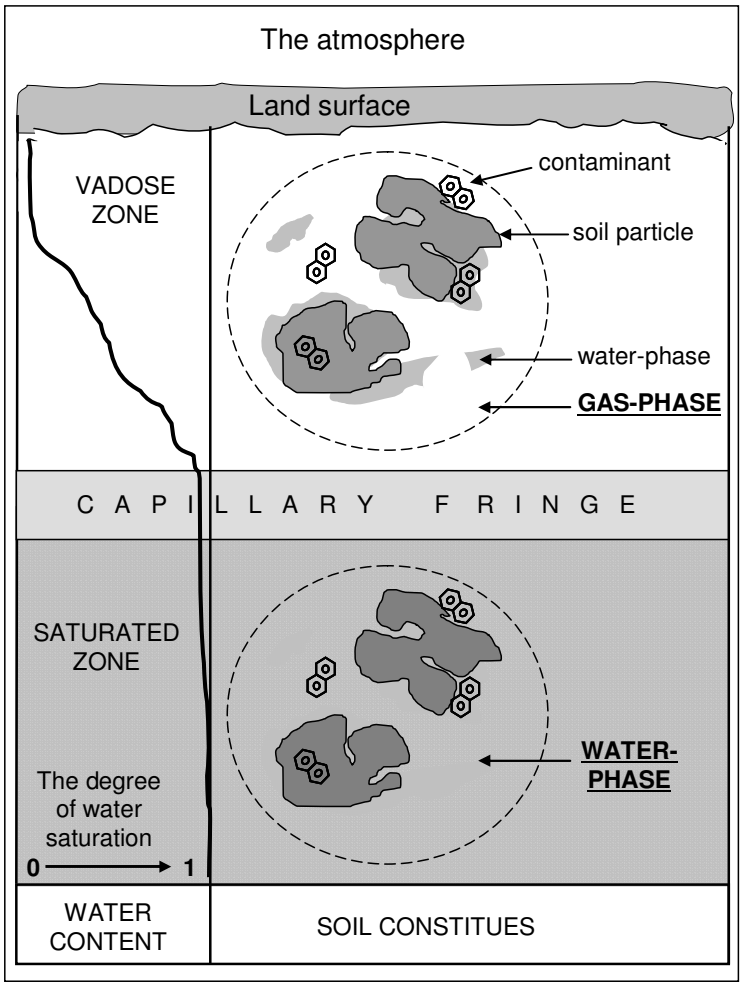

Figure 1.1. Schematic illustration of terrestrial ecosystem.

So far, microbiological research in the vadose zone has been restricted to documenting the presence, abundance, diversity and viability of microbial populations. Hence, it still remains a fairly unknown compartment of terrestrial ecosystem (19). Limited information exists on, e.g., the interplay between the diffusive transport of volatile contaminants and the spatio-temporal distribution of the bacteria, and their influence on contaminant degradation (12).

1.3.2 Microbial activity in the vadose zone

A view of the vadose zone as a sterile or barely populated region of soil has dominated until the 1970s, picturing the subsurface microbial communities as not very important for the

ecology or fertility of soil system (20, 21). Relatively harsh environmental conditions existing in such habitats are mostly caused by changes in nutrients availability, fluctuations in the soil temperature and low amount of water (13). In consequence, the unsaturated subsurface zones are normally inhabited by three to four orders of magnitude lower microbial biomass than the water-saturated soils (10). It is known that under such circumstances some indigenous bacteria develop suitable adaptation strategies allowing them to cope with the environmental stress (13). For instance, some microorganisms are known to synthesize sucrose and trehalose which help them to maintain cell membrane integrity, while others, to keep water molecules close to their membranes, produce higher amounts of the extracellular polymeric substances (EPS). Both mechanisms allow such microbes to survive at low water content (22, 23). However, although above mentioned adaptations increase the survivability of the vadose zone bacteria, it is known under the unsaturated conditions their activity, e.g., mobility is significantly reduced. It is caused by the discontinuous nature of aquatic microhabitats (13), and the tendency of the microbes to accumulate at the air-water interfaces which further restricts their movement through the water-unsaturated soils (16). As such air-water boundary layers contain the highest densities of bacterial cells (13) they are of a special interest for the biodegradation of volatile contaminants present in the vadose zone.

Microbial degradation of volatile contaminants has received considerable attention in recent years (24). Despite lower biomass the vadose zone environments appear to have higher potential to influence their transport and environmental fate (14). It has been demonstrated that, when passing through the unsaturated subsurface, many volatile compounds are intercepted and degraded by the indigenous microbes. Hence, rich in microbes the vadose subsurface are believed to be an effective natural bio-filter removing contaminants vapors from terrestrial ecosystem. By preventing their transport to other soil compartments bacterial activities are of a particular importance for bioremediation of soils and aquifers contaminated

with such chemicals (18). The concept of the vadose zone as a natural bio-filter is schematically shown on Figure 1.2.

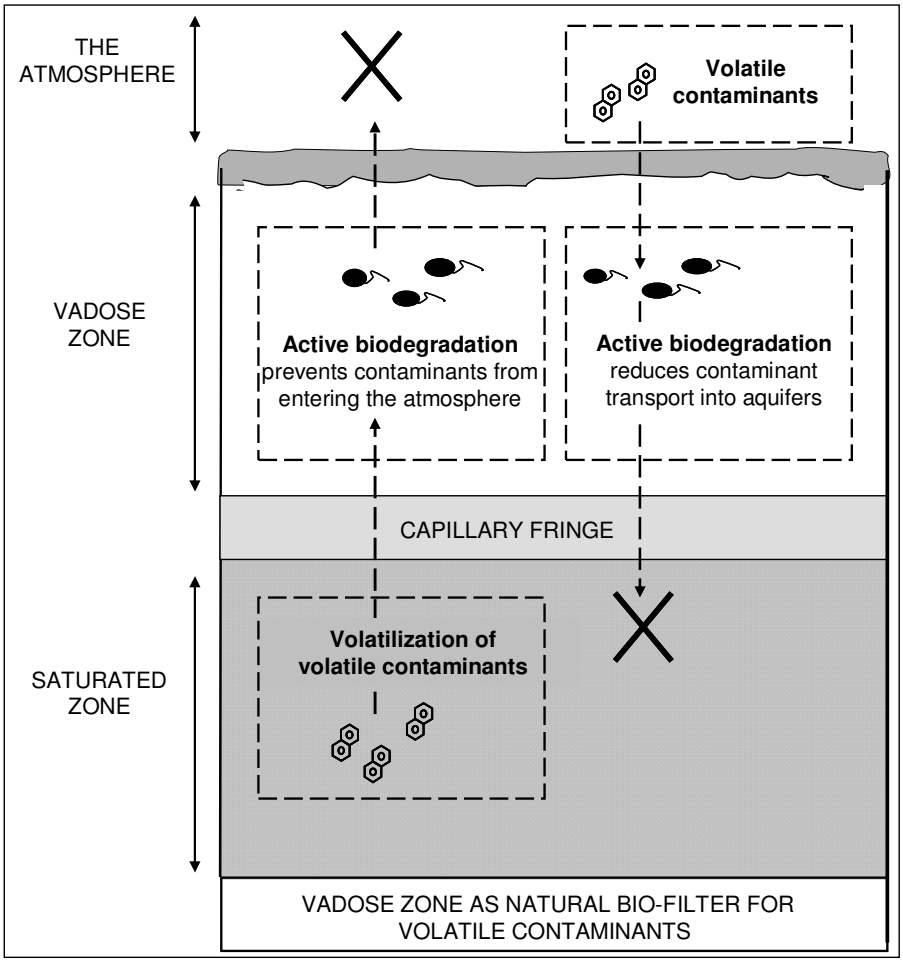

Figure 1.2. Microbial processes taking place in the vadose zone.

1.3.3 Volatile contaminants in the vadose zone

According to the definition approved by the Australian Department of Environment and Heritage (2003) '*any chemical compound based on carbon chains or rings (and also containing hydrogen) with a vapor pressure greater then 2 mm of mercury (mm Hg) at 25 degree Celsius (°C)'* is considered as volatile contaminant. Furthermore, '*these compounds may contain oxygen, nitrogen and other elements. Substances that are specifically excluded are: carbon dioxide, carbon monoxide, carbonic acid, carbonate salts, metallic carbide, and methane'* (Australian Department of Environment and Heritage, 2003). Volatile compounds are mostly assigned to two major groups: (i) aliphatic hydrocarbons - alkanes and alkenes,

and (ii) aromatic hydrocarbons (25). Well-known volatiles include: alkyl benzenes (e.g., *o*-xylen, *m*-xylen, *p*-xylen, toluene), aromatic hydrocarbons (e.g., naphthalene, benzene), ethers (e.g., MTBE), chlorinated alkanes (e.g., chloroethane, chloromethane, tetrachloromethane), chlorinated alkenes (e.g., vinyl chloride, 1,1-dichloroethane), or chlorinated aromatics (e.g., chlorobenzene, 1,2-dichlorobenzene) (26). The tendency of volatile contaminants to move from the aqueous- into the air-filled pores of the vadose zone is influenced by their vapor pressure, water solubility, octanol-water partition coefficient, polarity, air-water partition coefficient or fugacity (27, 26).

Volatile contaminants enter the vadose zone from multiple of sources. Very often they are released during petroleum spills and exist as non-aqueous phase liquids (NAPLs) floating on groundwater or being bound to soil particles. As some NAPLs are denser than water, they migrate below the water table and act as a long term contamination source (28, 29). Such contaminated groundwaters pose a serious risk for terrestrial ecosystem. Due to volatilization processes they may enter back to the vadose zone, where they may rapidly move to other soil compartments, or be released into the atmosphere affecting human health (15). Interestingly, some volatiles (i.e. ethanol, hexane, octane or benzaldehyde) are released by soil inhabiting bacteria and fungi as, so-called secondary metabolites. They may be used as indicators of microbial activity and community abundance, or may be utilized by bacteria as an efficient infochemicals allowing inter-microbial communication. As such infochemicals were shown to have negative, positive or neutral influence on other soil bacteria and fungi, they play an important role in shaping soil microbial communities (30, 31). Furthermore, very often volatile contaminants are released into the atmosphere due to, e.g., incomplete combustion of organic matter or industrial activities (32). From there they may be transported by, so-called above-ground vegetation, and via plant leaves may be directly incorporated into soil (33). Some examples of the above described pathways by which volatile contaminants enter soil system are shown on Figure 1.3.

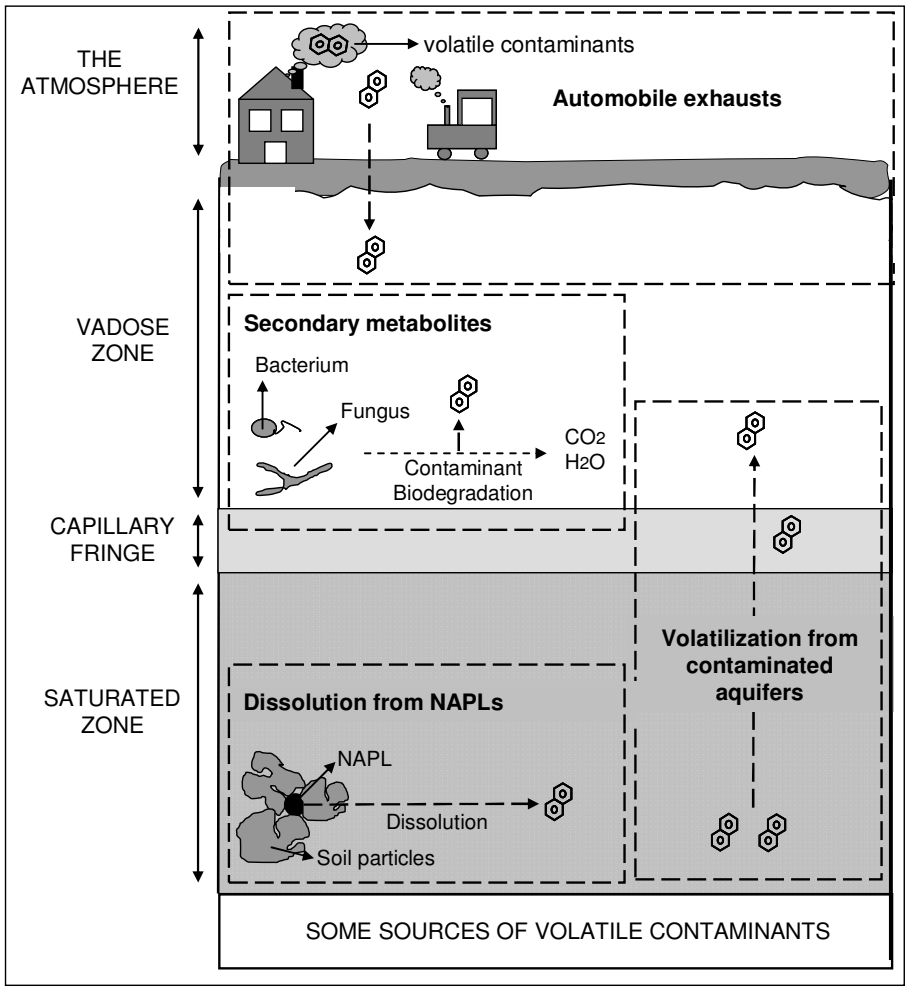

Fig.1.3. Illustration demonstrating multiple sources of volatile contaminants and their possible transport pathways though soil.

Vapor-phase contaminants are transported through the unsaturated subsurface mostly by the diffusion processes (34). As reported in literature, some were found even at a distant of 20 meters away from their initial contamination source. Therefore, in contrast to negligible advection processes (14), horizontal and vertical diffusive transport is considered as fast and efficient pathway for the above mentioned contaminants (24, 35).

1.4 Microbial degradation of vapor-phase contaminants in the vadose zone

Effective biodegradation of soil contaminants requires optimal environmental conditions (i.e. soil temperature, pH or water content), and the presence of available substrates (36, 37). As only compounds which are available for bacterial uptake can be degraded, their

bioavailability is as an excellent measure of the efficiency of the substrate biotransformation (38, 39). Quantitatively it can be described by the bioavailability number (*Bn*) which takes into account the mass transfer of contaminants to microbial cells, and its intrinsic activity of degrading bacteria to transform them (38). Usually, at high mass transfer rate the biodegradation is controlled by the metabolic bacterial activity (high *Bn*), and when the mass transfer decreases or when the population size increases, the mass transfer becomes the rate limiting step, reducing the overall rate of the biodegradation processes (low *Bn*) (40).

It is known that microbial degradation of environmental contaminants can serve different functions for a degrading organism including (i) assimilative biodegradation that generates energy and carbon, (ii) co-metabolic degradation that although degrades substrates it does not generate energy and carbon for the cell metabolism, or (iii) intracellular detoxification of potentially toxic impacts (41). All processes are controlled by the contaminant's bioavilability. Hence, depending on the bioavailability the same compound simultaneously may serve as a food source and exert toxic effects on the same microorganisms. This indicates that the bioavailability for biodegradation may be significantly different from the bioavailability for toxic effects, despite the fact that bioaccessible pool of the same contaminant may be an identical (39). Therefore, the assessment of microbial activity should take into account the contrasting processes of the bioavilability of such contaminant for biodegradation and toxicity.

Microbial degradation of the substrate which is used by the bacteria as carbon and energy source can be described by Best equation written as:

$$q = q_{\max} \frac{Cd + Km + q_{\max} k^{-1}}{2 q_{\max} k^{-1}} \left\{ 1 - \left[1 - \frac{4 Cd q_{\max} k^{-1}}{\left(Cd + Km + q_{\max} k^{-1} \right)^2} \right]^{1/2} \right\}$$

where q_{max} is the maximum conversion flux that can be achieved by a cell (M T^{-1}), *Cd* is the distant contaminant concentration (M L^{-3}), *Km* is the cell surface concentration (M L^{-3}), *k* mass transfer constant (L^3 T^{-1}) (for the derivation of this equation, see the reports of Bosma

et al. (38), Simoni et al. (42), and Best (43)). It assumes the steady-state conditions achieved when the transport flux and the rate of substrate degradation equal each other. Furthermore, as Best equation describes substrate uptake in relation to the contaminant mass transfer potential in the environment surrounding microbial cells, it evaluates the relative physical and biological contributions to the overall degradation rate. However, the above mentioned concept is valid if the substrate is the only rate limiting substance, and when its high concentrations have no inhibitory effects on the degradation rate. Yet, in terrestrial systems microorganisms are very often exposed to elevated concentrations of various environmental contaminants, even those metabolizable ones. Higher concentration of substrate, product, cell or other inhibitory substances may, e.g., inhibit microbial growth. If the substrate is present at concentrations exceeding the threshold limits tolerated by bacteria and hence inhibits microbial growth, such phenomenon is commonly known as substrate inhibition (44). Under such circumstances at low substrate concentrations microbial growth is normally reduced by it low bioavailability, whereas at high concentrations cell development is usually inhibited by enhanced substrate bioavailability. Hence, the highest biodegradation rates are typically observed at an intermediate substrate bioavilability, i.e. at conditions representing a compromise of acceptable inhibition and sufficient substrate supply to metabolically active cells (45). Several mathematical models have been developed to quantify inhibitory effects of the target substrates on microbial growth (44, 45). However, their applications to the water-unsaturated systems are limited and, hence, information about the influence of enhanced bioavilability of vapor-phase contaminants on the activity of the bacteria present at the air-water interfaces is still scarce. Such knowledge is of a great importance for the remediation of volatile contaminants, as the air-water associated bacteria are usually exposed to high amounts of contaminants vapors. So far, microbial degradation of such compounds was mostly approximated by methods which require their partitioning from the gas- into the liquid-phase where biodegradation takes place. Among such approaches commonly used are

biofilters (BFs), biotrickling filters (BTF), bioscrubbers, or membrane bioreactors (44). *In situ* the biodegradation of volatile contaminants was mainly assessed by measuring oxygen and carbon dioxide concentration profiles. Although such measurements allow to estimate the spatio-temporal contaminants degradation taking place in the subsurface soils (24, 28, 46), they do not provide any information on the role of contaminant vapors on the spatio-temporal distribution of soil microbial populations, nor on their activity.

1.5 Bacterial strategies influencing contaminant bioavailability

Unlike planktonic bacteria surrounded by relatively thick diffusive boundary layer, the bacteria present at the air-water interfaces are most likely covered by very thin water film, which possibly do not act as an effective diffusive barrier to vapor-phase contaminants. Therefore, one may assume such bacteria to be directly exposed to enhanced bioavilability of volatile contaminants. This may inhibit, e.g., microbial growth and/or activity. This concept is schematically shown on Figure 1.4, where the gas-phase of the petri dish imitates the vadose zone conditions and agar represents the water-saturated zone. It demonstrates that unlike bacteria embedded in a liquid medium and exposed to less pronounced dissolved contaminant gradient, the bacteria present at the air-water interface are directly exposed to volatile contaminant gradient via the gas-phase (both gradients are shown as light grey triangles).

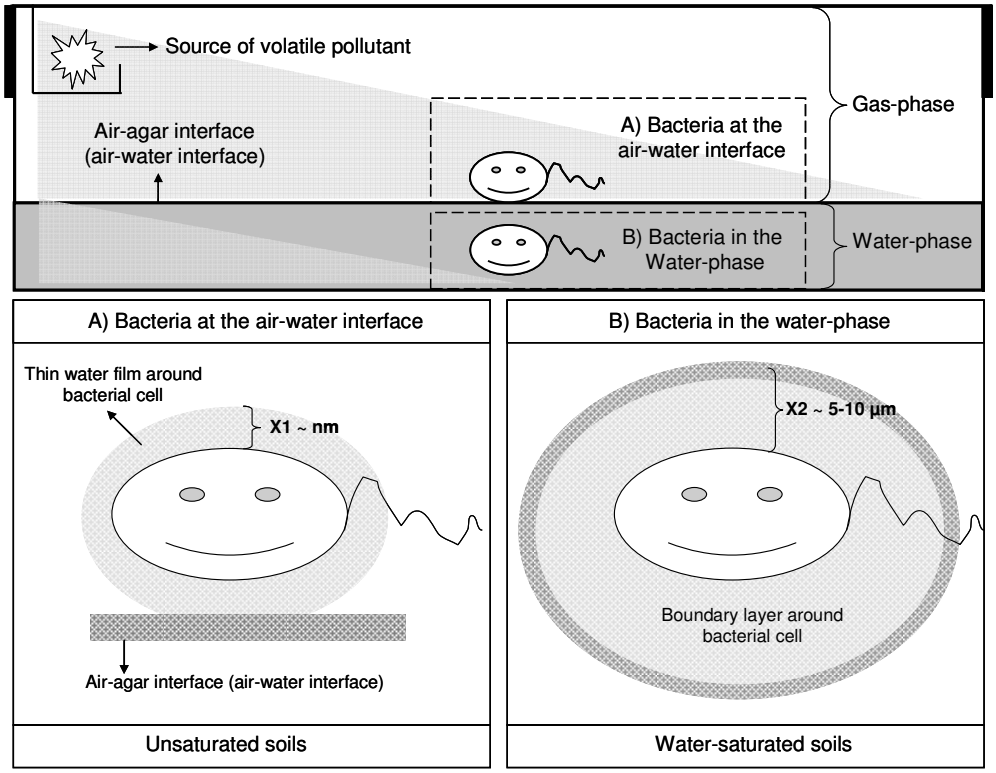

Figure 1.4. A petri dish microcosm mimicking selected features of unsaturated and saturated soils.

In order to survive under the conditions of the enhanced bioavailability of vapor-phase contaminant gradients, the air-surface associated bacteria need to develop suitable adaptation strategies allowing them to alleviate high contaminant bioavailability.

One of such strategy may be the consumption of potentially inhibitory substrates. As microbial degradation of environmental chemicals may function as intracellular detoxification mechanism (41), by contaminant degradation bacteria may reduce their extent of exposure to such contaminants. Hence, it may be an important strategy regulating the bioavailability of vapor-phase contaminants. Via their substrate utilization microbial populations reduce contaminant concentrations to levels allowing for further growth, and thus theoretically consumption could be an efficient detoxification mechanism developed by bacteria under environmental stress, i.e. in the presence of potentially toxic or inhibitory chemicals. Several studies have documented the ability of the bacteria to degrade and thus detoxify different environmental contaminants. For instance, Juhasz *et al.* (2000) studied the ability of *Stenotrophomonas maltophilia* strain VUN 10,003 to degrade and detoxify polycyclic

aromatic hydrocarbons (PAHs). Degradation of PAHs was assessed by measuring the reduction in their concentration, which was later linked to the mutagenic potential measured in a mutagenicity assay (AmesTest). As the reduction in PAHs concentration correlated well to the reduction of mutagenic potential, the author concluded that microbial degradation reduced the toxicity of these compounds (47).

An important adaptation strategy developed by bacteria is dispersal, which allows microbes to position themselves with respect to contaminants bioavilability (48). Bacteria may exhibit so-called twitching (e.g., *Pseudomonas aeruginosa*), gliding on water-wet surfaces (e.g., myxobacteria, cyanobacteria) or chemotactic swimming along fungal mycelia (e.g., *Pseudomonas putida*) (49, 50). Whereas twitching cells use extension and retraction of pili as a driving force for cells dispersal, in gliding the movement of outer cell membrane components are used to push the cell back and forwards. In addition, some bacteria (e.g., *Escherichia coli* or *Salmonella typhpimurium*) exhibit movement on solid or semi-solid surfaces, mechanism known as bacterial swimming or swarming, which may also enhance contaminant bioavailability (51).

Taxis represents a sophisticated strategy allowing motile microbial populations to navigate in response to gradients of various chemical and physical parameters. Bacteria may exhibit tactic response towards gradients of light (phototaxis), oxygen (aerotaxis), temperature (thermotaxis) or chemicals (chemotaxis) (1). Such behavior of motile bacteria is driven by receptors located at the cell surface, which as sensing elements, monitor changes in the environment and provide cells with the information about the actual strengths of target stimuli (52). Since such informations are transmitted extremely fast, microbial taxis is an immediate adaptation strategy allowing microbial populations to respond rapidly to environmental changes. A special type of tactic response is energy taxis, which makes use of sensing the intracellular energy level. Changes in energy levels are linked with electron transport systems and, thus, any physicochemical stimuli affecting the transport of electrons,

results in bacterial movement towards locations providing more energy (53). Therefore, it is sometimes difficult to distinguish energy taxis from other tactic behaviors. Chemotaxis plays a particularly important role for bacteria. It has a big ecological relevance, as swimming towards substrates increases its bioavailability while, conversely, fleeing from inhibitory substances reduces exposure (54).

1.5.1 Bacterial chemotaxis

Bacterial chemotaxis is the self-directed movement of flagellated bacteria along chemical gradients towards higher or lower concentrations, referred to as positive and negative chemotaxis, respectively (55). The ability of flagellated bacteria to sense contaminant gradients and bias their movement according to contaminants concentration profile has competitive advantages over non-motile and non-chemotactic strains as it allows microbial cells to move towards the most desirable niches where the conditions for survival and growth are optimal (53, 56, 57). Swimming patterns of chemotactic bacteria can be described as sequences of forward movements (so called '*runs'*) being interrupted by sudden cell reorientation (so called '*tumbles'*) followed in swimming in a changed direction. Chemotactic bacteria normally swim with speed ranging from 20-60 μm sec^{-1}, with runs lasting up to several seconds and tumbles taking a fraction of a second (58, 59). Bacteria 'run' towards chemoattractants for prolonged periods of time, and they tumble earlier when approaching chemorepellents (52).

Bacteria can exhibit chemotaxis in the presence of metabolizable or non-metabolizable chemicals, which was the reason to further classify bacterial chemotaxis:

(1) *'Metabolism-independent'* chemotaxis, where swimming along gradients does not depend on the uptake and chemoeffector utilization (56). These bacteria show chemotactic response to non-metabolizable analogues of metabolizable chemoattractants, and may swim towards non-metabolizable chemoattractants even

away from metabolizable compounds. Furthermore, mutation taking place in the chemoattractant metabolism pathway does not affect bacterial chemotaxis. In metabolism-independed chemotaxis transmembrane chemoreceptors (so called chemotaxis transducers) transmit the information about environmental changes from outside the cell to the inner part of the cell and via *'two-component regulatory system'* influence the direction of flagella rotation. *Pseudomonas putida* and *Bacillus subtilis* are among the bacteria that exhibit metabolism-independed chemotaxis (54)*;*

(2) *'Metabolism-dependent'* chemotaxis, where the chemoeffector needs to be consumed to provoke the chemotactic response of the bacteria. Metabolism-depended chemotactic bacteria do not show chemotactic response towards substrate analogues and their chemotaxis is affected by mutation in the chemoeffector metabolism pathway. Chemotaxis metabolism-depended was found in *Escherichia coli* towards proline, glycerol or succinate (54).

Bacterial chemotaxis can be assessed using quantitative as well as qualitative methods. Among techniques which allow to measure bacterial chemotaxis the most commonly used is *'capillary assay'*, which was introduced by Pfeffer in 1886, 1888 first as qualitative approach and later provided quantitative picture of chemotactic response along chemoeffectors' gradients, as well (60). Other methods to measure chemotaxis include *'Motility plate assay'* (58), *'Drop assay'* (61), *'Stopped flow diffusion chamber'* (SFDC) or *'Diffusion gradient chamber'* (DGC) (58), or agaroze-plug assay, commonly used approach to study bacterial chemotaxis towards volatile compounds (62).

1.5.2 Ecological relevance of bacterial chemotaxis

Chemotaxis has been reported in literature towards various environmental contaminants, mostly towards water soluble ones. It is known that positive chemotaxis along contaminant gradients increases the bioavailability of soil contaminants, as it improves the contact

between degrader organisms and patchy contaminants (63, 64). Thus, swimming along contaminant gradients may play a significant role in terrestrial ecosystems (53, 65). However, despite the fact that bacterial chemotaxis is a well-known phenomenon the knowledge regarding their swimming along concentration gradients of vapor-phase contaminants is scarce. There were some attempts to test chemotactic response of the bacteria towards volatile compounds, such as toluene or chlorinated ethanes. However, these studies have used an agarose-plug assay, where chemotactic water-bound bacteria were exposed to likewise agarose-embedded contaminants (48, 67). Thus, they tended not to reflect conditions found in the subsurface vadose zone soils, where air-surface associated bacteria are most likely influenced by vapor-phase contaminant gradients. As such volatiles have usually high vapor pressure, they can travel large distances and form vapor-phase gradients in heterogeneous soil systems. As, chemotactic dispersal within such microbial 'odor landscapes' (70) can affect the dynamics of microbial ecosystems, the knowledge of chemotactic swimming along vapor-phase contaminant gradients is of a great importance for the ecology of their biodegradation (71).An overview of known chemotactic strains and their target volatile chemicals, with the original literature is given in Table 1.1.

Table 1.1. Bacterial chemotaxis towards environmental contaminants.

Target chemical	Bacterial strain	Reference
BTEX compounds		
Benzene	*Pseudomonas putida* F1	(66)
Toluene	*Pseudomonas putida* F1	(66)
	Ralstonia picketti PK01	
	Burkholderia cepacia G4	(67)
	Pseudomonas stutzeri OX1	
Ethylbenzene	*Pseudomonas putida* F1	(66)
Polycyclic aromatic hydrocarbons/Biphenyl		
Naphthalene	*Pseudomonas putida* G7	(61)
	Pseudomonas sp. NCIB9816-4	
	Pseudomonas alcaligenes 8A	(68)
	Pseudomonas stutzeri 9A	
	Pseudomonas putida 10D	
Phenanthrene	*Pseudomonas putida* 10D	(68)
Anthracene, Pyrene	*Pseudomonas putida* 10D	(68)
Biphenyl	*Pseudomonas putida* G7	(61)
Aliphatics		
Hexadecane gas oil	*Flavimonas oryzihabitans*	(69)
Vinylchloride	*Pseudomonas stutzeri* OX1	(67)
	Burkholderia cepacia G4	

Chapter 2
Microbial growth on vapor-phase gradients of naphthalene

2.1 Microbial growth with vapor-phase substrate[1]
2.2 Walking the tightrope of bioavailability: Growth dynamics of PAH degraders on vapor-phase PAH[2]

[1] Environmental Pollution. 2011, 159, 858-864.
[2] Microbial Biotechnology. submitted.

This chapter aims at studying the interplay between the diffusive transport of vapor-phase naphthalene and its repercussion on the spatio-temporal growth of naphthalene-degrading bacteria *Pseudomonas putida* (NAH7) G7.

In the first part of this chapter investigates the spatio-temporal growth of the planktonic bacteria on vapor-phase naphthalene. Obtained results have demonstrated that despite the high NAPH gas-phase diffusivity microbial growth was strongly depended on its distance to the substrate source, and for a given distance on the amount of bacteria competing for the NAPH. Mass transfer limitation of *P.putida* G7 cells was more apparent at longer distances from the source and in the presence of an elevated microbial biomass. As a result, microbial growth was inversely correlated with the distance from the NAPH.

The second part of this chapter focuses on the spatio-temporal growth of the air-surface associated bacteria and hence studies microbial growth at the conditions of enhanced bioavilability of vapor-phase NAPH. Obtained results were in agreement with the previous findings at larger distances from the NAPH. Yet, at shorter locations the growth of *P.putida* G7 was strongly inhibited revealing negative correlation between growth, and distance to vapor-phase substrate or bacterial cell numbers. However, at immediate distance to the source competition between degrading organisms increased the growth rates, suggesting that high bioavailability of gas-phase NAPH inhibits microbial growth, unless sufficient substrate consumption is provided. Hence, increased catabolic activity of the bacteria alleviated inhibitory effects of vapor-phase NAPH by reducing its concentrations to levels allowing for optimal growth.

Obtained results indicate at a significant role of the vadose zone as a natural bio-filter for gas-phase volatile contaminants emanating from contaminated groundwater or soil.

Environmental Pollution 159 (2011) 858–864

Contents lists available at ScienceDirect

Environmental Pollution

journal homepage: www.elsevier.com/locate/envpol

Microbial growth with vapor-phase substrate

Joanna Hanzel, Martin Thullner, Hauke Harms, Lukas Y. Wick*

UFZ – Helmholtz Centre for Environmental Research, Department of Environmental Microbiology, Permoserstrasse 15, 04318 Leipzig, Germany

Suspended bacteria have a high efficiency to degrade vapor-phase naphthalene and effectively influence vapor-phase naphthalene concentration gradients at the centimeter scale.

ARTICLE INFO

Article history:
Received 20 September 2010
Received in revised form
22 December 2010
Accepted 28 December 2010

Keywords:
Vapor-phase contaminants
Vadose zone
Bioavailability
Biodegradation
Mass transfer
P. putida PpG7 (NAH7)

ABSTRACT

Limited information exists on influences of the diffusive transport of volatile organic contaminants (VOC) on bacterial activity in the unsaturated zone of the terrestrial subsurface. Diffusion of VOC in the vapor-phase is much more efficient than in water and results in effective VOC transport and high bioavailability despite restricted mobility of bacteria in the vadose zone. Since many bacteria tend to accumulate at solid-water, solid-air and air–water interfaces, such phase boundaries are of a special interest for VOC-biodegradation. In an attempt to evaluate microbial activity toward air-borne substrates, this study investigated the spatio-temporal interplay between growth of *Pseudomonas putida* (NAH7) on vapor-phase naphthalene (NAPH) and its repercussion on vapor-phase NAPH concentrations. Our data demonstrate that growth rates of strain PpG7 were inversely correlated to the distance from the source of vapor-phase NAPH. Despite the high gas phase diffusivity of NAPH, microbial growth was absent at distances above 5 cm from the source when sufficient biomass was located in between. This indicates a high efficiency of suspended bacteria to acquire vapor-phase compounds and influence headspace concentration gradients at the centimeter-scale. It further suggests a crucial role of microorganisms as biofilters for gas-phase VOC emanating from contaminated groundwater or soil.

1. Introduction

The vadose zone plays an important role as natural biofilter. It is where volatile organic contaminants emanating from polluted aquifers are degraded by aerobic microbes (Hohener et al., 2006; Marr et al., 2006). Biotransformation in the vadose zone also limits the transfer of atmosphere- or soil-bound contaminants to aquifers (Konopka and Turco, 1991) hence improving groundwater quality (Squillace et al., 2004). Until the 1970s a view of the vadose zone as a sterile or sparsely populated region dominated (Chapelle, 1999). Since then, microbiological research in the vadose zone has largely focused on documenting the presence, abundance, diversity of microbes and influence of water potential on their activity (Dechesne et al., 2010; Holden and Fierer, 2005). Nevertheless, the water-unsaturated subsurface is still a fairly unknown compartment of terrestrial ecosystems. Limited information exists on bacterial activity in the unsaturated zone of subsurface systems and on the influence of entrapped air on diffusive pollutant transport (Konopka and Turco, 1991; Batterman et al., 1996; Harms, 1996).

Whereas the mobility of bacteria in unsaturated systems is restricted by air-filled pores, VOC diffusion is more efficient in the vapor-phase than in water (Schwarzenbach et al., 2003) and allows for effective VOC transport even over longer distances. Vapor-phase contaminants, for instance, have been found to travel up to 20 m through air-filled soil within few hours after a contamination incident (Christophersen et al., 2005). Vapor-phase diffusion, however, is controlled by the temperature and the soil physical properties porosity, water content, and tortuosity of the soil pore network (for a review: Kristensen et al., 2010; Choi and Smith, 2005). At the microscopic scale the transport of chemicals is controlled primarily by diffusion through spatially and temporally variable liquid and gas phases. As a result, the small scale distribution of chemicals, nutrients and their fluxes greatly impact the activity and distribution of microbes in the vadose zone (Wang and Or, 2010). Surface-attached microcolonies and biofilms harbor most of the microbes in the vadose zone (Young and Crawford, 2004). Since many bacteria furthermore accumulate at solid-air and air–water interfaces, these three types of phase boundaries are of special interest for the VOC-biodegradation in unsaturated soil zones, such as the capillary fringe above contaminated aquifers (Konopka and Turco, 1991) and in technical biofilters (Mudliar et al., 2010). Due to the relatively high availability of water, oxygen and

* Corresponding author.
E-mail address: lukas.wick@ufz.de (L.Y. Wick).

0269-7491/$ – see front matter © 2011 Elsevier Ltd. All rights reserved.
doi:10.1016/j.envpol.2010.12.032

VOC emanating from the groundwater, the vadose zone is a hotspot of microbial activity. It is in fact believed to host one of the highest prokaryotic densities of all biosphere compartments (Whitman et al., 1998). Accordingly it has a higher degradation capacity than saturated soil (Andersen et al., 2008), where diffusion is impeded by constituents with high resistance to diffusion like clayey materials or organic matter (Luthy et al., 1997; Semple et al., 2007). In an attempt to evaluate microbial activity toward air-borne substrates, this study tested the hypothesis that the diffusive transport of the model VOC naphthalene (NAPH) governs the spatio-temporal establishment of NAPH-degrading bacteria. We took the growth of *Pseudomonas putida* PpG7 (NAH7) (Dunn and Gunsalus, 1973), a strain with well-known growth characteristics (Ahn et al., 1998; Marx and Aitken, 1999; Filonov et al., 1997), as a quantitative indicator of the vapor-phase substrate transport in a model vadose system. Our goal was to link the spatial distribution of microbial growth and activity at the cm-scale to vapor-phase diffusion gradients of the organic substrate growth retrace from a remote source. We observed that competition between bacteria located at various distances from the NAPH source greatly affected the distribution of the newly emerging biomass and NAPH degradation activity.

2. Material and methods

2.1. Bacteria and culture conditions

P. putida PpG7 (NAH7) (Dunn and Gunsalus, 1973) is an aerobic soil bacterium degrading the semi-volatile polycyclic aromatic hydrocarbon naphthalene (NAPH) with known kinetics (Ahn et al., 1998; Marx and Aitken, 1999). Strain PpG7 was grown at 25 °C on a gyratory shaker (150 rpm) in 100-mL Erlenmeyer flasks containing 50 mL of liquid mineral medium (Wick et al., 2001) in the presence of 1.5 g l^{-1} of solid NAPH (>98%, Fluka; crystals as obtained by the provider). Cells used as inoculum for vapor-phase growth experiments were harvested in the late exponential phase (48 h of growth), centrifuged and washed twice with mineral medium (MM) and re-suspended in MM to obtain a bacterial suspension of an $OD_{600,Cary}$ of approx. 0.08 (measured in a quartz cuvette of 1 cm path length in a Cary 400 Scan (Varian) spectrophotometer) that corresponded to approx. 8×10^7 cfu ml^{-1} or 32 $\mu g_{dry\ weight}$ ml^{-1}. This cell density corresponded to an OD_{600} of approx. 0.14 when analyzed in a multi-well plate by an automated multi-well spectrophotometer (GENius Plus, Tecan Deutschland GmbH). A highly linear correlation ($r^2 > 0.99$, $n = 27$) of $OD_{600,Cary} = 2.20OD_{600} \times -0.18$ was found. Assuming this relation and a measured constant conversion factor of 323 $mg_{dry\ weight}$ cell biomass per $OD_{600,Cary}$, the cell to OD_{600} conversion function ($K_{OD/c}$) as given in Table 1 is derived. Bacteria in viability assays were quantified as colony forming units (cfu) on Luria Broth (LB) agar (2% w/v) using automated spiral plating and cell counting systems (Meintrup DWS Laborgeräte GmbH, Germany).

Table 1
List of parameters used in this report.

Symbol	Definition	Value (Reference)	Unit
A	Areal cross section for NAPH-flux		cm^2
c_0	Gas-phase concentration at NAPH crystal	0.56[a]	mg L^{-1}
d	Distance between the well and cover plate	0.1	cm
D_g	Diffusivity (gas phase)	2.3×10^{-2} [a]	m^2 h^{-1}
J	Mass flux of NAPH		mg h^{-1} cm^{-2}
$K_{OD/c}$	Cell to OD conversion function	$710 \times OD - 58$	$mg_{dry\ weight}L^{-1}$
m_{mol}	Molar mass of NAPH	1.28×10^{5}	mg mol^{-1}
P^0	Vapor pressure of NAPH	1.07×10^{-4} [a]	atm
R_{well}	Radius of well	0.35	cm
R_g	Ideal gas constant	8.206×10^{-2}	L atm mol^{-1} K^{-1}
s	Distance between two wells in a row	0.1	cm
T	Temperature	298.15	K
V_{well}	Volume of cell suspension in well	2×10^{-4}	L
Y	Cell yield coefficient	0.60[b]	g g^{-1}

[a] (Schwarzenbach et al., 2003).
[b] (Filonov et al., 1997).

2.2. Growth on vapor-phase NAPH

Growth of strain PpG7 with vapor-phase NAPH was assessed in tightly closed, sterile 96-multi-well plates (Nunc TC microwell 96F, Sigma–Aldrich; dimensions: 12.5 × 8.5 × 0.9 cm) as laboratory model for spatially distributed water pockets in the unsaturated soil zone. 50 mg of solid NAPH was placed in each well of the first row (Fig. 1). NAPH crystals remained visible throughout the experiment. All other wells or a selection were subsequently filled with bacterial suspensions as follows. In one growth experiment the influence of the distance of *P. putida* PpG7 inocula from the source of NAPH vapor was tested ('distance experiment'). Using different microwell plates, 200 μL of cell suspension ($OD_{600} \approx 0.08$) was filled in each of the eight wells of one row located either at 0.9, 1.7, 2.5, 3.3, 4.1, 5.8 or 7.4 cm from the NAPH source (cf. Fig. 1) while all other wells were left empty. Cultivation was performed at approx. 25 °C. Identical experiments in the absence of NAPH served as controls. In a second growth experiment, the influence of substrate competition between inoculated wells at different distances from the source of NAPH vapor was tested ('competition experiment'). All wells except those containing NAPH in row 1, were filled with 200 μL of cell suspension ($OD_{600} \approx 0.08$). Identical experiments in the absence of NAPH served as controls. Growth of strain PpG7 in inoculated wells was quantified by half-hourly analysis of the OD_{600} for 70 h using an automated multi-well spectrophotometer with automated agitation for 20 s prior to each analysis for homogenizing the cell suspensions. To minimize losses of humidity and volatile NAPH, multi-well plates were tightly sealed with Teflon tape. Loss of humidity checked by repeated weighing was negligible (<1.5 mg h^{-1}). In order to exclude boundary effects, only data obtained from wells within the rectangle confined by C2 and F10 (Fig. 1) were used for this study.

2.3. Analysis of spatio-temporal concentrations of NAPH in MM

In order to demonstrate the presence of vapor-phase NAPH concentration gradients in the multi-well plates' headspace, MM NAPH concentrations were measured at room temperature (ca. 20 °C). Shortly, 50 mg of solid NAPH was placed in each well of the first row of sealed, sterile 96-multi-well plates as described above for the 'distance experiments' (Fig. 1). Except for the eight wells of one row (i.e. the wells A2-H2, A5-H5, A7-H7, or A10-H10 located at different distances from the NAPH source) which were inoculated with 200 μL of cell suspension ($OD_{600} \approx 0.08$), all other wells were filled with 200 μL of sterile MM. At given intervals (24, 48, and 72 h) the NAPH containing MM was removed using glass pipettes and transferred to HPLC vials containing microliter inserts allowing for minimal headspace only. NAPH was analyzed by high performance liquid chromatography (HPLC) (Shimadzu class-VP) on an RP-18 column (Nucleosil 100-5 C18 4mmID) using an isocratic mobile phase (MeOH/water (90:10 v/v); flow: 1 mL min^{-1}) and UV-spectroscopy (250 nm) for the detection of NAPH that was based on a 6-point calibration curve with NAPH dissolved in MM covering the full range of its solubility.

3. Quantitative estimation of NAPH degradation rates and gas phase concentration gradients

For each well, the observed rate of biomass formation and the substrate requirement for biomass maintenance are assumed to reflect the rate r of NAPH degradation:

$$r = \frac{1}{Y} \cdot \left(\frac{\partial m_{bac}}{\partial t} + M \cdot m_{bac} \right) \quad (1)$$

Y is the growth yield factor and M the maintenance factor. For simplicity and due to the lack of reliable estimates for this strain M will be set to zero in the remainder of this study. The bacterial biomass m_{bac} in a volume V_{well}, is $m_{bac} = c_{bac} \cdot V_{well}$. The concentration of bacteria c_{bac} is linked to the optical density OD measured in the automated sampling system via an OD dependent conversion function $K_{OD/c}$: $c_{bac} = K_{OD/c}(OD)$. With this the NAPH degradation rate in a well can be expressed using measured optical densities and their changes during an interval Δt.

$$r = V_{well} \cdot \frac{1}{Y} \cdot \frac{\Delta K_{OD/c}(OD)}{\Delta t} \quad (2)$$

Input values needed for the calculation (Table 1) were either defined by the experimental setup (i.e. V_{well}), measured independently (i.e. $K_{OD/c}$) or taken from the literature (i.e. Y).

To calculate NAPH concentrations c_{NAPH} along the well plate, steady state was assumed for NAPH concentrations and degradation rates, and diffusion was assumed to be the only process

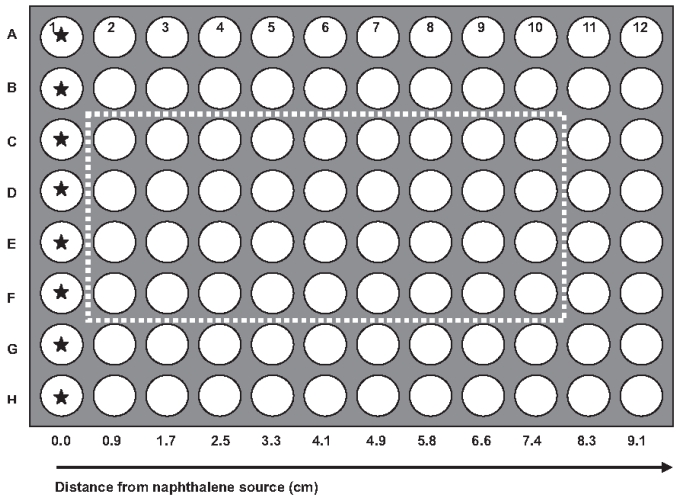

Fig. 1. Schematic view of a 96-multi-well plate used to quantify growth of *P. putida* PpG7 (NAH7) on vapor-phase naphthalene emanating from crystals in wells A1-H1 (symbolized by stars). Data of Figs. 2–4 represent averages and standard deviations of data obtained from wells within the rectangle between C2 and F10.

of NAPH transport in the gas phase. Applying these assumptions to the 'distance experiment', the diffusive NAPH mass flux J from the NAPH crystals to the inhabited row at distance Δx is equal to the degradation rate determined for wells in this row using Eq. (2):

$$J = D \cdot \frac{\Delta c_{NAPH}}{\Delta x} \cdot A = r \quad (3)$$

The gas phase diffusion coefficient D is taken from the literature. The cross sectional area A available for the gas flux to an inhabited well is defined by a rectangle of distance d between the well plate and its cover plate, the diameter of a well R_{well} and the distance s between two wells in a row (Table 1): $A = d \times (2R_{well} + s)$. It is thus assumed that the horizontal diffusion of gaseous NAPH limits the flux and not its vertical migration into the individual wells. With this relation the gas phase NAPH concentration at a well can be expressed as

$$c_{NAPH} = c_0 - \frac{r \cdot \Delta x}{D \cdot d \cdot (2R_{well} + s)} \quad (4)$$

where c_0 is the concentration at zero distance from the NAPH crystals given by the NAPH vapor pressure P^0, the molar mass m_{mol} of NAPH, the gas constant R_g and the temperature T: $c_0 = (P^0 \cdot m_{mol})/(T \cdot R_g)$. The volatilization of NAPH crystals is thus assumed to be fast enough to maintain a permanent equilibrium between crystals and gas phase concentrations at zero distance from the crystals.

For the competition experiment the calculation of NAPH degradation rates and concentration gradients was generally conducted as above. The only difference is that the flux between the crystals and wells at distance Δx is now assumed to be given by the accumulated rate r_{acc} of the well at this distance and of all those located at larger distances:

$$J = r_{acc}(\Delta x) = \sum_{x > \Delta x} r(x) \quad (5)$$

with each individual $r(x)$ calculated using Eq. (2). Analogously, the NAPH concentration at a well is calculated by replacing r with r_{acc} in Equation (4).

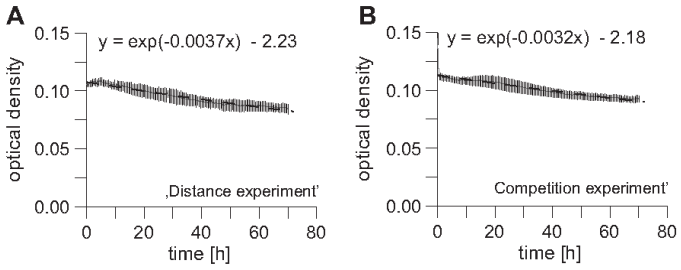

Fig. 2. Growth curves of *P. putida* PpG7 (NAH7) in control experiments the absence of vapor-phase NAPH obtained from 'distance experiments' (panel A) and 'competition experiments' (panel B). Growth data are averages (gray line) and standard deviations of data obtained from wells in C2–F10 as indicated in Fig. 1. The exponential fit is shown as black dashed line.

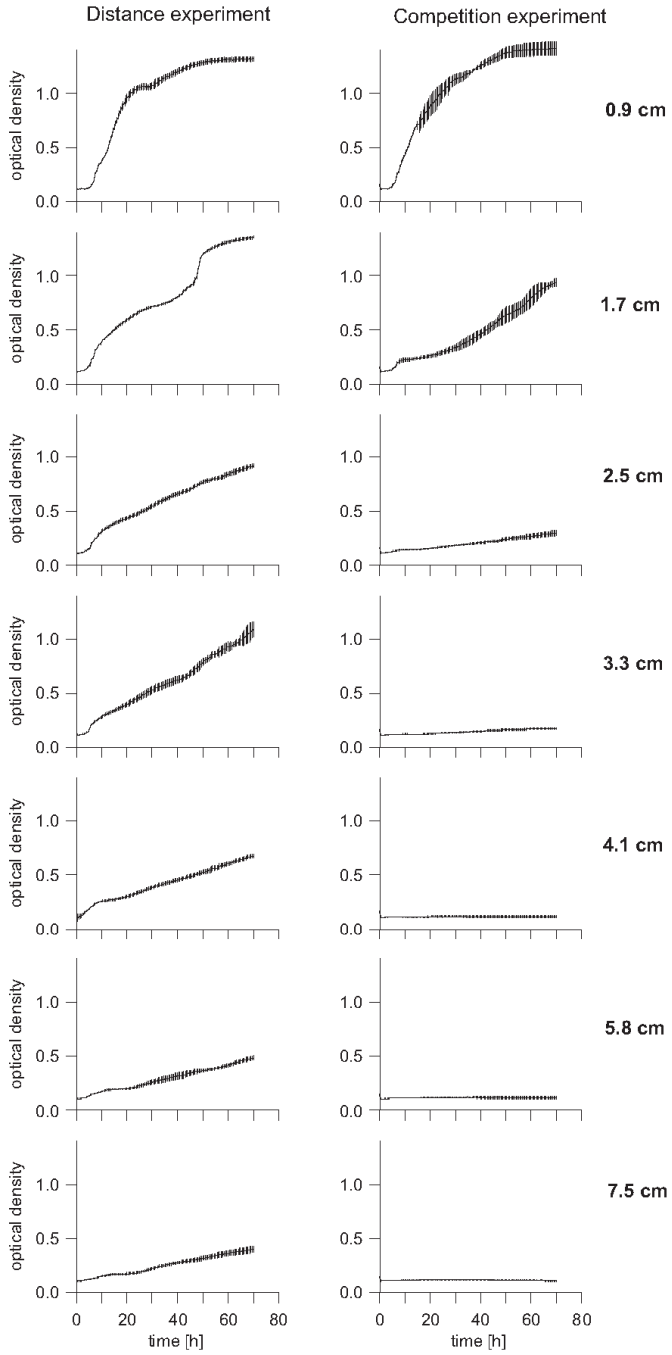

Fig. 3. Spatio-temporal growth of *P. putida* (NAH7) G7 on vapor-phase NAPH in the absence and presence of competition between wells located at different distances from the source. Growth data are averages and standard deviations of data obtained from wells C2 – F10 as indicated in Fig. 1.

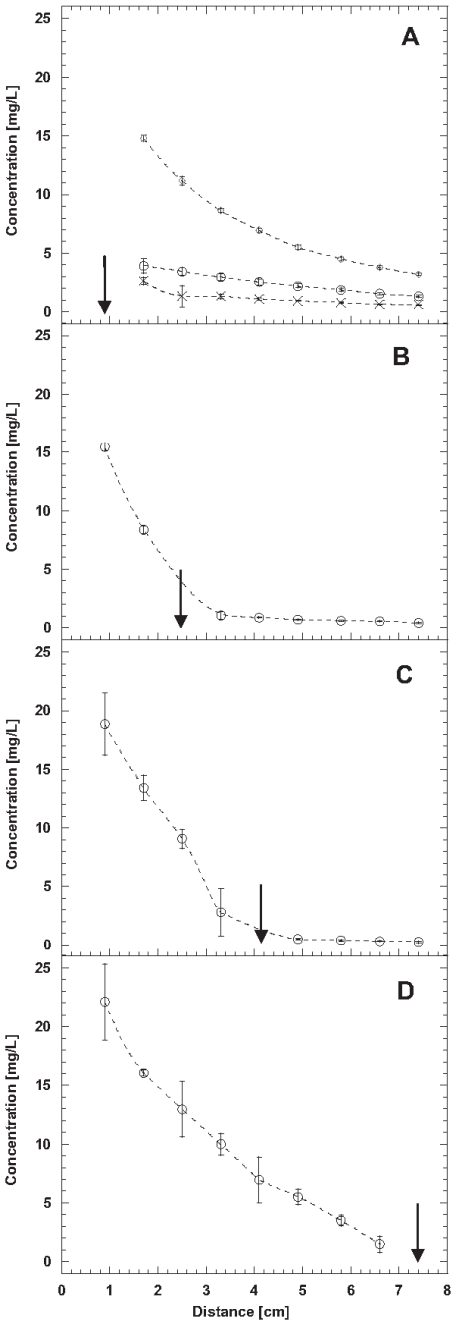

Fig. 4. Aqueous NAPH concentrations at given distances from the NAPH source measured in experimental set-ups similar to 'distance experiments' after 24 h of incubation (empty circles): Panels A, B, C, and D depict averages and standard deviations of NAPH concentration obtained from wells C2 – F10 in individual experiments in presence of PpG7 bacteria growing either in wells A2-H2 (A), A5-H5 (B), A7-H7 (C), and A10-H10 (D). Locations of microbial activity are indicated by the arrows. Crosses and rhomboids in panel A additionally represent NAPH concentrations detected after 48 and 72 h. As such data in Panels B–D was highly similar to the values measured after 24, they are not depicted for better readability of the figure.

4. Experimental results

4.1. Growth of strain PpG7 with vapor-phase NAPH

Control experiments in the absence of NAPH resulted in minimal reduction of the OD in the range of -4×10^{-4} OD h^{-1} for both types of experiments (Fig. 2). The small decrease of OD, however, could not be unequivocally related to the bacteria's viability in separate experiments (data not shown). In the presence of solid NAPH as sole carbon and energy source strain PpG7 exhibited efficient growth with rates depending on the distance of the wells to the NAPH source and the microbial biomass present (Fig. 3). The left side of Fig. 3 depicts growth curves of strain PpG7 in 'distance experiments'. Rates of OD_{600} increase as a measure of cell growth were inversely correlated with the distance from the NAPH source. After a lag period (approx. 5 h) and short periods of exponential growth (approx. 5–15 h) phases of apparently linear growth were typically observed at the different sampling locations. Apparent growth rates assessed in the period 30–45 h decreasing from ca. 1.9×10^{-2} OD h^{-1} (i.e. 100% at $x = 0.9$ cm) to 4.1×10^{-3} OD h^{-1} (i.e. 22% at $x = 7.5$ cm). In competition experiments similar apparent growth rates of 2.0×10^{-2} OD h^{-1} were observed close to the NAPH source ($x = 0.9$ cm). On the contrary, growth rates of strain PpG7 declined rapidly to 50, 12, and 6% at $x = 1.7$, 2.5, 3.3 cm and dropped below the detection limit at 4.2 cm from the NAPH source and beyond.

4.2. NAPH concentrations in MM as indicator for vapor-phase NAPH gradients

In order to demonstrate the presence of vapor-phase NAPH concentration gradients in the multi-well plates' headspace, spatio-temporal NAPH concentrations in the MM were measured. Except for the data shown in Fig. 4A highly similar NAPH profiles were detected at all intervals tested suggesting steady state conditions to be achieved with less than a day. For better readability Fig. 4B–D hence depicts the finding of the 24 h of incubation interval only. This data reveals clear distance-dependant quasi linear decrease of aqueous NAPH concentrations in wells ranging from close to the maximal solubility to below 1 mgL^{-1} behind zones of microbial activity. By linear extrapolation of the NAPH concentration profiles (e.g. in Fig. 5B–D) to a hypothetical distance of zero cm to the NAPH source a maximal solubility of NAPH in MM of approx. 24 ± 1 mgL^{-1} ($n = 9$) is calculated (extrapolation not shown). This value is close to the maximal solubility of NAPH in pure water at $T = 20$ °C (approx. 26 mg L^{-1} (Schwarz, 1977)). Given an ionic strength of in the range of 10^{-1} M of the MM used an even lower NAPH solubility has to be expected. Fig. 4A reveals an approximate three fold increase of the NAPH concentration after 72 h and points at reduced microbial NAPH consumption rates in wells A2-H2, as is also reflected by the first panel of the left row in Fig. 3.

5. Discussion

5.1. Mass-transfer limited growth on vapor-phase NAPH

Growth of *P. putida* (NAH7) G7 on vapor-phase NAPH as sole carbon and energy source was followed to investigate the influence of vapor-phase NAPH fluxes on microbial consumption and *vice versa*. Growth data show that, despite the high vapor-phase

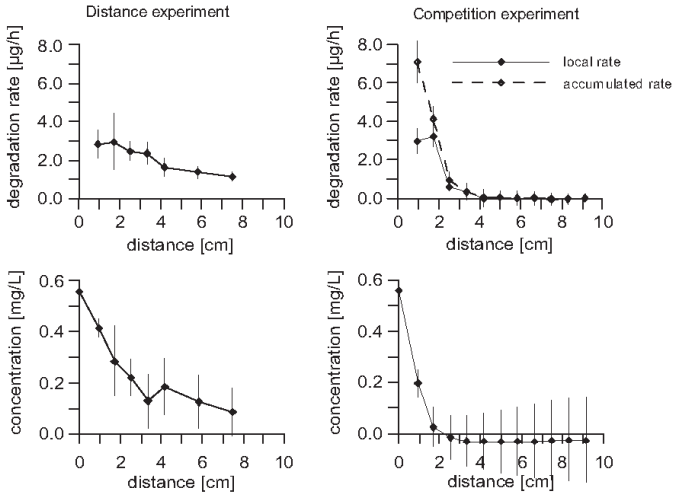

Fig. 5. Calculated NAPH degradation rates (panel A using Eq. (2), and panel B using Eqs. (2) and (5)) and corresponding NAPH concentration profiles (panel C using Eq. (4), and panel D using Eq. (4) with accumulated rates) at given distances from the NAPH source in competition and 'distance experiments'. Results shown are averages and standard deviations for the time interval $30 < t < 45$ h.

diffusivity of NAPH (Table 1), growth of *P. putida* cells strongly depended on its distance to the NAPH source and for a given distance on the numbers of bacteria competing for the air-borne substrate. Linear growth (i.e. continuously declining specific growth) at higher distances points at transfer limitation of vapor-phase NAPH (Wick et al., 2001). Bioavailability for compound degradation is a dynamic process determined by the rate of physical mass transfer to microbial cells relative to their intrinsic catabolic activity (Johnsen et al., 2005). At high transfer rates, the realized degradation rate (Wick et al., 2001) is predominantly controlled by the metabolic potential of the bacteria, whereas at decreasing transfer rates and/or growing microbial consumption the substrate mass transfer may become the limiting factor. Diffusive transport of NAPH to cells is best described by Fick's first law of diffusion (Eq. (3)). According to this law, the NAPH mass flux depends on the space coordinate in the direction of the transport Δx and the vapor-phase concentration difference Δc_{NAPH} between the substrate source and substrate-consuming cells, with the latter being the drivers of the diffusive mass flux. Mass transfer limitation of NAPH-degrading PpG7 is thus more severe at longer distances from the source (Fig. 3 left) and/or in the presence of an elevated microbial consumption potential, particularly when the competing microbes are located closer to the substrate source as in the competition experiments (Fig. 3 right). Using growth data (Fig. 3) spatially-resolved headspace NAPH concentrations (Fig. 5) can be inferred (Eqs. (1–5)) and, *vice versa* provide a useful quantitative estimate showing that observed growth data qualitatively and quantitatively support the hypothesis of air phase diffusion limited growth. Further note that the quantitative estimates given in Fig. 5 are based on data obtained from the 30–45 h growth interval. We are aware that type and length of the different growth phases at the different sampling locations exhibited some degree of variability. Fig. 3, nevertheless suggests that growth of strain PpG7 at the interval of 5 and 15 h is more exponential than linear, while at later stages (i.e. between 30 and 45 h) its growth rates appear to be relatively constant at all sampling locations. To achieve a high degree of consistence and for better comparison between the measured data and our quantitative estimates we hence decided to select a single time period (between 30 and 45 h) for all sampling locations. This time period seemed (i) to be independent of unknown initial growth effects (e.g. lag phases, growth on internal storage products), (ii) to exhibit *quasi* constant growth rates at each sampling location, and (iii) to lack unexpected growth behavior as e.g. observed after 45 h in wells A3 to H3 in the 'distance experiments' (Fig. 3). Fig. 5 illustrates that calculated NAPH concentrations in the headspace and corresponding NAPH degradation rates sharply drop within a few centimeters. Such estimated headspace NAPH gradients were underpinned by analyzing the NAPH concentrations in MM-filled wells in response to the multi-well plates' headspace NAPH gradients (Fig. 4). Assuming sufficiently fast vertical migration of NAPH into the individual wells MM-borne NAPH hence supports both, the spatial vapor-phase NAPH concentration gradients considered in this study and the drastic effects of microbial activity on vapor-phase NAPH concentrations as proposed by Fig. 5B and D. Although based solely on measured data from this study or from the literature, the presented quantitative estimates are subject to several uncertainties and simplifications (e.g., maintenance effects, conversion of OD to cell activity, vertical diffusive transport into the wells etc.) and are thus not meant as a fully quantitative description of the reactive transport of NAPH in the system. However, the quantitative estimates in Fig. 5 unambiguously show that changes of vapor-phase concentrations and degradation rates heavily depended on the amount of biomass and its spatial distribution. This becomes even more explicit in the competition experiment which demonstrated that bacteria located close to the source of vapor-phase NAPH strongly suppressed the growth of remoter bacteria.

5.2. Relevance for VOCs contaminated unsaturated subsurface soils

This study showed that in presence of metabolically active microorganisms vapor-phase NAPH is effectively depleted within centimeters from the NAPH source. This finding is of a great importance for understanding the fate of VOC in heterogeneous vadose soil zones, as they can be found above the capillary fringe of VOC-contaminated groundwater. Our results suggest that, given

the right conditions for microbial activity, the zone next to a reservoir of VOC may act as a highly effective natural biofilter preventing long distance subsurface transport of volatile groundwater contaminants through soil and to the atmosphere. Likewise microbial activity may play a crucial role in shallow unsaturated soils by keeping VOC in soil from migrating to groundwater (Franzmann et al., 1999) or, *vice versa*, for VOC emanating from groundwater. This appears to be of special relevance for vertical soil filters designed for groundwater remediation, which have been recently suggested for the treatment of VOC-contaminated groundwater (Salmon et al., 1998; Knight et al., 1999; Wallace and Kadlec, 2005; Eke and Scholz, 2008; Tang et al., 2009) provided that they prevent atmospheric emissions (De Biase et al., submitted). The observed effective removal of vapor-phase NAPH in this study may further underpin the efficacy of phyllosphere bacteria for the degradation of air-borne gases or VOC (De Kempeneer et al., 2004; Sandhu et al., 2007; Waight et al., 2007). They may act as important biofilters in constructed wetlands for groundwater treatment, plantations for the purpose of contaminant phytoextraction and green belts along highways or around industrial sites.

Acknowledgments

Funding European grant European MC-EST20984 grant (RAISE-BIO) is greatly acknowledged. Additional funding was provided by the Helmholtz Association via the program topic "CITE-Chemicals in the Environment", and grant VG-NG-338 ("GReaT MoDE"). The authors wish to thank an anonymous reviewer for the helpful input as well as Jana Reichenbach, Oliver Scheer and Birgit Würz for skilled technical help.

References

Ahn, I.S., Ghiorse, W.C., Lion, L.W., Shuler, M.L., 1998. Growth kinetics of *Pseudomonas putida* G7 on naphthalene and occurrence of naphthalene toxicity during nutrient deprivation. Biotechnol. Bioeng. 59, 587–594.

Andersen, R.G., Booth, E.C., Marr, L.C., Widdowson, M.A., Novak, J.T., 2008. Volatilization and biodegradation of naphthalene in the vadose zone impacted by phytoremediation. Environ. Sci. Technol. 42, 2575–2581.

Batterman, S., Padmanabham, I., Milne, P., 1996. Effective gas-phase diffusion coefficients in soils at varying water content measured using a one-flow sorbent based technique. Environ. Sci. Technol. 30, 770–778.

Chapelle, F.H., 1999. Bioremediation of petroleum hydrocarbon-contaminated ground water: the perspectives of history and hydrology. Ground Water 37, 122–132.

Choi, J.W., Smith, J.A., 2005. Geoenvironmental factors affecting organic vapor advection and diffusion fluxes from the unsaturated zone to the atmosphere under natural conditions. Environ. Eng. Sci. 22, 95–108.

Christophersen, M., Broholm, M.M., Mosbaek, H., Karapanagioti, H.K., Burganos, V.N., Kjeldsen, P., 2005. Transport of hydrocarbons from an emplaced fuel source experiment in the vadose zone at airbase Vaerlose, Denmark. J. Contam. Hydrol. 81, 1–33.

De Biase, C., Reger, D., Schmidt, A., Jechalke, S., Reiche, N., Martinez-Lavanchy, P.M., van Afferden, M., Mayer, U., Oswald, S.E., Thullner, M., Treatment of volatile organic contaminants in a vertical flow filter: relevance of different removal processes. Ecol. Eng. (submitted).

De Kempeneer, L., Sercu, B., Vanbrabant, W., Van Langenhove, H., Verstraete, W., 2004. Bioaugmentation of the phyllosphere for the removal of toluene from indoor air. Appl. Microbiol. Biotechnol. 64, 284–288.

Dechesne, A., Owsianiak, M., Bazire, A., Grundmann, G.L., Binning, P.J., Smets, B.F., 2010. Biodegradation in a partially saturated sand matrix: compounding effects of water content, bacterial spatial distribution, and motility. Environ. Sci. Technol. 44, 2386–2392.

Dunn, N.W., Gunsalus, I.C., 1973. Transmisible plasmid coding early enzymes of oxidation in *Pseudomonas putida*. J. Bacteriol. 114, 974–979.

Eke, P.E., Scholz, M., 2008. Benzene removal with vertical-flow constructed treatment wetlands. J. Chem. Technol. Biotechnol. 83, 55–63.

Filonov, A.E., Duetz, W.A., Karpov, A.V., Gaiazov, R.R., Kosheleva, I.A., Breure, A.M., Filonova, I.F., vanAndel, J.G., Boronin, A.M., 1997. Competition of plasmid-hearing *Pseudomonas putida* strains catabolizing naphthalene via various pathways in chemostat culture. Appl. Microbiol. Biotechnol. 48, 493–498.

Franzmann, P.D., Zappia, L.R., Power, T.R., Davis, G.B., Patterson, B.M., 1999. Microbial mineralisation of benzene and characterisation of microbial biomass in soil above hydrocarbon-contaminated groundwater. Fems Microbiol. Ecol. 30, 67–76.

Harms, H., 1996. Bacterial growth on distant naphthalene diffusing through water, air, water-saturated, and unsaturated porous media. Appl. Environ. Microbiol. 62, 2286–2293.

Hohener, P., Dakhel, N., Christophersen, M., Broholm, M., Kjeldsen, P., 2006. Biodegradation of hydrocarbons vapors: comparison of laboratory studies and field investigations in the vadose zone at the emplaced fuel source experiment, Airbase Vaerlose, Denmark. J. Contam. Hydro.l 88, 337–358.

Holden, P.A., Fierer, N., 2005. Microbial processes in the vadose zone. Vadose Zone J. 4, 1–21.

Johnsen, A.R., Wick, L.Y., Harms, H., 2005. Principles of microbial PAH degradation. Environ. Pollut. 133, 71–84.

Knight, R.L., Kadlec, R.H., Ohlendorf, H.M., 1999. The use of treatment wetlands for petroleum industry effluents. Environ. Sci. Technol. 33, 973–980.

Konopka, A., Turco, R., 1991. Biodegradation of organic compounds in vadose zone and aquifer sediments. Appl. Environ. Microbiol. 57, 2260–2268.

Kristensen, A.H., Henriksen, K., Mortensen, L., Scow, K.M., Moldrup, P., 2010. Soil physical constraints on intrinsic biodegradation of petroleum vapors in a layered subsurface. Vadose Zone J. 9, 137–147.

Luthy, R.G., Aiken, G.R., Brusseau, M.L., Cunningham, S.D., Gschwend, P.M., Pignatello, J.J., Reinhard, M., Traina, S.J., Weber, W.J., Westall, J.C., 1997. Sequestration of hydrophobic organic contaminants by geosorbents. Environ. Sci. Technol. 31, 3341–3347.

Marr, L.C., Booth, E.C., Andersen, R.G., Widdowson, M.A., Novak, J.T., 2006. Direct volatilization of naphthalene to the atmosphere at a phytoremediation site. Environ. Sci. Technol. 40, 5560–5566.

Marx, R.B., Aitken, M.D., 1999. Quantification of chemotaxis to naphthalene by *Pseudomonas putida* G7. Appl. Environ. Microbiol. 65, 2847–2852.

Mudliar, S., Giri, B., Padoley, K., Satpute, D., Dixit, R., Bhatt, P., Pandey, R., Juwarkar, A., Vaidya, A., 2010. Bioreactors for treatment of VOCs and odours - a review. J. Environ. Manage. 91, 1039–1054.

Salmon, C., Crabos, J.L., Sambuco, J.P., Bessiere, J.M., Basseres, A., Caumette, P., Baccou, J.C., 1998. Artificial wetland performances in the purification efficiency of hydrocarbon wastewater. Water Air Soil Pollut. 104, 313–329.

Sandhu, A., Halverson, L.J., Beattie, G.A., 2007. Bacterial degradation of airborne phenol in the phyllosphere. Environ. Microbiol. 9, 383–392.

Schwarz, F.P., 1977. Determination of temperature-dependence of solubilities of polycyclic aromatic-hydrocarbons in aqueous-solutions by a fluorescence method. J. Chem. Eng. Data 22, 273–277.

Schwarzenbach, R.P., Gschwend, P.M., Imboden, D.M., 2003. Environmental Organic Chemistry, first ed. John Wiley & Sons, Inc., Hoboken (NJ).

Semple, K.T., Doick, K.J., Wick, L.Y., Harms, H., 2007. Microbial interactions with organic contaminants in soil: definitions, processes and measurement. Environ. Poll 150, 166–176.

Squillace, P.J., Moran, M.J., Price, C.V., 2004. VOCs in shallow groundwater in new residential/commercial areas of the United States. Environ. Sci. Technol. 38, 5327–5338.

Tang, X.Q., Eke, P.E., Scholz, M., Huang, S.L., 2009. Processes impacting on benzene removal in vertical-flow constructed wetlands. Bioresour. Technol. 100, 227–234.

Waight, K., Pinyakong, O., Luepromchai, E., 2007. Degradation of phenanthrene on plant leaves by phyllosphere bacteria. J. Gen. Appl. Microbiol. 53, 265–272.

Wallace, S., Kadlec, R., 2005. BTEX degradation in a cold-climate wetland system. Water Sci. Technol. 51, 165–171.

Wang, G., Or, D., 2010. Aqueous films limit bacterial cell motility and colony expansion on partially saturated rough surfaces. Environ. Microbiol. 12, 1363–1373.

Whitman, W.B., Coleman, D.C., Wiebe, W.J., 1998. Prokaryotes: the unseen majority. PNAS 95, 6578–6583.

Wick, L.Y., Colangelo, T., Harms, H., 2001. Kinetics of mass transfer-limited bacterial growth on solid PAHs. Environ. Sci. Technol. 35, 354–361.

Young, I.M., Crawford, J.W., 2004. Interactions and self-organization in the soil-microbe complex. Science 304, 1634–1637.

Walking the tightrope of bioavailability: Growth dynamics of PAH degraders on vapour-phase PAH

Joanna Hanzel, Martin Thullner, Hauke Harms, Lukas Y. Wick*

UFZ – Helmholtz Centre for Environmental Research, Department of Environmental Microbiology, 04318 Leipzig. Germany

Running title: Walking the tightrope of bioavailability

Intended for: Microbial Biotechnology

* Corresponding author: Mailing address: Helmholtz Centre for Environmental Research UFZ. Department of Environmental Microbiology, Permoserstrasse 15. 04318 Leipzig, Germany. Phone: +49 341 235 1316, Fax: +49 341 235 1351, E-mail: lukas.wick@ufz.de.

Abstract

Microbial contaminant degradation may either result in the utilization of the compound for growth or act as a protective mechanism against its toxicity. Bioavailability of contaminants for nutrition and toxicity has opposite consequences which may have resulted in quite different bacterial adaptation mechanisms; these may particularly interfere when a growth substrate causes toxicity at high bioavailability. Recently, it has been demonstrated that a high bioavailability of vapour-phase naphthalene (NAPH) leads to chemotactic movement of NAPH-degrading *Pseudomonas putida* (NAH7) G7 away from the NAPH source. To investigate the balance of toxic defense and substrate utilization, we tested the influence of the cell density on surface-associated growth of strain PpG7 at different positions in vapour-phase NAPH gradients. Controlled microcosm experiments revealed that high cell densities increased growth rates close (< 2 cm) to the NAPH source, whereas competition for NAPH decreased the growth rates at larger distances despite the high gas phase diffusivity of NAPH. At larger distance, less microbial biomass was likewise sustained by the vapour-phase NAPH. Such varying growth kinetics is explained by a combination of bioavailability restrictions and NAPH-based inhibition. To account for this balance, a novel, integrated 'Best-equation' describing microbial growth influenced by substrate availability and inhibition is presented.

Key words: Best equation, biodegradation, bioavailability, inhibition, naphthalene, vapour-phase, *Pseudomonas putida* (NAH7) G7.

Introduction

Effective biodegradation of soil contaminants requires both adequate environmental conditions and a suitable availability of the compounds to the degrading organisms. The average bulk concentration of a contaminant, however, is not an appropriate measure for its availability, since bioavailability needs to be seen as the dynamic interplay of the mass transfer (flux) of a compound to a microbial cell and its metabolic potential to degrade it (Bosma et al., 1997): At high transfer rates, degradation hence is predominantly controlled by the metabolic potential of the bacteria, whereas low transfer rates may limit both the microbial growth rates and the amount of biomass sustained. Reversibly, the bioavailability may also become limiting when the catabolic capacity of a microbial biomass exceeds the capacity of its environment to deliver it as often can be found in soil environments (Johnsen et al., 2005). The bioavailability of a compound can adequately be quantified by the bioavailability number (*Bn*) which takes into account the mass transfer of a compound to microbial cells and the intrinsic activity of these cells to transform it (Bosma et al., 1997). For the assumed situation of steady-state (i.e. when the transport flux and the rate of degradation of the substrate equal each other) the so-called Best Equation (Best, 1955) describes substrate uptake in relation to the contaminant mass transfer potential in the environment surrounding a cell; i.e. it evaluates the relative physical and biological contributions to the overall degradation rate.

Microbial contaminant degradation may either result in the utilization of the contaminant for growth or contribute to the protection against contaminant toxicity depending on its flux to individual cells. The bioavailability of a compund hence is 'Janus-faced', i.e. bioavailabilty is essential and likely promoted by the target organism for assimilative uptake, whereas a too high bioavailabilty of compounds may lead to toxic effects and provokes avoidance strategies of target organisms. Although the bioaccessible compound pool for both effects may be identical the exposure of organisms to environmental chemicals hence has opposite consequences and may lead to quite different bacterial adaptation mechanisms depending on

the compounds bioavailability. These may interfere, when a growth substrate causes toxicity at high bioavailability, leading to a tightrope walk that is often overlooked in bioremediation studies where one tends to assume that effective pollutant-utilizing bacteria tolerate any exposure to these substrates. Intracellular NAPH, for instance, has been reported to be toxic to *Pseudomonas putida* (NAH7) G7 unless it is metabolized (Ahn et al., 1998), e.g. under oxygen-, nitrogen- or nutrient limiting conditions (Ahn et al., 1998; Park et al., 2004; Pumphrey and Madsen, 2007). According to Pumphrey et al. (2007) likely hypotheses for explaining the inhibitory effect of NAPH are: (i) NAPH itself is directly inhibitory or toxic when present at high concentrations; (ii) the NAPH metabolism leads to the accumulation of toxic or inhibitory metabolites (or reactive oxygen species (George and Hay, 2011)) at elevated NAPH bioavailability to the cells; or (iii) both NAPH and its metabolites cause growth inhibition. Recently, it also has been demonstrated in controlled laboratory systems that the high bioavailability of vapour-phase NAPH induced negative chemotaxis, i.e. a down-gradient movement of NAPH-degrading *Pseudomonas putida* (NAH7) G7 away from a solid NAPH point source. Surprisingly this occurred even at gaseous concentrations lower than aqueous concentrations that induced chemoattraction (Hanzel et al., 2010).

Knowledge of how and where microbial populations develop in vapour phase-substrate gradients is of great importance for a better understanding of the degradation of volatile organic compounds (VOC), as found for instance in the vadose zone of terrestrial environments. The goal of the study was (i) to experimentally elucidate the tightrope walk of substrate bioavailability for assimilative growth and growth inhibition of strain PpG7 in vapour-phase NAPH gradients and (ii) to qualitatively reflect microbial growth in a novel kinetic model combining assimilative growth driven by substrate (bio-)availability and inhibition/toxicity.

Results

Growth on vapour-phase NAPH

Growth of NAPH-degrading strain *Pseudomonas putida* (NAH7) G7 on the surface of agar exposed to vapour-phase NAPH was studied in Petri dish microcosms with an emphasis on influences of cell density and distribution. As illustrated in Fig. 1A, all microcosms contained a central minimal medium agar (MMA) disk (A) and/or concentric MMA rings of varying diameters (B, C, D), which were positioned at various distances from the central NAPH point source. Two different inoculation patterns were tested: In a *'high competition'* scenario (HCS) (Fig. 1B) all agar patches (A-D) were simultaneously present and homogeneously inoculated with 4.5×10^{8} cfu cm^{-2}, whereas in *'low competition'* scenarios (LCS) each of the inoculated patches (A, B, C or D) was placed in a separate Petri dish (Fig. 1C). Similar to previous studies vapour-phase NAPH emanating from the point source led to cm-scale vapour-phase NAPH gradients (cf.: (Hanzel et al., 2010; Hanzel et al., 2011) as expressed by distinct biomass distribution patterns after 8, 20, 30, 48 and 72 hours of incubation (Fig. 2). The biomass was approximated by colony forming unit (cfu) analysis on LB-agar after sacrificing the individual patches. The cfu data reveal that higher total numbers of widely distributed cells in the HCS facilitated growth close to the NAPH source (A and B) with three times higher cell numbers per cm^{-2} than at more distant locations (C and D). In the LCS, growth on patch A was at least 60% lower than in the HCS at all sampling times. Lower biomass than in the HCS was detected after 8 h on all patches (A-D) in the LCS (Fig. 2). With increasing cell numbers and NAPH consumption in the LCS, the biomass in position B became similar in both scenarios and even exceeded that in the HCS by up to 60 % on patches C and D.

An analysis of average growth rates until 72 h further illustrates these effects (Fig. 3). The different inoculum pattern in the HCS led to an about two-fold accelerated growth rate of the

cells on patch A, yet kept the growth rate of the cells on patch B uninfluenced, or reduced it by about 60% at more distant locations from the NAPH source (patches C and D; Fig. 3).

Kinetic description of bacterial growth influenced by substrate toxicity and competition

To explain the observed growth patterns in terms of microbial growth kinetics, we modified an established concept for growth under bioavailability restrictions so that it accounts for toxic growth inhibition. When transport flux and the rate of substrate degradation equal each other (i.e. at quasi-steady state conditions) the so-called Best Equation (Best, 1955) describes the relative physical and biological contributions to the overall degradation rate. In the following, an extended version of this concept is proposed which allows for the description of microbial growth in a domain where substrate consumption for assimilation and for detoxification occurs. The dynamics of bacterial substrate degradation is commonly expressed using Michaelis-Menten kinetics (Nelson and Cox, 2004):

$$r_{\mathrm{deg}} = k_m \cdot \frac{c_b}{K_s + c_b} \qquad (1)$$

with k_m as maximum degradation rate per unit biomass, K_s as Michaelis-Menten constant, and c_b as the bioavailable concentration of the substrate. If the bioavailable concentration differs from the total bulk concentration c_{tot} of the substrate, i.e. if bioavailability restrictions need to be considered, the link between these two concentrations can be expressed using a linear exchange model (Hesse et al., 2010; Baveye and Valocchi, 1989; Button, 1991; Thullner et al., 2007) describing the exchange rate r_{ex}:

$$r_{ex} = \lambda \cdot \left(c_{tot} - c_b\right) \qquad (2)$$

with λ as exchange rate parameter influenced by the mass transfer processes controlling substrate bioavailability. Typically, λ increases with the mobility (e.g., diffusion coefficient) of the substrate and decreases with the distance to be covered by the mass transfer process. When rates for mass flux and substrate degradation equal each other and assuming (quasi-)

steady state conditions at the micro scale ($r_{deg} = r_{ex}$), Eq. 1 and 2 can be combined to the so-called Best Equation (Best, 1955; Bosma et al., 1997; Simoni et al., 2001),

$$r_{Best} = \frac{K_s \lambda}{2} \cdot \left(1 + \frac{c_{tot}}{K_s} + \frac{k_m}{K_s \lambda}\right) \cdot \left(1 - \sqrt{1 - \frac{4 \frac{c_{tot}}{K_s} \frac{k_m}{K_s \lambda}}{\left(1 + \frac{c_{tot}}{K_s} + \frac{k_k}{K_s \lambda}\right)^2}}\right) \quad (3)$$

which allows expressing the degradation rate as a function of the bulk concentration in the presence of bioavailability restrictions. The smaller the bulk concentration and the smaller the bioavailability number $Bn = K_s\lambda/k_m$ the higher the influence of bioavailability restriction on the degradation rate. The above concept is valid and established if the substrate is the only rate limiting substance and if high substrate concentrations have no inhibitory effects on the degradation rate. To address the latter – as necessary for the present study – the simple Michaelis-Menten kinetics (Eq. 1) needs to be expanded. From the different approaches proposed to include such inhibition terms into growth rate expressions we here discuss an example:

$$r_{\deg} = k_m \cdot \frac{c_b}{K_s + c_b} \cdot \frac{K_i}{c_b + K_i} \quad (4)$$

proposed for non-competitive inhibition (Lehninger, 2004), with K_i as inhibition constant. Eq. 4 is also commonly used to address inhibition effects in reactive transport simulations (Thullner et al., 2007). To combine this expanded rate expression with bioavailability restrictions (Eq. 2) in analogy to the above derivation of the Best Equation leads to bioavailable concentrations fulfilling the equation

$$c_b^3 + \left(1 + c_{tot} + K_i\right) \cdot c_b^2 + \left(K_s \cdot K_i + \frac{K_i \cdot k_m}{\lambda} - \left(K_i + K_s\right) \cdot c_{wt}\right) \cdot c_b - K_s \cdot K_i \cdot c_{tot} = 0 \quad (5)$$

It is not possible to express the general solution of Eq. 5 and the resulting degradation rate in a closed form (which would be an expanded Best Equation considering inhibition effects, too). However, for specific parameter values a numerical solution for c_b can be obtained from Eq.

5, which can then be used to calculate rate values using Eq. 2 or 4. The link between the growth rate of a bacterial species B and the above presented degradation rates is the given assuming a constant yield factor *Y*:

$$\frac{\partial B}{\partial t} = Y \cdot r_{\text{deg}} \cdot B \qquad (6)$$

which in the simplest case (Michaelis-Menten kinetics, no bioavailability restriction, no inhibition effects) results in the established Monod-type growth kinetics (Monod, 1949; Thullner et al., 2007), or in an extended version of it considering bioavailability and substrate inhibition.

The theoretically predicted influence of substrate inhibition on degradation rates is shown for an arbitrary but representative example (Fig. 4A) to demonstrate the differences between the considered rate expressions (Eq. 1 in the absence of inhibition effects, and Eq. 4 in the presence of inhibition effects; cf. Material and Methods). Omission of inhibition effects results in a rate monotonously increasing with substrate concentration. In turn, when consideration of inhibition effects leads to predicted maximum rates at a concentration of $c_b = (K_i \cdot K_s)^{1/2}$. At concentrations of $c_b < (K_i \cdot K_s)^{1/2}$ the rate is decreasing due to substrate limitation while higher concentrations of $c_b > (K_i \cdot K_s)^{1/2}$ lead to a rate decrease due to substrate inhibition. Similar observations were made using alternative expressions suggested in the literature (e.g., (Mulchandani and Luong, 1989)) to describe rate inhibition effects (results not shown). Fig. 4B relates the influence of inhibition to changes of the substrate degradation rates (and hence of bacterial growth rates) at varying substrate bioavailability conditions: In the absence of inhibition degradation rates are highest when the substrate is highly bioavailable (i.e. lower values for *1/Bn*), whereas reduction of substrate bioavailability (e.g., due to increased distance or increased competition as in the LCS or HCS) leads to concomitant decrease of the degradation rates. Interestingly, the degradation rates at all bioavailability conditions (values of *1/Bn*) are lower in the presence of inhibition (Fig. 4A & B). While at low bioavailability

inhibition effects remain small, differences grow significantly larger at high bioavailability conditions. Figure 4B further reveals that inhibition leads to highest degradation rates at intermediate substrate bioavailability conditions representing a compromise of moderate inhibition and sufficient substrate supply to a metabolically active cell.

Discussion

Bacterial growth influenced by substrate toxicity and competition

In an attempt to evaluate the microbial utilization of a potentially inhibitory vapour-phase substrate, we tested influences of initial biomass and its location relative to an NAPH point source. Our data reveal that growth rates of *P. putida* depended on their distance to the NAPH source and were influenced by the spatial distribution and abundance of catabolically-active cells in the microcosm. This is explained by the formation of cm-scale, vapour-phase NAPH-gradients forming around a NAPH point source, which have previously been demonstrated in similar laboratory test tracks despite of the high diffusivity of NAPH in air (Hanzel et al., 2010; Hanzel et al., 2011). In these studies the volatilization of NAPH from a solid spot source resulted in distinct gradients in the headspace of a Petri dish with average vapor-phase NAPH concentrations near the source close to the equilibrium concentration ($\approx 3 \times 10^{-7}$ mol L^{-1}) and an approximately 3-fold drop along a Petri dish's transect (Hanzel et al 2010). Petri dishes hence emerge as ideal experimental reactors to study the spatio-temporal interplay of varying NAPH bioavailability and microbial growth. Our data are in good agreement with previous studies considering bioavailability as a dynamic process influenced by the rate of physical mass transfer to microbial cells relative to their intrinsic catabolic activity (e.g., Bosma et al., 1997; Wick et al., 2001). As convection is apparently absent in our closed microcosms, the NAPH flux is best described by Fick's first law of diffusion (Schwarzenbach et al., 2003) implying that bioavailability of vapour-phase NAPH decreases with distance as has been demonstrated in a recent study (Hanzel et al 2011). The higher amount of bacterial

cells present in the HCS leads to a reduced per cell bioavailability of NAPH compared to the LCS. The complex effect of additional biomass results from the fact that additional NAPH consumption reduces toxicity under conditions of high bioavailability, while it consumes sought-after substrate under conditions of low biodiversity. It thus either buffers toxic effects by removing vapour-phase NAPH or intensifies the competition for substrate. Figs. 2 and 3 indicate that bacteria located close to the NAPH source benefit from the buffer effect of additional biomass, while those located at larger distances suffer from additional competitors. The position of the transition zone, where buffer and competition effects compensate each other, depends on the overall degradation capacity in the system. With ongoing growth, it moves closer to the NAPH source, as can be seen from intersecting biomass curves of positions B, C and D (Fig. 2). In earlier studies, the complex interplay between toxic and nutrition effects were not seen, since NAPH bioavailability was too low to exert toxicity (Harms, 1996; Hanzel et al., 2011).

Kinetic description of bacterial growth influenced by substrate toxicity and competition

Although Fig. 4 reflects an arbitrary example, the predicted relation between substrate inhibited degradation/growth rates and bioavailability is also suitable to explain the observations made in this study. At the initial stage of the experiment ($t < 8$ hours) cell concentrations on the individual patches do not result in bioavailability restrictions. Substrate bioavailability is similar all over the system and competition effects are rather moderate: The resulting growth rate distribution in the LCS showed moderate variability with distance to the NAPH spot source with rates accounting for 35-55% of the rates found at higher competition in HCS at all sampling locations (data not shown). We here consider this initial situation to be represented by the high bioavailability region in Fig. 4B (i.e. low values for *1/Bn*) where the lower substrate bioavailability to individual cells in HCS has an apparent positive impact on microbial rates. At a later stage of the experiment ($t > 8$ hours) spatial gradients and

differences between HCS and LCS in the experimental growth rates are addressed to the non-monotonous dependency of the substrate inhibited growth rate on bioavailability. Figure 3 reflects average growth rates after 72 hours for HCS and LCS. In the HCS continuous decrease of the growth rates is observed at increasing distances from the NAPH source. In contrast to LCS at close distance to the NAPH source however, the high competition for NAPH significantly favours bacterial growth (i.e. the bioavailability of NAPH to the PpG7 cells still appears to be on the left-hand side of the optimum as shown in Fig. 4B). At more distant locations, however, distance to the NAPH source had negative effect on NAPH bioavailability. This is reflected by decreased growth rates of strain PpG7 and, hence, proposes a bioavailability scenario as represented by the right-hand side of the optimum in Fig. 4B. Not surprisingly, such distance effect was amplified in the HCS, where competition led to limited NAPH bioavailability and subsequent lowered growth rates strain PpG7 (Fig. 3). It appears that increasing cell density led to rising competition for the NAPH, higher distance-dependant limitations of NAPH bioavailability and lowered growth rates in the system (i.e., a situation as described by the optimum (patches A & B) or the right-hand side of the optimum in Fig. 4B (patches C & D)).

Ecological relevance

Our results suggest that vapour-phase contaminant gradients may inhibit growth of pollutant-degrading bacteria unless sufficient substrate consumption is present. This might be of a great importance for remediation of VOCs-contaminated systems like the vadose zone of terrestrial environments where degrading bacteria present at air-water or air-solid interfaces (Schäfer et al., 1998) are exposed to high amounts of contaminants vapours. The data secondly underline the importance of high active biomass and concomitant effective reduction of their exposure to inhibitory (toxic) substrates in order to create environments favourable for survival, which may influence the exposure dynamics and ecology of entire microbial communities and hence

actively shape environments beneficial for enhanced biodegradation. Microbial toxicity tests hence should generally take special focus on a contaminant's bioavailability and bioaccessibility in a give environment i.e. both on its chemodynamics and on the adaptative mechanisms employed by microorganisms to avoid and/or transform toxic compounds to levels suitable for effective biotransformation.

Material and Methods

Bacteria and culture conditions.

The aerobic NAPH-degrading soil bacterium *Pseudomonas putida* PpG7 (NAH7) (Dunn and Gunsalus, 1973) was grown at 25°C in 100-mL Erlenmeyer flasks containing 50 mL of liquid mineral medium (MM) on a gyratory shaker (150 rpm) (Wick et al., 2001) in the presence of 1.5 g L^{-1} of solid NAPH (> 98%, Fluka; crystals as obtained by the provider). Inocula used for the growth experiments were harvested after 48 hours of growth in the late exponential phase, centrifuged, washed twice with MM and re-suspended in MM to obtain final bacterial suspension with an optical density at 600 nm (OD_{600}) of ca. 0.3 corresponding to ca. 3×10^7 cfu mL^{-1}. Cells were quantified as colony forming units (cfu) after 3 days of incubation at room temperature on Luria Broth agar (2% w/v) using an automated spiral plating and cell counting system (Meintrup GmbH). Mineral medium agar (MMA; 1.5 % (w/v)) was used for growth experiments as detailed below.

Growth of P. putida (NAH7) G7 on vapour-phase NAPH.

On the basis of former data (Hanzel et al., 2010) growth experiments were performed at room temperature in Teflon tape-sealed, upside-down positioned Petri dishes (diameter: 9 cm) containing 20 mg NAPH as sole carbon and energy source. NAPH was centrally placed in the lid (Fig. 1A) with solid NAPH being visible until the end of the experiment. As illustrated in

Fig.1 the Petri dishes contained a disk-shaped central MMA disk (patch A; diameter 0.5 cm) and/or three concentric, ring-shaped MMA patches (width: 0.5 cm) of increasing outer diameters (i.e. 3.4, 6.2, and 9 cm for patches B, C, D) corresponding to average distances of 1.1, 2.1, 3.3 and 4.9 cm from the NAPH point source. The total surface areas of patches A, B, C, and D were 0.2 cm^2, 4.2 cm^2, 8.5 cm^2, and 12.7 cm^2 and all patches were inoculated at a density of ca. 4.5×10^8 cfu cm^{-2} (i.e. using 5 µL of cell suspension of an $OD_{578} \approx 0.3$ per cm^{-2}). Two growth scenarios resulting in differential competition for the substrate were tested. In a *'high competition experiments'* all four agar patches were placed in the same Petri dish and homogeneously inoculated whereas in the *'low competition experiments'* each patch was placed in a separate Petri dish and inoculated (Fig. 1B). Growth of PpG7 bacteria on vapour-phase NAPH was approximated by cfu analysis after 0, 8, 20, 30, 48 and 72 hours (t_0, t_8, t_{20}, t_{30}, t_{48}, t_{72}) of incubation. Therefore, the entire patch A or four equally-sized and equally-distributed segments (surface area: 0.75 cm^2) of each of the patches B-D were harvested. Extracted bacteria were suspended in 9-mL of PBS-buffer, vortexed for 1 min, sonicated (2×1 min with a break of 30 sec) and spread on LB plates. All experiments were performed in triplicate. Colony forming units (cfu) shown in Figs. 2-4 represent cfu averages and standard errors from three independent experiments as outlined in Fig. 1. The cfu of all platings were calculated using two different dilutions calculated according to: $cfu_{total} = ((cfu_{\text{at lower dilution}}) + (cfu_{\text{at higher dilution}}/10))/1.1$ (Süßmuth et al. 1987).

Acknowledgements: Funding by the European grant MC-EST 20984 (RAISEBIO) is greatly acknowledged. Further funding was provided by the Helmholtz Association via the program topic "CITE-Chemicals in the Environment", and grant VG-NG-338 (GReaT MoDE). The authors wish to thank J. Reichenbach, O. Scheer and B. Würz for skilled technical help.

References

Ahn, I.S., Ghiorse, W.C., Lion, L.W., and Shuler, M.L. (1998) Growth kinetics of *Pseudomonas putida* G7 on naphthalene and occurrence of naphthalene toxicity during nutrient deprivation. *Biotechnol Bioeng* **59**: 587-594.

Baveye, P., and Valocchi, A. (1989) An evaluation of mathematical-models of the transport of biologically reacting solutes in saturated soils and aquifers. *Water Resour Res* **25**: 1413-1421.

Best, J.B. (1955) The interference of intracellular enzymatic properties from kinetic data obtained on living cells. I. Some kinetic considerations regarding an enzyme enclosed by a diffusion barrier. *J Cell Comp Physiol* **46**: 1-27.

Bosma, T.N.P., Middeldorp, P.J.M., Schraa, G., and Zehnder, A.J.B. (1997) Mass transfer limitation of biotransformation: Quantifying bioavailability. *Environ Sci Technol* **31**: 248-252.

Button, D.K. (1991) Biochemical basis for whole-cell uptake kinetics: Specific affinity, oligotrophic capacity, and the meaning of the Michaelis constant. *App Environ Microbiol* 57: 2033-2038.

Cerniglia, C.E. (1992) Biodegradation of polycyclic aromatic hydrocarbons. *Biodegrad* **3**: 351-368.

Dunn, N.W., and Gunsalus, I.C. (1973) Transmisible plasmid coding early enzymes of oxidation in *Pseudomonas putida*. *J Bacteriol* **114**: 974-979.

George, K.W. and Hay, A.G. (2011) Bacterial strategies for growth on aromatic compounds. Adv. Appl. Microbiol. **74**: 2-25.

Hanzel, J., Harms, H., and Wick, L.Y. (2010) Bacterial chemotaxis along vapor-phase gradients of naphthalene *Environ Sci Technol* **44**: 9304-9310.

Hanzel, J., Thullner, M., Harms, H., and Wick, L.Y. (2011) Microbial growth with vapor-phase substrate. *Environ Poll* **159**: 858-864.

Harms, H. (1996) Bacterial growth on distant naphthalene diffusing through water, air, water-saturated, and unsaturated porous media. *Appl Environ Microbiol* **62**: 2286-2293.

Hesse, F., Harms, H., Attinger, S., and Thullner, M. (2010) Linear exchange model for the description of mass transfer limited bioavailability at the pore scale. *Environ Sci Technol* **44**: 2064-2071.

Johnsen, A.R., Wick, L.Y., and Harms, H. (2005) Principles of microbial PAH degradation. *Environ Poll* **133**: 71-84.

Monod, J. (1949) The growth of bacterial cultures. *Ann Rev Microbiol* **3**: 371-394.

Mulchandani, A., and Luong, J.H.T. (1989) Microbial inhibition-kinetics revisited. *Enzyme Microb Technol* **11**: 66-73.

Nelson, D.L., and Cox, M.M. (2004) *Lehninger Principles of Biochemistry*: W. H. Freeman.

Park, W., Jeon, C.O., Cadillo, H., DeRito, C., and Madsen, E.L. (2004) Survival of naphthalene-degrading Pseudomonas putida NCIB 9816-4 in naphthalene-amended soils: toxicity of naphthalene and its metabolites. *Appl Microbiol Biotechnol* **64**: 429-435.

Pumphrey, G.M., and Madsen, E.L. (2007) Naphthalene metabolism and growth inhibition by naphthalene in *Polaromonas naphthalenivorans* strain CJ2. *Microbiology-SGM* **153**: 3730-3738.

Schäfer, A., Harms, H., and Zehnder, A.J.B. (1998) Bacterial accumulation at the air-water interface. *Environ Sci Technol* **32**: 3704-3712.

Schwarzenbach, R.P., Gschwend, P.M., and Imboden, D.M. (2003) *Environmental Organic Chemistry*. Hoboken (NJ): John Wiley & Sons, Inc.

Simoni, S.F., Schäfer, A., Harms, H., and Zehnder, A.J.B. (2001) Factors affecting mass transfer limited biodegradation in saturated porous media. *J Contam Hydrol* **50**: 99-120.

Süssmuth, R., Eberspächer, J., Haag, R., and Springer, W. (1987) *Biochemisch-mikrobiologisches Praktikum*. Stuttgart, New York: Thieme.

Thullner, M., Regnier, P., and Van Cappellen, P. (2007) Modeling microbially induced carbon degradation in redox-stratified subsurface environments: Concepts and open questions. *Geomicrobiol J* **24**: 139-155.

Wick, L.Y., Colangelo, T., and Harms, H. (2001) Kinetics of mass transfer-limited bacterial growth on solid PAHs. *Environ Sci Technol* **35**: 354-361.

Figure Legends

Figure 1. Cross section (A) and birds view (B) of the experimental setup for studying growth of NAPH-degrading surface-associated bacteria *Pseudomonas putida* (NAH7) G7 on vapour-phase NAPH of variable bioavailability. The numbers in panel A refer to the average distances in cm of the patches sampled to the solid NAPH. Panel B shows the experimental scenario to assess for increased inter-microbial competition ('high competition', sampling locations are symbolized by the light-colored areas), whereas panel C depicts the four scenarios to mimic lower competition scenarios ('low competition, sampling locations are symbolized by the light-colored areas).

Figure 2. Spatio-temporal growth of MMA-surface associated *P. putida* (NAH7) G7 on vapour-phase NAPH at different distances (patch A, B, C, and D, i.e. at 1.1, 2.1, 3.3, and 4.9 cm) from the NAPH spot source at conditions mimicking high (diamonds) and low (squares) microbial competition. Growth is reflected by cfu that are surface-area normalized and represent averages and standard errors (1 sigma) from four locations taken of MMA patches obtained from three independent experiments.

Figure 3. Spatially resolved growth rates *P. putida* (NAH7) G7 during 72 h of growth on vapour-phase NAPH emanating from a spot source. High and low competition experiments are represented by diamonds and squares, respectively. Data represent averages and standard errors from three independent experiments.

Figure 4. Influence of substrate inhibition on microbial degradation (and growth) rates. Panel A) Rate dependency on bioavailable substrate concentration considering the presence (Eq. 4) and absence of substrate inhibition effects (Eq. 1) assuming $K_i=3K_s$. Panel B) Rate

dependency on bioavailable substrate concentration as expressed by the bioavailability number *Bn* considering the presence (Eq. 5 combined with Eq. 2 or 4) and absence (Eq. 3) of substrate inhibition effects assuming $c_{tot}=10K_s$ and $K_i=3K_s$. Note that high bioavailability is represented by low values of *1/Bn*.

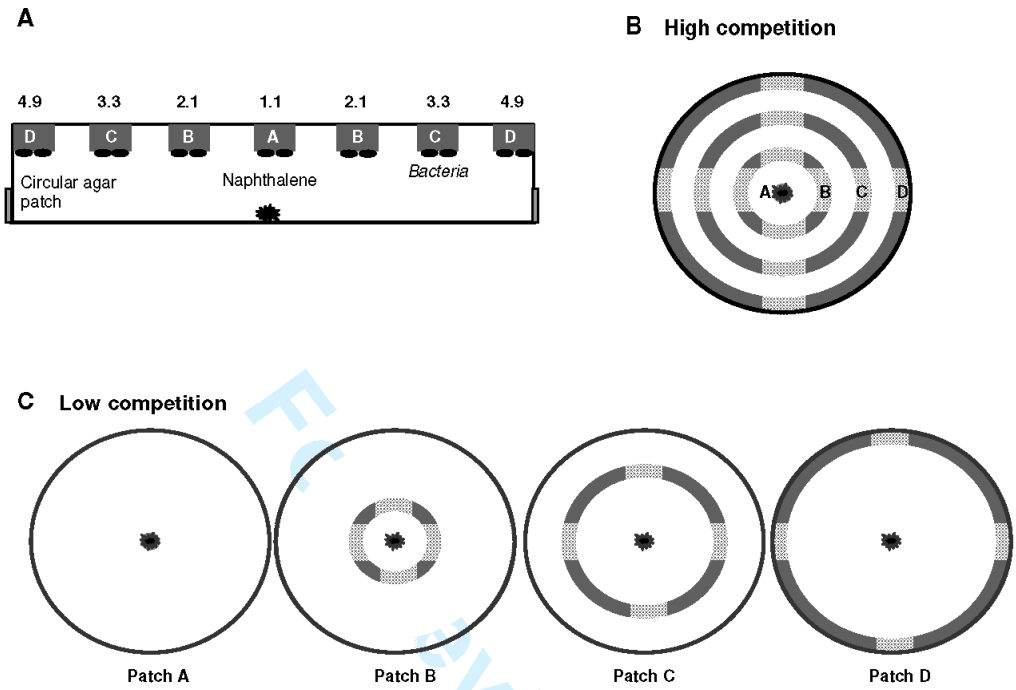

Figure 1

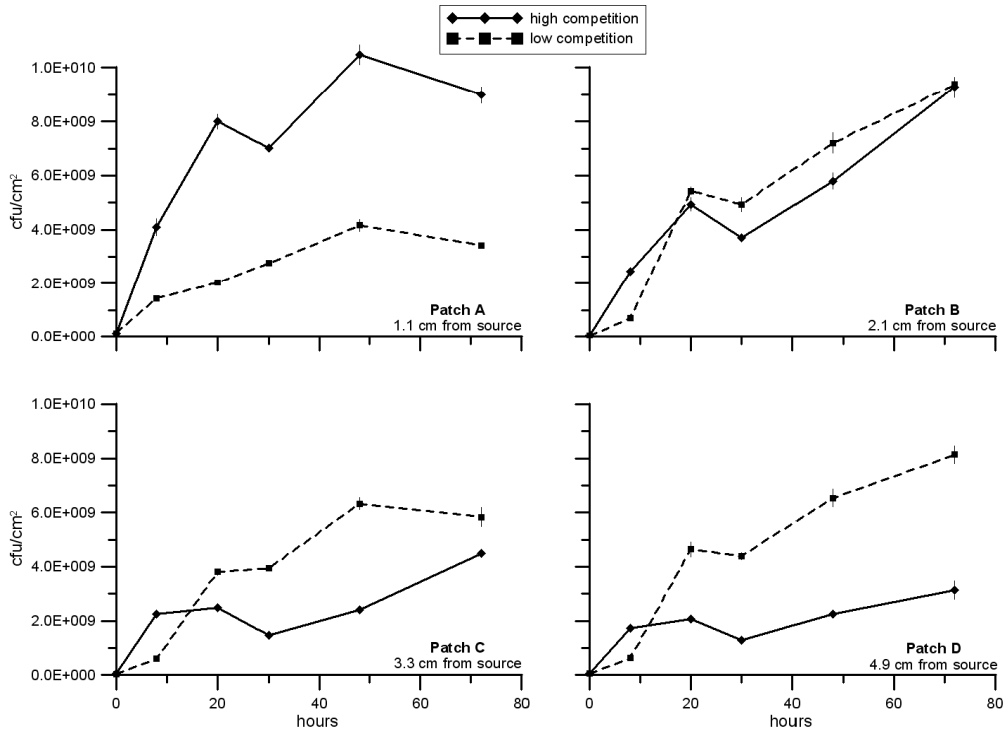

Figure 2

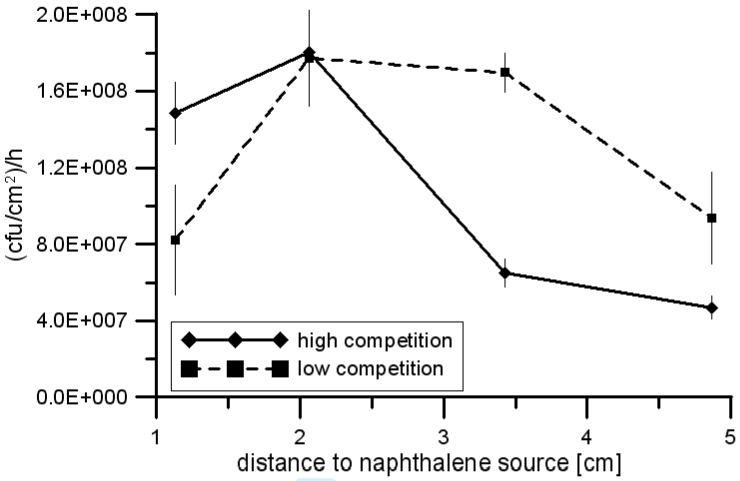

Figure 3

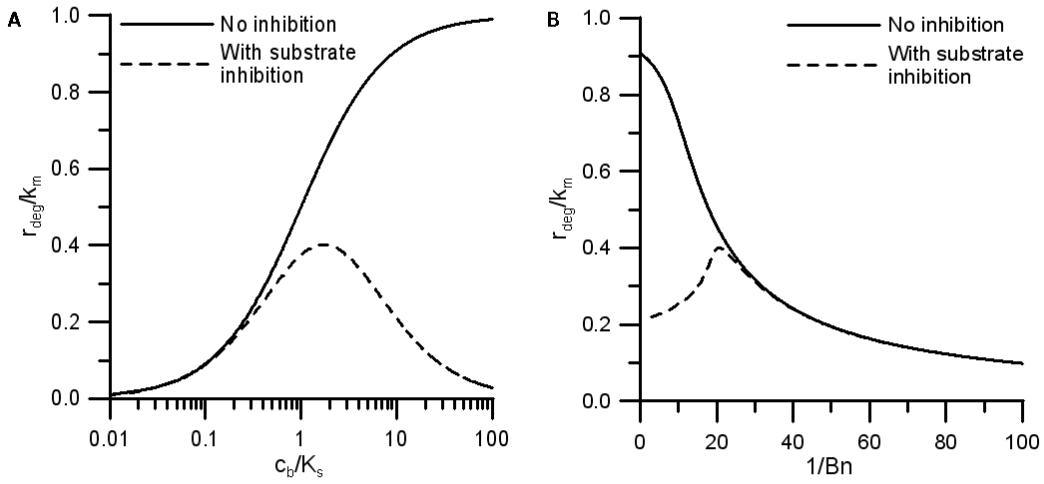

Figure 4

Supporting Information:

Walking the tightrope of bioavailability: Growth dynamics of PAH degraders on vapour-phase PAH

Joanna Hanzel, Martin Thullner, Hauke Harms, Lukas Y. Wick*

UFZ – Helmholtz Centre for Environmental Research, Department of Environmental Microbiology, 04318 Leipzig. Germany

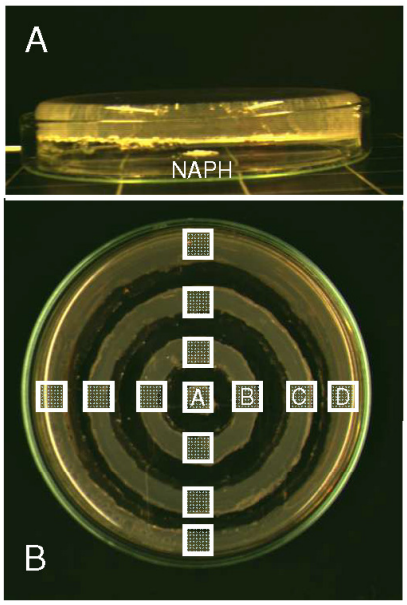

Figure S1. Photographs of the side (A) and birds view (B) of the experimental scenario to assess for increased inter-microbial competition ('high competition'; approximate sampling locations are symbolized by the light-colored squares) for studying growth of surface-associated *Pseudomonas putida* (NAH7) G7 on vapour-phase NAPH. The position of NAPH addition is marked in panel A, whereas letters in panel B refer to the name of the patches sampled. Please note that the Teflon-tape seals surrounding the Petri-dishes were removed for better clarity of the photographs.

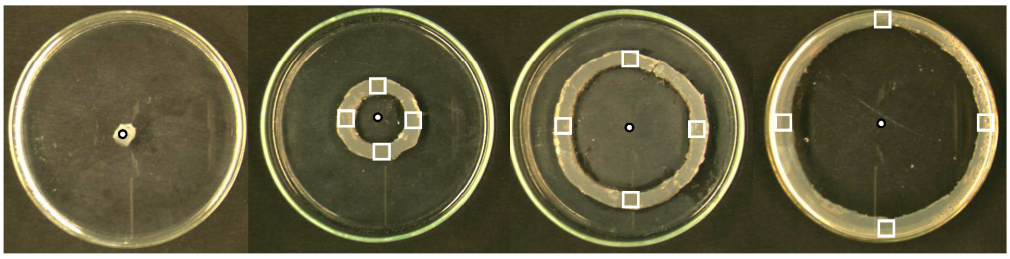

Figure S2. Photographs of the birds view (B) depicting the four scenarios to mimic lower competition scenarios ('low competition; sampling locations are symbolized by the light-colored areas) for studying growth of surface-associated *Pseudomonas putida* (NAH7) G7 on vapour-phase NAPH prior to addition of NAPH. The position of NAPH addition is marked by the light colored circles. Please also note that the Teflon-tape seals surrounding the Petri-dishes were removed for better clarity of the photographs.

Chapter 3

Microbial chemotaxis influenced by vapor-phase gradients of naphthalene

[1] Environmental Science and Technology. 2010, 44, 9304-9310.

This chapter studies the role of naphthalene gradients developing in the headspace of microcosms, on tactic response and growth of chemotactic naphthalene-degrading bacteria *Pseudomonas putida* (NAH7) G7.

Chapter 3.1 examines whether and to which extent *P.putida* G7 cells chemotactically follow vapor-phase NAPH gradients under non-growth conditions. Obtained results demonstrated that the bacteria were able to sense vapor-phase NAPH gradients and to chemotactically respond to its headspace concentrations by moving away from the solid source (negative chemotaxis). Surprisingly, after prolonged period of time *P.putida* G7 appeared to have alleviated potential NAPH stress by, e.g., 'diving' into the agar, where cells were chemotactically attracted by the aqueous NAPH gradients formed in response to the vapor-phase gradients.

By using the same experimental-setup but modifying conditions, chapter 3.2 studies chemotaxis and growth of *P.putida* G7 under the influence of gas-phase NAPH gradients. Obtained results demonstrated that after exhibiting negative chemotaxis, the bacteria changed the location of initial settlement and moved towards NAPH source, showing positive chemotaxis and growth on potentially inhibitory substrate. Hence, catabolically active bacteria reduced gas-phase NAPH concentrations to levels allowing to approach NAPH source and substrate consumption was thus showed to be an effective detoxification mechanism.

Environ. Sci. Technol. **2010**, *44*, 9304–9310

Bacterial Chemotaxis along Vapor-Phase Gradients of Naphthalene

JOANNA HANZEL, HAUKE HARMS, AND LUKAS Y. WICK*

UFZ, Helmholtz Centre for Environmental Research, Department of Environmental Microbiology, 04318 Leipzig, Germany

Received March 10, 2010. Revised manuscript received October 26, 2010. Accepted November 3, 2010.

The role of bacterial growth and translocation for the bioremediation of organic contaminants in the vadose zone is poorly understood. Whereas air-filled pores restrict the mobility of bacteria, diffusion of volatile organic compounds in air is more efficient than in water. Past research, however, has focused on chemotactic swimming of bacteria along gradients of water-dissolved chemicals. In this study we tested if and to what extent *Pseudomonas putida* PpG7 (NAH7) chemotactically reacts to vapor-phase gradients forming above their swimming medium by the volatilization from a spot source of solid naphthalene. The development of an aqueous naphthalene gradient by air–water partitioning was largely suppressed by means of activated carbon in the agar. Surprisingly, strain PpG7 was repelled by vapor-phase naphthalene although the steady state gaseous concentrations were 50–100 times lower than the aqueous concentrations that result in positive chemotaxis of the same strain. It is thus assumed that the efficient gas-phase diffusion resulting in a steady, and possibly toxic, naphthalene flux to the cells controlled the chemotactic reaction rather than the concentration to which the cells were exposed. To our knowledge this is the first demonstration of apparent chemotactic behavior of bacteria in response to vapor-phase effector gradients.

Introduction

The suffix "-taxis" refers to the ability of microorganisms to navigate along physicochemical gradients of ecologically relevant information (infotaxis) (*1*) such as stimuli affecting physiological energy levels (energy taxis) (*2*). Bacterial chemotaxis is the self-directed movement of flagellated bacteria along chemical gradients toward higher or lower concentrations (positive or negative chemotaxis). It enables bacteria to position themselves in environments favorable for survival (*2*–*4*). Chemotaxis hence may play an important role in terrestrial ecosystems (*2*, *5*). The fluxes and the distribution of chemoeffector signals in such environments depend heavily upon the physical conditions at different size scales (*6*). Soil systems are further characterized by high fragmentation of the aquatic microhabitats, large variations in the availability of water, nutrients, and substrates, as well as steep concentration gradients at and along phase boundaries (*7*). Positive chemotaxis along contaminant gradients increases the bioavailability of soil contaminants, as it improves the contact between degrader organisms and patchy contaminants (*8*, *9*). Directed swimming of microbes may occur at up to 1.7–3.5 m d^{-1} (*10*), which is in the same range as typical groundwater flow velocities. Chemotaxis may thus be important for the transport of bacteria and their access to patchy contaminations in saturated systems (*3*, *9*, *11*, *12*). Under unsaturated conditions, however, microbial mobility is significantly reduced due to the discontinuity of water pockets (*7*). The tendency of hydrophobic bacteria to accumulate at the air–water interface may also restrict their mobility (*13*). In such habitats alternative dispersal mechanisms such as gliding, twitching, and sliding on water-wet surfaces (*14*) or chemotactic swimming along continuous networks such as fungal mycelia (*15*, *16*) may become important. Limited mechanistic information exists on bacterial activity and dispersal in the unsaturated zone of subsurface. For instance nothing is known about the dispersal of air–water interface-associated microbes under the influence of vapor-phase contaminant gradients as they likely exist in the vadose zone (e.g., above the capillary fringe of contaminated aquifers). This may be due to the erroneous assumption that the high efficiency of gaseous diffusion impedes the formation of relevant gaseous concentration gradients. However, the presence of such gaseous gradients has been systematically demonstrated by microbial growth on vapor-phase naphthalene (NAPH) (*17*). In the present study we investigated if vapor-phase NAPH provoked chemotactic movement of NAPH-degrading *Pseudomonas putida* (NAH7) PpG7 (*18*) and its nonchemotactic derivative *P. putida* G7.C1 (pHG100), respectively. The hypothesis tested was if and to what extent surface-associated bacteria react chemotactically to vapor-phase gradients formed by the volatilization of a spot source of solid NAPH. To our knowledge this is the first demonstration of an apparent chemotactic response of bacteria being exposed to a vapor-phase effector gradient.

Material and Methods

Used Strains and Inoculum Preparation. Chemotactic *P. putida* PpG7 (NAH7) and its nonchemotactic derivative *P. putida* G7.C1 (pHG100) are both motile by means of polar flagella and able to degrade NAPH (*18*, *19*). Conjugative transfer of pHG100 to NAH7-cured *P. putida* G7.C1 leads to strain G7.C1 (pHG100) able to grow on NAPH as sole carbon and energy source, likely by using chromosomally encoded ortho pathway genes to degrade catechol generated as an intermediate of NAPH degradation (*18*). Strains PpG7 and G7.C1 (pHG100) are motile by means of polar flagella and exhibit insignificant differences in motility, as well as in physicochemical surface properties (*3*, *9*, *11*, *12*). They were grown at 25 °C on a gyratory shaker (150 rpm) in 100-mL Erlenmeyer flasks containing 50 mL of liquid minimal medium (*20*) in the presence of 1.5 g of solid NAPH (>98%, Fluka). Cells used in the experiments were harvested in the late exponential phase after 48 h of growth, the remaining NAPH was removed by filtration, and the cells were centrifuged (7800*g*, 10 min) to preserve the flagella and avoid loss of motility (*12*). The cells were then washed three times in cold 10 mM potassium phosphate buffer saline (PBS, pH = 7.2) and suspended in PBS to obtain a suspension containing $\approx 1.2 \times 10^9$ cells L^{-1} (optical density at 578 nm $\approx$ 12). Cells were quantified as colony forming units (cfu) after 3 days of incubation at room temperature on Luria Broth agar (2%

* Corresponding author mailing address: UFZ Helmholtz Centre for Environmental Research, Department of Environmental Microbiology, Permoserstrasse 15, 04318 Leipzig, Germany; phone: +49 341 235 1316; fax: +49 341 235 1351; e-mail: lukas.wick@ufz.de.

10.1021/es100776h
Published on Web 11/16/2010

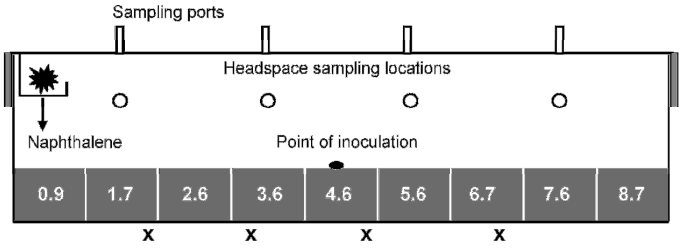

FIGURE 1. Cross section of the experimental setup applied for assessing bacterial chemotaxis along vapor- and agar-phase NAPH gradients. Sampling locations of headspace NAPH analysis and placement of SPME fibers for the assessment of freely dissolved NAPH in the agar are indicated by circles and crosses, respectively. Numbers reflect the distance to the NAPH source in centimeters.

w/v) using an automated spiral plating and cell counting system (Meintrup GmbH).

Instrumental Analysis. NAPH concentrations were analyzed by headspace gas chromatography (GC) with a flame ionization detector (FID) or mass spectroscopy (MS) detection (HP 6890 Series; Agilent Technologies). Gas-phase injection was automated using a headspace autosampler (G 1888; Agilent Technologies) with an oven temperature of 45 °C and an injection volume of 1 mL. A fused silica capillary column (Optima δ-3, length 60 m, inside diameter 0.32 mm, film thickness 0.35 mm; Macherey-Nagel) was used with a split of 50:1 and run isothermally at 180 °C for 6.5 min. The FID was operated at 280 °C and helium was used as carrier gas with initial flow 2 mL min^{-1}. For GC-MS analysis a 30-m HP5MS capillary column (Agilent Technologies) and splitless injection of a 1-μL sample using an automatic HP septumless PTV injector (Agilent Technologies) was used. Helium served as carrier gas at 1.0 mL min^{-1}. The oven temperature was kept at 50 °C for 2 min, 15 °C min^{-1} to 160 °C, and then 40 °C min^{-1} to 300 °C.

Chemotaxis Experiments. Experiments were performed in Petri dishes (diameter 9 cm) containing 30 mL of nutrient-free PBS swimming agar (0.3%) to avoid bacterial growth: The agar was allowed to stabilize for 1.5 h prior to inoculation with 5 μL of cell suspension (OD_{578} = 12) carefully placed with a syringe onto the agar at the center of the plate avoiding any physical damage of the agar surface. The plate was closed immediately after inoculation with its lid holding 20 mg of solid NAPH placed in a small open sterile aluminum holder at the edge of the Petri dish (4.6 cm from the inoculation point) in a way avoiding direct contact to the agar (Figure 1). All plates were tightly sealed with Teflon tape to minimize the loss of gaseous NAPH. The spatiotemporal distribution of bacteria was approximated by quantifying cell numbers in agar cores simultaneously taken at distances of 0.9, 1.7, 2.6, 3.5, 4.6, 5.6, 6.7, 7.6, and 8.7 cm from NAPH by sacrificing triplicate plates right after inoculation (t_0) and after 6, 20, 50, and 95 h (t_6, t_{20}, t_{50}, t_{95}) of incubation. Cores of the entire agar depth (volume: 300 μL) were taken using sterile glass tubes (0.4 cm i.d.) equipped with rubber suckers, the contents were carefully rinsed with 1 mL of sterile 10 mM PBS to tared test tubes to determine the exact volumes, and the number of cells was quantified as described above.

Experiments with Agar Containing Activated Carbon (AC). To minimize freely dissolved (i.e., bioavailable (*21*)) NAPH in the agar, experiments with swimming agar containing 0.85 g mL^{-1} uniformly distributed AC powder (AC-agar) were performed. The AC (Sigma Aldrich, Darco G-60, −100 mesh) was sterilized twice, dried overnight at 180 °C, and kept in a desiccator prior to use. All experiments were performed at least in triplicate.

Viability Experiments. Viability and growth of strain PpG7 on nutrient-deprived PBS agar (10 mM, 2% agar (w/v)) in presence of vapor-phase NAPH was tested in Petri dishes by exposing PpG7-inoculated ($5.5 \times 10^7 \pm 7.0 \times 10^6$ cfu ($n = 3$)) circular PBS-agar patches (diameter 20 mm, height 4 mm) at two different distances (ca. 1.5 and 4.5 cm) to NAPH crystals mounted to the lid of the Petri dish as described before. After 0.2, 20, and 50 h of NAPH-exposure individual Petri dishes were sacrificed and the number of cells was quantified by cfu on LB agar as described above.

Quantification of Agar- and Vapor-Phase NAPH. Gradients developing around solid NAPH in both the vapor- and agar-phase were measured in the absence of bacteria. (A) *Vapor-phase NAPH gradients* were measured by removal of 2 mL of the headspace with an airtight glass syringe and subsequent injection to a gastight 10-mL headspace GC vial and analyzed by headspace GC. Samples were removed at 1.7, 3.6, 5.6, and 7.6 cm from the NAPH source by sacrificing individual plates and measuring only one position per plate (Figure 1). Both the small volume sampled (2 mL, i.e., ca. 3% of the headspace volume) and the sacrifice of individual plates allowed for a spatially discrete analysis of the vapor-phase NAPH concentration. (B) The presence of *agar-dissolved NAPH gradients* was demonstrated by analyzing NAPH concentrations in the agar cores as obtained above. Samples were immediately placed into 10-mL headspace GC vials, tightly closed, and heated to 50 °C for 30 min to vaporize the NAPH prior to headspace GC. (C) *Total NAPH in AC-agar* was quantified by GC-MS. After removal at 0.9, 2.6, 4.6, 6.7, and 8.7 cm distance from the source, the samples were dried with 10 g of anhydrous Na_2SO_4, extracted for >10 h with 6 mL of toluene (>99.9%, Merck) containing NAPH-d_8 (10 ng μL^{-1}) as internal standard. Extracts were analyzed without further treatment.

Quantification of Freely Dissolved NAPH in Agar by Solid-Phase Microextraction (SPME). Silica fibers coated with a thin layer of polydimethylsiloxane (PDMS) were used to quantify freely dissolved NAPH in the agar in either the presence or the absence of AC. SPME fibers (Polymicro Technologies, Inc., Phoenix, AZ) were cut into 1-cm long pieces and washed twice with methanol and bidistilled water as described earlier (*21*). Four fibers were placed inside the agar at given distances (1.9, 3.4, 4.3, and 6.8 cm) from the NAPH using sterile needles (Figure 1). The fibers were recovered at t_6, t_{20}, and t_{50}, and carefully cleaned using paper tissue to remove agar and AC. The fibers were subsequently placed into 1-mL gas chromatography vials, extracted with 100 μL of toluene (containing 10 ng μL^{-1} NAPH-d_8) for 8 h on a horizontal shaker, and analyzed by GC-MS. Freely dissolved concentrations were calculated from triplicate 9-point external calibration. Twenty mL of mineral medium agar was spiked with increasing amounts of NAPH in methanol (0−1250 μg L^{-1}; n = 10; methanol, < 0.2% (v/v)). To each vial a 1-cm SPME fiber was added and shaken for 24 h to attain equilibrium, removed, and treated as detailed above. The mass of NAPH sorbed to the PDMS coating (n) was converted to a concentration using the volume of PDMS per unit length of fiber (V_{PDMS} = 13.55 ± 0.02 μL m^{-1}) and the PDMS/agar partition coefficient (K_{PDMS}) according to

$C_{diss} = n/K_{PDMS} * V_{PDMS}$ (*21*). The data were plotted as NAPH concentration in the agar versus concentration in the PDMS. The resulting relationship was highly linear ($r^2 = 0.96$) with the slope giving the dimensionless PDMS/agar partition coefficient. Equilibrium between the PDMS fiber and the agar was estimated by quantifying the PDMS-associated NAPH after exposure of the fibers for 0.5, 1, 3, 5, 20, 30, 50, and 95 h to the agar and was reached within about 5 h.

Results

NAPH Concentrations in Gas- and Water-Phase Compartments. Volatilization of solid NAPH in the headspace resulted

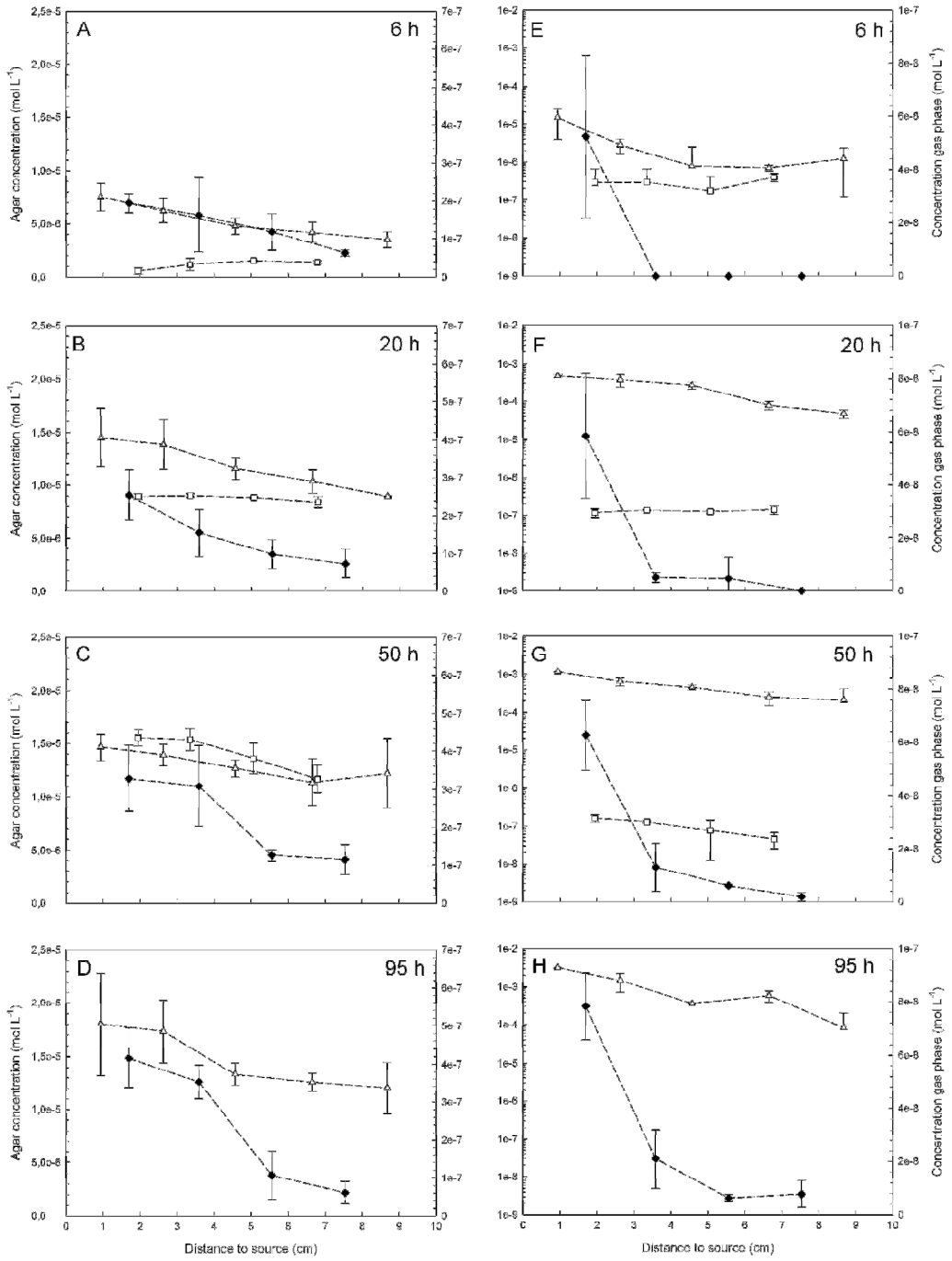

FIGURE 2. Profiles of total NAPH in the headspace (filled rhomboids, right *y*-axis) and agar (open triangles, left *y*-axis) as well as freely dissolved NAPH concentrations in agar (open squares, left *y*-axis) at t_0, t_{20}, t_{50}, and t_{95} without bacteria in absence (A–D) and presence (E–H) of AC. Data represent the averages and the standard deviations of three independent experiments.

TABLE 1. Relative Abundance of *P. putida* PpG7 (NAH7) Cells and Average Concentrations of Total and Freely Dissolved Concentrations in Agar and Headspace in the Presence and the Absence of AC (For a Depiction of the Distribution of Cells Please Refer to Figure 3)

	agar					agar and AC			
time (h) /distance to source (cm)[a]	fraction mobilized bacteria (%)		average concentration (mol L^{-1})			fraction mobilized bacteria (%)	average concentration (mol L^{-1})		
	PpG7[b]	G7.C1 (pHG100)[c]	headspace[d]	$agar_{tot}$[e]	SPME[f]	PpG7[b]	headspace[d]	$agar_{tot}$[e]	SPME[f]
6:0.9–3.7	0	0	1.8×10^{-7}	6.9×10^{-6}	8.8×10^{-7}	0	2.6×10^{-8}	8.2×10^{-6}	2.9×10^{-7}
6:5.6–8.7	100	0	9.1×10^{-8}	3.8×10^{-6}	1.5×10^{-6}	0	bdl[g]	9.7×10^{-7}	2.8×10^{-7}
20:0.9–3.7	15	0	2.0×10^{-7}	1.4×10^{-5}	9.0×10^{-6}	25	3.2×10^{-8}	4.2×10^{-4}	1.3×10^{-7}
20:5.6–8.7	85	100	8.6×10^{-8}	9.7×10^{-6}	8.7×10^{-6}	75	2.4×10^{-9}	6.3×10^{-5}	1.3×10^{-7}
50:0.9–3.7	73	0	3.2×10^{-7}	1.4×10^{-5}	1.6×10^{-5}	8	3.8×10^{-8}	8.9×10^{-4}	1.4×10^{-7}
50:5.6–8.7	26	100	1.2×10^{-7}	1.2×10^{-5}	1.3×10^{-5}	92	3.9×10^{-9}	2.3×10^{-4}	6.1×10^{-8}
95:0.9–3.7	46	53	3.9×10^{-7}	1.8×10^{-5}	n.a.[h]	56	5.0×10^{-8}	2.3×10^{-3}	n.a.[h]
95:5.6–8.7	54	47	8.4×10^{-8}	1.2×10^{-5}		44	7.0×10^{-9}	3.3×10^{-4}	

[a] Cf. Figure 1. [b] Relative fraction of cells of chemotactic *P. putida* (NAH7) PpG7 dispersing from point of inoculation (derived from the average of $n = 3$ independent experiments). [c] Relative fraction of cells of nonchemotactic *P. putida* G7.C1 (pHG100) dispersing from point of inoculation (derived from the average of $n = 3$ independent experiments). [d] 0.9–3.7: average 1.7 and 3.6 cm samples; 5.6–8.7: average of 5.6 and 7.6 cm samples. [e] Total NAPH concentration per volume of agar or AC-agar. 0.9–3.7: average of 0.9, 1.7; 2.6, and 3.6 cm samples; 5.6–8.7: average of 5.6, 6.7, 7.6, and 8.7 cm samples. [f] Freely dissolved NAPH concentration per volume of agar. 0.9–3.7: average of 1.9 and 3.4 cm samples; 5.6–8.7: average of 4.3 and 6.8 cm samples. [g] Below detection limit. [h] Not analyzed.

in distinct gradients in both the vapor and the agar phase (Figure 2) even in the absence of NAPH-degrading bacteria. The average (t_6–t_{95}) vapor-phase NAPH concentration near the source ($\approx 3 \times 10^{-7}$ mol L^{-1}, i.e., close to the equilibrium concentration as calculated by Henry's law) dropped about 3-fold along the plate's transect (Figure 2) yet remained over time as a result of continuous NAPH dissolution in the agar. As a result of fast air–agar exchange, similar, yet less pronounced NAPH gradients were detected in the agar (Figure 2). To estimate the truly dissolved NAPH, i.e., NAPH that is freely available to the bacteria in the agar, non-exhaustive solid-phase microextraction (SPME) was applied at t_6, t_{20}, and t_{50} using a fiber–agar partitioning coefficient ($K_{PDMS} = 138 \pm 11$; $n = 3$). This value is in the magnitude of literature values determined in water of $K_{PDMS} = 524$ (*22*). Chemoeffector concentrations in sterile AC-agar controls were further analyzed. AC acts as an efficient sink for NAPH and creates steep vapor-phase NAPH gradients as it drives high mass fluxes into the agar. AC also significantly reduced the freely bioavailable NAPH and its spatial gradients and thus may be used to minimize a chemotactic response of *P. putida* within the agar. AC-agar further reduced the overall gas-phase concentrations of NAPH significantly (about 10-fold; Table 1). Fortunately for our purpose, vapor-phase gradients in the presence of AC (although at 10-fold lower concentrations) were characterized by an 80% concentration drop (Figure 2). Total NAPH concentrations in AC-agar increased ca. 300-fold between t_6 and t_{95} and reflects the effectiveness of AC-agar as a sink of NAPH vapor. Only 1% of the total NAPH was freely dissolved and exhibited a relatively flat gradient at t_{50} (Figure 2G).

Spatiotemporal Variations of the Abundance of Bacteria in Response to NAPH. Dispersal of PpG7 in response to vapor-phase NAPH gradients was assessed by quantifying the cell distribution on the swimming agar over time. Distinct spatial distribution patterns of strain PpG7 were observed during the experiment. Although known for positive chemotaxis to water-dissolved NAPH, PpG7 cells at the air–agar interface avoided the zones of highest vapor-phase NAPH concentrations, i.e., were repelled by increasing vapor-phase NAPH concentrations up to t_{20} (Table 1). Interestingly, this trend was reversed at t_{50}, when >70% of the mobilized cells were found in the half of the plate next to the NAPH source (Figure 3C, Table 1). This is likely due to diving of the initially surface-associated cells into the agar and subsequent chemotactic swimming along aqueous NAPH gradients (Figure 2). No preferred mobilization to NAPH and avoidance of high NAPH concentrations (t_{20}, t_{50}), however, was observed when the nonchemotactic derivative G7.C1 (PHG100) was used (Figure 3, Table 1). Likewise PpG7 cells on AC-agar were repelled by vapor-phase NAPH at all times after t_6 (Figure 3F–H) with up to 92% (t_{50}) of mobilized bacteria avoiding the NAPH source (Table 1). Controls in the absence of NAPH consistently resulted in symmetrical distribution of PpG7 cells both in agar and AC-agar (data not shown). In separate experiments the potential toxic effect of gas-phase NAPH of as high as $c_g \approx 3 \times 10^{-7}$ mol L^{-1} on the viability of PpG7 cells was tested on PBS agar. Exposure to NAPH did not influence the viability of the bacteria, as 99 ± 13, 110 ± 5, and 74 ± 25% ($n = 3$) of the cfu placed onto the agar remained culturable after 0.2, 20, and 50 h of NAPH exposure independent of the distance to the NAPH crystal. Controls in the absence of NAPH showed similar viability, i.e., 99 ± 13, 110 ± 5, and 108 ± 29% ($n = 3$) after identical intervals. This data simultaneously suggest that nutrient-deprived PBS agar did not allow for apparent bacterial growth, i.e., that the spatiotemporal distribution of the cells in the presence of NAPH-gradients was due to dispersal rather than microbial growth and/or inhibition. The absence of microbial growth was further underpinned by recovery rates estimated from the cfu retrieved from all sampling locations relative to the initial cfu inoculated. Bacterial recovery ranged from 29% (t_6) to 17% (t_{95}) in agar and from 4% (t_6) to 10% (t_{95}) in AC-agar. Interestingly, recovery of bacteria from AC-agar remained consistently low at all sampling times likely due to strong AC–bacteria interactions and subsequent reduced extraction efficiency.

Discussion

Chemotactic Response of Surface-Associated *P. putida* (NAH) G7 to Vapor-Phase NAPH. Several studies have examined the chemotactic responses of bacteria toward volatile compounds such as ethylene, benzene, and chlorinated ethenes (*23*, *24*). These studies, however, have used plug agarose assays (*25*) exposing water-bound bacteria to the likewise agarose-embedded chemoeffectors. They thus tended to neglect situations likely to be found in unsaturated porous media, where bacteria may be under the influence

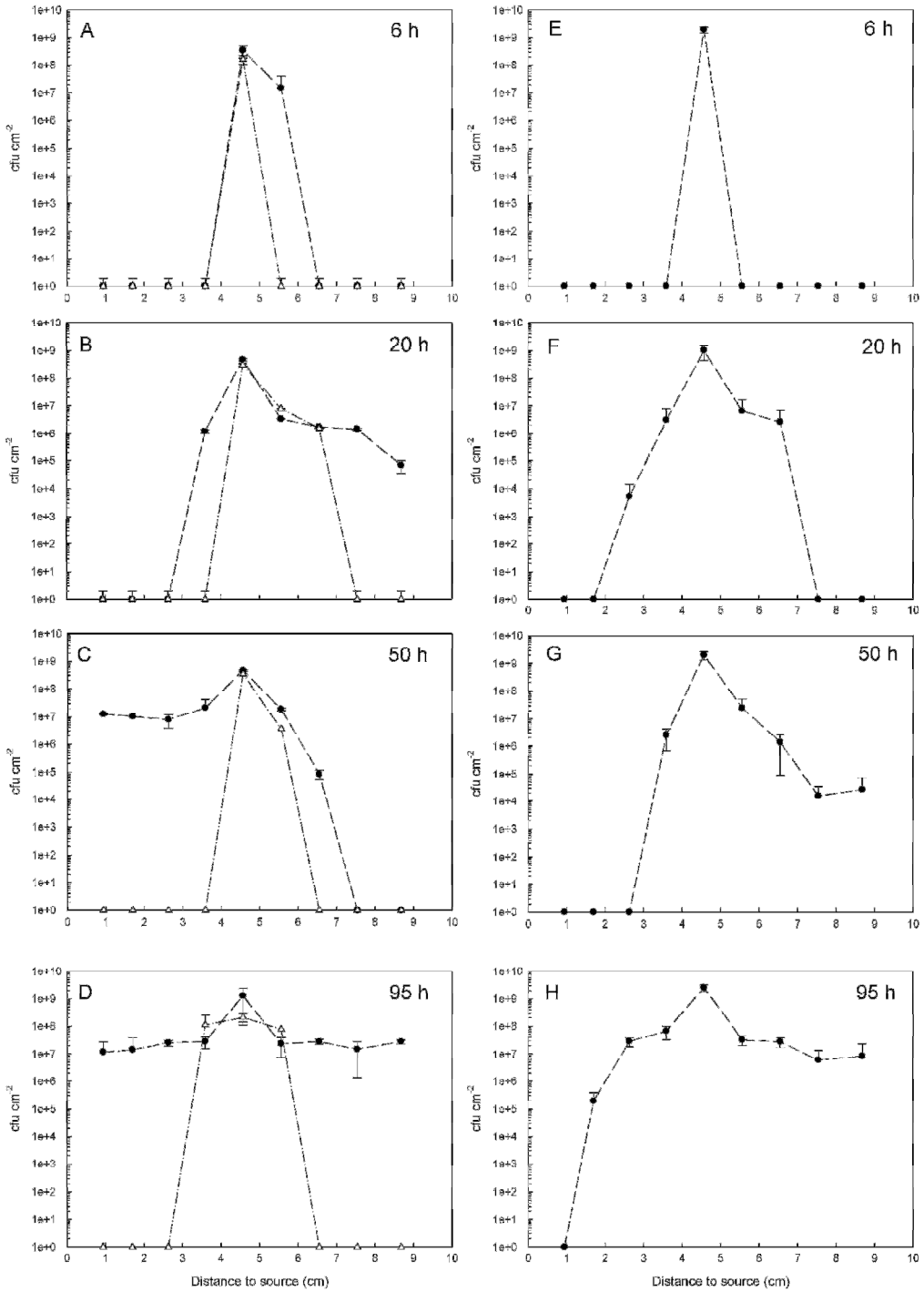

FIGURE 3. Spatial distribution of *P. putida* (NAH7) G7 (circles) and *P. putida* (NAH7) G7.C1(pHG100) (triangles) at t_6, t_{20}, t_{50}, and t_{95} in nutrient-free swimming agar in the absence (A−D) and presence (E−H) of AC. Bacteria were inoculated at 4.6 cm from the NAPH source. Data represent the averages and the standard deviations of three independent experiments.

of vapor-phase chemicals, e.g., emanating from contaminated aquifers. Bacteria present in or near air−water interfaces are likely to be important for natural attenuation processes of subsurface volatiles. In the present study we tested whether and to what extent chemotactic bacteria can sense and follow vapor-phase NAPH gradients present in the gaseous phase

next to their aqueous habitat. NAPH crystals were placed in the headspace above agar that allowed swimming of *P. putida* PpG7 while preventing its growth by the use of nutrient-deprived agar for the sake of easy quantification of the strain's dispersal. Strain PpG7 exhibits a well described chemotaxis along gradients of NAPH in aqueous environments (*4, 9, 26*). Figure 3 illustrates that the presence of a NAPH spot source in the headspace resulted in directed dispersal of strain PpG7 in the plate. Controls in the absence of NAPH consistently resulted in symmetrical distribution of PpG7 cells in agar and AC-agar. Surprisingly and contrary to literature describing rapid positive chemotaxis of PpG7 to waterborne NAPH even at $c_{w,sat}$ (*27*), bacteria were repelled by gas-phase NAPH up to t_{20} (Figure 3, Table 1), whereas at t_{50} 75% of cells were found in the half of the plate next to NAPH and equal numbers in both halves were observed at t_{95}, respectively. Strain PpG7 hence appeared to be repelled by vapor-phase NAPH gradients ("negative chemotaxis"). The development of NAPH gradients was verified in the absence of PpG7 cells (which by means of biodegradation may give rise to even steeper vapor-phase NAPH gradients). Distinct gradients along the sampled transects were measured with 3–4-fold enhanced NAPH concentrations next to the source (Table 1). Bacteria exposed to vapor-phase NAPH hence appear to have alleviated potential NAPH stress by either interfacial swimming downgradient vapor-phase NAPH gradients (t_6–t_{20}) and/or by "diving" into the agar, where they were chemotactically attracted by *horizontal* aqueous NAPH gradients formed in response to the vapor-phase NAPH gradients (Figure 2) finally leading to the apparent equal distribution of the cells after 95 h (Figure 3D). Due to NAPH exchange at the headspace–agar interface we further expect *vertical* NAPH gradient to form within the agar with higher concentrations close to the headspace interface and hence to initially (i.e., t_6–t_{20}) result in a "chemotactic focusing" or "chemotactic trap" for chemotactic bacteria at the headspace–agar interface. The role of chemotaxis for bacterial response to vapor-phase NAPH was further examined by using derivative strain G7.C1 (PHG100), known to lack chemotaxis to NAPH. Strain G7.C1 (PHG100) got consistently repelled by vapor-phase NAPH and lacked any targeted dispersal toward the NAPH at t_0–t_{50} (Table 1). Slight avoidance of vapor-phase NAPH by this nonchemotactic derivative strain (Figure 3) may be due to energy-taxis-induced motility. Energy taxis is broadly defined as a behavioral response to stimuli that affect cellular energy levels and encompasses responses that are directly linked to electron transport/energy generation (*2*). Any potentially toxic effect of vapor-phase NAPH (as indicated by avoidance of increasing vapor-phase NAPH gradients by the wild-type strain) hence may have affected the dispersal of strain G7.C1 (PHG100) and may explain the observations found. To minimize formation of aqueous NAPH-gradients, similar experiments were performed with AC suspended in the agar. AC indeed minimized dissolved NAPH concentrations in the agar (*28*) and left vapor-phase NAPH as the principle chemoeffector to strain PpG7. Dissolved NAPH was approximated by equilibrium SPME (*29*). Due to the relatively long time needed to reach equilibrium between the SPME fiber and the agar, however, SPME at t_6 and t_{20} may underestimate freely dissolved NAPH. This is seen by constantly increasing SPME-calculated concentrations from t_6 to t_{50} (Figures 2A–C). Despite the significant reduction, freely dissolved NAPH still formed weak gradients in AC-agar (Figure 2). Likewise vapor-phase NAPH gradients were detected in presence of AC although at 10-fold reduced concentration relative to the variant without AC (Table 1). Nonetheless, clear avoidance of PpG7 cells to vapor-phase NAPH was observed, underpinning the observation that even vapor-phase NAPH as dilute as 10^{-8} mol L^{-1} is sufficient to repel chemotactic PpG7 cells, which are known to be normally attracted by up to 10^6-fold higher aqueous concentrations of NAPH.

The reasons for these opposing chemotactic responses remain unresolved at present. We assume, however, that different NAPH fluxes to the receptors at the cells' surfaces cause these different behaviors. The average suspended bacterium is surrounded by a 5–10-μm thick aqueous diffusive boundary layer for NAPH (*30*). In contrast, bacteria at a solid–air interface are likely to be covered by very thin water films unlikely to act as diffusive barriers to gaseous NAPH ($D_g \approx 6.4 \times 10^{-6}$ m^2 s^{-1}) to the cell envelope. Roughly assuming that bacteria on agar may exhibit a behavior similar to ideal solid surfaces, such films were in the range of nanometers (corresponding to 5–10 layers of water molecules (*31*)) and would result in high NAPH fluxes to the cells and chemotactic receptors (as has also been observed from the high sensitivity of bioreporter bacteria to vapor-phase NAPH (*32*)). Despite higher nominal NAPH concentrations in the agar, diving of the cells into the agar hence may have decreased the NAPH flux to the cells due to the formation of a diffusive boundary layer around their surface and, hence, significantly reduced diffusivity of NAPH in the aqueous environment ($D_w \approx 6.7 \times 10^{-10}$ m^2 s^{-1}). One may speculate that the transfer efficiency of a chemoeffector rather than its bulk concentration determines the chemotactic behavior of bacteria. This assumption was corroborated in control habitats with AC placed close to the NAPH source only. Dispersal of PpG7 cells at t_{20} and at t_{50} showed that bacteria still avoided this region characterized by low aqueous-phase and high vapor-phase NAPH concentrations (data not shown).

Relevance for the Ecology of Microbial Contaminant Degradation. Our data reveal that vapor-phase chemical gradients influence the chemotactic dispersal and the spatiotemporal distribution of contaminant degrading bacteria. Such "olfactory" swimming thus is a behavioral adaptation allowing microorganisms to locate contaminant sources or to position themselves at a distance representing a compromise of acceptable toxicity and sufficient substrate supply as for instance shown in plug chemotaxis assays using chlorinated ethenes (*33*). This simultaneously illustrates that bioavailability for biodegradation (i.e., energy-tactically promoted by the target organisms) may be very different from bioavailability for toxic effects (i.e., chemotactically avoided), although the bioaccessible pool for both effects may be identical (*34*). Although chemotaxis has been described to require at least some solubility of the target chemical, i.e., sufficient to generate an aqueous-phase concentration gradient (*35*), it is theoretically possible that also poorly soluble contaminants give rise to chemotaxis via their gas-phase distribution at concentrations as low as 10^{-9} mol L^{-1} when present in unsaturated porous media. Air-exposed bacteria become increasingly important for the biodegradation of vapor-phase contaminants in technical filters as well as in the phyllosphere (*36, 37*). Microbial species furthermore produce unique, situation-specific profiles of secondary metabolites of which many are volatile at environmental conditions (*38, 39*). Positive, negative, or neutral interactions have been described among a very wide range of soil bacteria and fungi (*40*) including inhibitory growth effects of microbial volatiles against other microorganisms or inhibition/stimulation of fungal growth (*41*). Because of their high vapor pressure such volatile metabolites can effectively travel large distances and form vapor-phase gradients in heterogeneous soil. Chemotactic dispersal within such microbial "odor landscapes" (*6*) hence can affect the dynamics of microbial ecosystems and the ecology of contaminant biodegradation (*42*).

Acknowledgments

Funding from European grant MC-EST 20984 (RAISEBIO) is greatly acknowledged. We thank B. Würz, J. Reichenbach, and R. Remer for skilled technical help. We further thank Prof. C. S. Harwood (University of Washington) for the provision of *P. putida* G7.C1 (pHG100).

Literature Cited

(1) Vergassola, M.; Villermaux, E.; Shraiman, B. I. 'Infotaxis' as a strategy for searching without gradients. *Nature* **2007**, *445* (7126), 406–409.
(2) Alexandre, G.; Greer-Phillips, S.; Zhulin, I. B. Ecological role of energy taxis in microorganisms. *FEMS Microbiol. Rev.* **2004**, *28* (1), 113–126.
(3) Pandey, G.; Jain, R. K. Bacterial Chemotaxis toward Environmental Pollutants: Role in Bioremediation. *App. Environ. Microbiol.* **2002**, *68* (12), 5789–5795.
(4) Pedit, J. A.; Marx, R. B.; Miller, C. T.; Aitken, M. D. Quantitative analysis of experiments on bacterial chemotaxis to naphthalene. *Biotechnol. Bioeng.* **2002**, *78* (6), 626–634.
(5) Ford, R. M.; Harvey, R. W. Role of chemotaxis in the transport of bacteria through saturated porous media. *Adv. Wat. Resour.* **2007**, *30*, 1608–1617.
(6) Moore, P.; Crimaldi, J. Odor landscapes and animal behavior: Tracking odor plumes in different physical worlds. *J. Mar. Syst.* **2004**, *49* (1–4), 55–64.
(7) Or, D.; Smets, B. F.; Wraith, J. M.; Dechesne, A.; Friedman, S. P. Physical constraints affecting bacterial habitats and activity in unsaturated porous media - A review. *Adv. Water Resour.* **2007**, *30* (6–7), 1505–1527.
(8) Harms, H.; Wick, L. Y. Dispersing pollutant-degrading bacteria in contaminated soil without touching it. *Eng. Life Sci.* **2006**, *6* (3), 252–260.
(9) Marx, R. B.; Aitken, M. D. Bacterial chemotaxis enhances naphthalnene degradation in a heterogeneous aqueous system. *Environ. Sci. Technol.* **2000**, *34*, 3379–3383.
(10) Frymier, P. D.; Ford, R. M.; Berg, H. C.; Cummings, P. T. 3-Dimensional tracking of motile bacteria near a solid planar surface. *Proc. Nat. Acad. Sci.* **1995**, *92* (13), 6195–6199.
(11) Ford, R. M.; Harvey, R. W. Role of chemotaxis in the transport of bacteria through saturated porous media. *Adv. Water Resour.* **2007**, *30* (6–7), 1608–1617.
(12) Velasco-Casal, P.; Wick, L. Y.; Ortega-Calvo, J. J. Chemoeffectors decrease the deposition of chemotactic bacteria during transport in porous media. *Environ. Sci. Technol.* **2008**, *42* (4), 1131–1137.
(13) Schäfer, A.; Harms, H.; Zehnder, A. J. B. Bacterial accumulation at the air-water interface. *Environ. Sci. Technol.* **1998**, *32*, 3704–3712.
(14) Harshey, R. M. Bacterial motility on a surface: Many ways to a common goal. *Annu. Rev. Microbiol.* **2003**, *57*, 249–273.
(15) Kohlmeier, S.; Smits, T. H. M.; Ford, R.; Keel, C.; Harms, H.; Wick, L. Y. Taking the fungal highway: Mobilization of pollutant degrading bacteria by fungi. *Environ. Sci. Technol.* **2005**, *39*, 4640–4646.
(16) Furuno, S.; Päzolt, K.; Rabe, C.; Neu, T.; Harms, H.; Wick, L. Fungal mycelia allow chemotactic dispersal of PAH-degrading bacteria in water-unsaturated systems. *Environ. Microbiol.* **2010**, *12*, 1391–1398.
(17) Harms, H. Bacterial growth on distant naphthalene diffusing through water, air, water-saturated, and unsaturated porous media. *Appl. Environ. Microbiol.* **1996**, *62*, 2286–2293.
(18) Grimm, A. C.; Harwood, C. S. Chemotaxis of *Pseudomonas* spp. to the polyaromatic hydrocarbon naphthalene. *Appl. Environ. Microbiol.* **1997**, *63* (10), 4111–4115.
(19) Dunn, N. W.; Gunsalus, I. C. Transmisible plasmid coding early enzymes of naphthalene oxidation in *Pseudomonas putida*. *J. Bacteriol.* **1973**, *114*, 974–979.
(20) Wick, L. Y.; Colangelo, T.; Harms, H. Kinetics of mass transfer-limited bacterial growth on solid PAHs. *Environ. Sci. Technol.* **2001**, *35* (2), 354–361.
(21) Smith, K. E. C.; Thullner, M.; Wick, L. Y.; Harms, H. Sorption to humic acids enhances polycyclic aromatic hydrocarbon biodegradation. *Environ. Sci. Technol.* **2009**, *43* (19), 7205–7211.
(22) Xia, X. R.; Baynes, R. E.; Monteiro-Riviere, N. A.; Riviere, J. E. Membrane uptake kinetics of jet fuel aromatic hydrocarbons from aqueous solutions studied by a membrane-coated fiber technique. *Toxicol. Mech. Methods* **2005**, *15* (4), 307–316.
(23) Liu, X. X.; Wood, P. L.; Parales, J. V.; Parales, R. E. Chemotaxis to pyrimidines and identification of a cytosine chemoreceptor in *Pseudomonas putida*. *J. Bacteriol.* **2009**, *191* (9), 2909–2916.
(24) Vardar, G.; Barbieri, P.; Wood, T. K. Chemotaxis of *Pseudomonas stutzeri* OX1 and *Burkholderia cepacia* G4 toward chlorinated ethenes. *Appl. Microbiol. Biotechnol.* **2005**, *66* (6), 696–701.
(25) Yu, H. S.; Alam, M. An agarose-in-plug bridge method to study chemotaxis in the Archaeon Halobacterium salinarum. *FEMS Microbiol. Lett.* **1997**, *156* (2), 265–269.
(26) Law, A. M. J.; Aitken, M. D. Bacterial chemotaxis to naphthalene desorbing from a nonaqueous liquid. *Appl. Environ. Microbiol.* **2003**, *69* (10), 5968–5973.
(27) Marx, R. B.; Aitken, M. D. Quantification of chemotaxis to naphthalene by *Pseudomonas putida* G7. *Appl. Environ. Microbiol.* **1999**, *65* (7), 2847–2852.
(28) Reichenberg, F.; Mayer, P. Two complementary sides of bioavailability: Accessibility and chemical activity of organic contaminants in sediments and soils. *Environ. Toxicol. Chem.* **2006**, *25*, 1239–1245.
(29) Poerschmann, J.; Zhang, Z. Y.; Kopinke, F. D.; Pawliszyn, J. Solid phase microextraction for determining the distribution of chemicals in aqueous matrices. *Anal. Chem.* **1997**, *69* (4), 597–600.
(30) Kampara, M.; Thullner, M.; Harms, H.; Wick, L. Y. Impact of cell density on microbially induced stable isotope fractionation. *Appl. Microbiol. Biotechnol.* **2009**, *81* (5), 977–985.
(31) vanOss, C. J. Hydrophobicity of biosurfaces - origin, quantitatve determination and interaction energies. *Colloids Surf., B* **1995**, *5*, 91–110.
(32) Werlen, C.; Jaspers, M. C. M.; van der Meer, J. R. Measurement of biologically available naphthalene in gas and aqueous phases by use of a *Pseudomonas putida* biosensor. *Appl. Environ. Microbiol.* **2004**, *70* (1), 43–51.
(33) Shitashiro, M.; Kato, J.; Fukumura, T.; Kuroda, A.; Ikeda, T.; Takiguchi, N.; Ohtake, H. Evaluation of bacterial aerotaxis for its potential use in detecting the toxicity of chemicals to microorganisms. *J. Biotechnol.* **2003**, *101* (1), 11–18.
(34) Semple, K. T.; Doick, K. J.; Wick, L. Y.; Harms, H. Microbial interactions with organic contaminants in soil: Definitions, processes and measurement. *Environ. Pollut.* **2007**, *150* (1), 166–176.
(35) Ortega-Calvo, J. J.; Marchenko, A. I.; Vorobyov, A. V.; Borovick, R. V. Chemotaxis in polycyclic aromatic hydrocarbon-degrading bacteria isolated from coal-tar- and oil-polluted rhizospheres. *FEMS Microbiol. Ecol.* **2003**, *44*, 373–381.
(36) Sandhu, A.; Halverson, L. J.; Beattie, G. A. Bacterial degradation of airborne phenol in the phyllosphere. *Environ. Microbiol.* **2007**, *9* (2), 383–392.
(37) Waightp, K. P. O.; Luepromchai, E. Degradation of phenanthrene on plant leaves by phyllosphere bacteria. *J. Gen. Appl. Microbiol.* **2007**, *53*, 265–272.
(38) Bruce, A.; Wheatley, R. E.; Humphris, S. N.; Hackett, C. A.; Florence, M. E. J. Production of volatile organic compounds by *Trichoderma* in media containing different amino acids and their effect on selected wood decay fungi. *Holzforschung* **2000**, *54* (5), 481–486.
(39) Minerdi, D.; Bossi, S.; Gullino, M. L.; Garibaldi, A. Volatile organic compounds: A potential direct long-distance mechanism for antagonistic action of *Fusarium oxysporum* strain MSA 35. *Environ. Microbiol.* **2009**, *11* (4), 844–854.
(40) Mackie, A. E.; Wheatley, R. E. Effects and incidence of volatile organic compound interactions between soil bacterial and fungal isolates. *Soil Biol. Biochem.* **1999**, *31* (3), 375–385.
(41) McKee, N. D.; Robinson, P. M. Production of the volatile inhibitors of germination and hyphal extension by *Geotrichum candidum*. *Trans. Br. Mycol. Soc.* **1988**, *91*, 157–190.
(42) Nijland, R.; Burgess, J. G. Bacterial olfaction. *Biotechnol. J.* **2010**, *5*, 974–977.

ES100776H

Substrate consumption as detoxification mechanism allowing bacteria to position themselves at a location suitable for optimal activity.

Abstract

The role of bacterial growth and chemotactic dispersal under the influence of vapor-phase contaminant gradients present in the unsaturated subsurface soil is still poorly understood. It is known that in the vadose zone the mobility of the bacteria is highly reduced, due to discontinuity of water pockets and the tendency of the bacteria to accumulate at the air-water interfaces. On the contrary, the diffusivity of volatile contaminants present in the subsurface is highly enhanced, resulting in higher bioavilability of volatile chemicals in the vadose zone relative to water-saturated environments. We have recently shown that enhanced naphthalene bioavilability in the vapor-phase led to negative chemotaxis, since chemotactic naphthalene-degrading bacteria *Pseudomonas putida* (NAH7) G7 surprisingly moved away from the naphthalene source already at concentrations lower than those being attractive in aqueous systems. In an attempt to test whether growth of the same strain on potentially inhibitory vapor-phase naphthalene can be used as detoxification mechanism, we exposed *P.putida* G7 to vapor-phase naphthalene under conditions allowing for growth. Our results revealed that by means of negative chemotaxis cells positioned themselves at a distance representing a compromise between acceptable toxicity and sufficient substrate supply to develop growth. By active degradation vapor phase-naphthalene concentrations were reduced to levels allowing chemotactic bacteria to change the location of initial settlement and exhibit positive chemotaxis and growth close to potentially inhibitory naphthalene spot source.

Introduction

The vadose zone, defined as the zone between the land surface and the groundwater table (12), has been considered for a long time as sterile or barely populated region of soil (20), and thus less important in soil ecology and its fertility (21). However, as later research in subsurface microbiology revealed that significant numbers of microbial populations inhabit the vadose zone environments (13), since then the unsaturated soils received increasing attention (12). Large variations in water availability and discontinuous nature of aquatic habitats result in the view of the vadose zone as rather harsh environment for microorganisms (13). Certain physiological adaptations have been recognized to be exhibited by the bacteria under the unsaturated conditions, allowing them to dwell at low water content (22, 23, 72). These, however, allow bacteria to survive rigorous water regimes, but do not enhance bacterial activity, e.g., mobility, which under unsaturated conditions is highly reduced relative to water-saturated soils (51). The tendency of motile bacteria to attach at the air-water interfaces further reduces their mobility (73). As such air-water interfaces are known to contain the highest microbial biomass (13), they are of a special interest for biodegradation of contaminants present in the subsurface. Of a particular interest are volatile contaminants, which due to fast and efficient diffusivity through the air-filled of the vadose zone (35), pose serious risk to groundwaters and other soil compartments (18). However, enhanced bioavailability of vapor-phase contaminants may also inhibit, e.g., bacterial dispersal, as it has been recently demonstrated with chemotactic naphthalene-degrading bacteria *Pseudomonas putida* (NAH7) strain G7 which exhibited negative chemotaxis when exposed to naphthalene via the gas-phase (78), although it is commonly known to be attracted by the dissolved concentration of naphthalene (79). By exhibiting negative chemotaxis bacteria were able to move to a distance representing a compromise of acceptable toxicity and sufficient substrate supply, as it has been previously demonstrated in plug chemotactic using chlorinated ethenes (80), or toluene (48). Therefore, bacterial chemotaxis is an excellent adaptation mechanism,

allowing chemotactic bacteria to find optimal conditions for their survival and further growth (81). By growth and contaminants degradation soil microbial populations could be useful in detoxification of potentially inhibitory concentrations of contaminants present in soil, as it has been previously demonstrated in liquid batch cultures (47, 82).

The aim of this study was to test whether growth of chemotactic naphthalene-degrading bacteria *Pseudomonas putida* (NAH7) G7 on potentially inhibitory vapor-phase naphthalene could be used as a detoxification mechanism reducing headspace NAPH concentrations to levels allowing chemotactic bacteria to closely approach NAPH spot sources. The influence of vapor-phase naphthalene gradients on growth and chemotactic response of the bacteria was investigated with vapor-phase NAPH supplied as the sole carbon substrate.

Material and Methods

Bacteria and culture conditions. Chemotactic naphthalene-degrading bacteria *Pseudomonas putida* (NAH7) G7 was cultivated, harvested and quantitatively analyzed as described in section 3.1.

Combined chemotaxis and growth experiments with vapor-phase NAPH. Chemotaxis and growth of *P.putida* G7 along vapor-phase gradients of naphthalene was approximated by quantitative (counts) and semi-quantitative (determination of colonized area) methods.

Quantitative analyzes of spatio-temporal growth and dispersal of P.putida G7 along vapor-phase gradients of naphthalene. Chemotactic NAPH-degrading bacteria were incubated in a mineral medium agar (0.3%), referred to as swimming agar, and exposed to vapor-phase gradients of naphthalene for 7, 21, 50 and 95 hours (t_7, t_{21}, t_{50}, t_{95}) (Figure 3.1). Growth and chemotactic response of *P.putida* G7 towards vapor-phase NAPH was determined by measuring spatial area of colonies formed close to NAPH source (sector A) and at further locations from the gas-phase substrate (sector B)

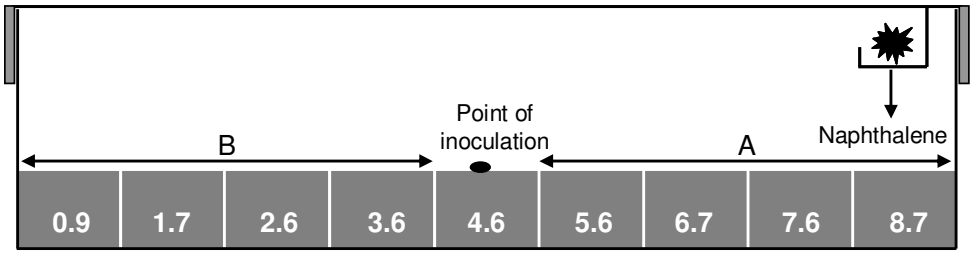

Figure 3.1. Schematic view of the experimental setup.

To minimize freely dissolved (i.e. bioavailable) NAPH concentrations in the agar, experiments with swimming agar containing activated carbon (AC) were performed. The preparation of the experiments, as well as samples harvesting and quantitative analyzes were performed according to the same regimes as described earlier in chapter 3, section 3.1.

Semi-quantitative method for growth and dispersal of P.putida G7 along vapor-phase NAPH gradients. The cells were spotted at the air-agar interface and exposed to vapor-phase NAPH for 21, 50 and 72 hours (t_{21}, t_{50}, and t_{72}) using the same experimental setup as in quantitative approach. Microbial growth and dispersal along gas-phase NAPH was approximated by photographic documentation, as well as by measuring visibly colonized surface area by the cells. The area colonized by the bacteria which are present at side of the Petri plate where NAPH crystals are present is compared to the area occupied by the bacteria present at the other side of the plate.

Results

Spatio-temporal growth and dispersal along vapor-phase gradients of NAPH. Chemotaxis and growth of *P.putida* G7 under the influence of vapor-phase NAPH were tested. Volatilization of a single spot source of solid NAPH in the headspace was expected to result in a directed vapor-phase NAPH gradients, according to previously findings (section 3.1, Figure 2). Based on former observations vapor-phase gradients of NAPH repelled chemotactic bacteria away from the source (section 3.1, Fig. 3). However, when testing the distribution of the cells at different periods available for movement, settlement and growth, obtained results

were not fully in accordance with previous observations. The bacteria present at the air-agar interface and exposed to vapor-phase substrate showed negative chemotaxis and growth after t_7 and t_{21}. As this trend was reversed, within t_{50} the cells changed the location of initial settlement, and moved towards the source, resulting in higher bacterial numbers found in close vicinity to NAPH hot spot at the end of the experiments (t_{95}). By quantifying bacterial numbers at the side of the Petri plate where NAPH crystals were placed (A) and at the other side of the plate (B) between t_7-t_{95}, the biomass colonizing the sector A increased by the factor of 5 (from $\approx 3 \times 10^5$ to 1×10^{10}), whereas occupying sector B - by the factor of 2 (from $\approx 8 \times 10^7$ to 2×10^9). This was reflected by the fact that *P.putida* G7 cells sensed and chemotactically responded to higher vapor-phase NAPH concentrations by active swimming along gas-phase gradients and developing growth in a vicinity to its hotpots, as shown by ca. 82% of the bacteria present in the half of the Petri dish next to the source (sector A) (Table 3.1).

Table 3.1. Relative abundance of *P.putida* G7 exposed to vapor-phase NAPH.

	Absence of AC		**Presence of AC**	
Time (h)/ Distance to NAPH (cm)	Sum cfu cm^{-2}	Fraction mobilized bacteria (%)	Sum cfu cm^{-2}	Fraction mobilized bacteria (%)
7: 0.9-3.7	2.85×10^5	0	n.a [(1)]	n.a
7: 5.6-8.7	7.62×10^7	100		
21: 0.9-3.7	1.39×10^7	5	1.28×10^8	52
21: 5.6-8.7	2.70×10^8	95	1.13×10^8	48
50: 0.9-3.7	2.92×10^9	72	8.54×10^7	70
50: 5.6-8.7	1.08×10^9	27	3.65×10^7	30
95: 0.9-3.7	1.03×10^{10}	82	8.22×10^8	76
95: 5.6-8.7	2.25×10^9	18	2.57×10^8	24

[(1)] Samples not analyzed.

Also photographic documentation (a), as well as measurements of the area colonized by the bacteria (b) showed significantly higher cell numbers in proximity to the substrate, where A indicates at directed movement and growth towards naphthalene source, B shows chemotactic movement away from gas-phase naphthalene (Fig. 3.2).

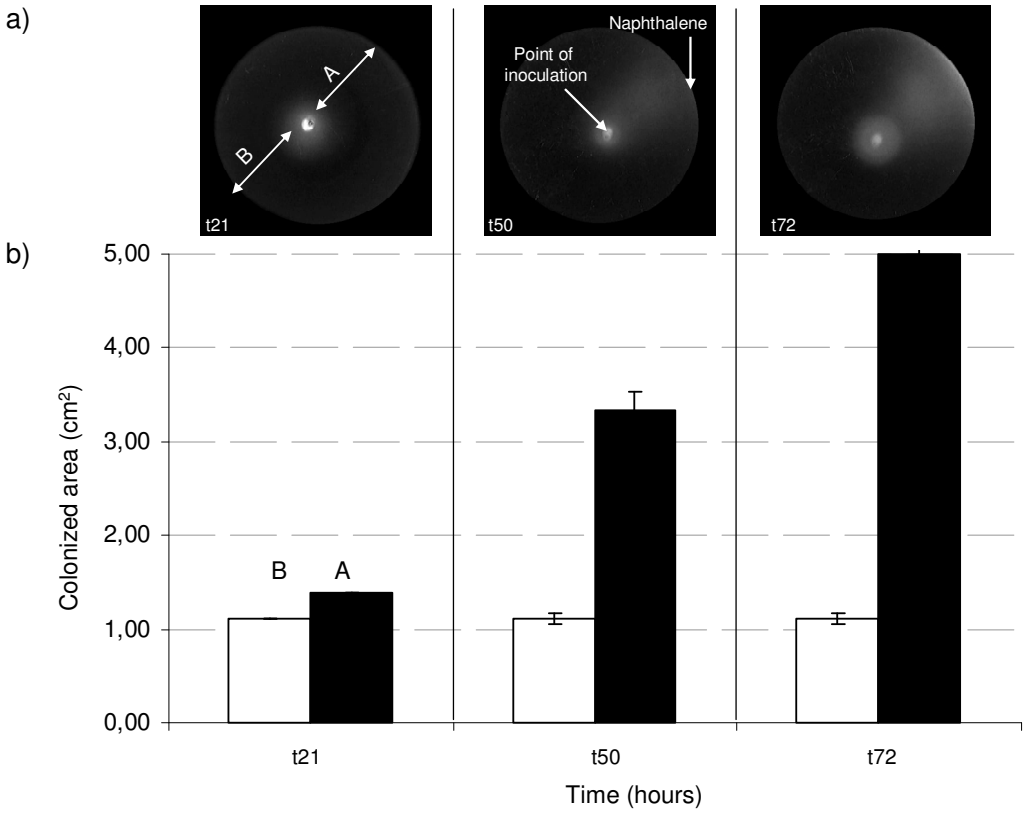

Figure 3.2. Semi-quantitative response of *P.putida* G7 towards vapor-phase NAPH.

Interestingly, a different response of the bacteria to vapor-phase gradients of NAPH was observed when agar with activated carbon (AC) was used. In AC-experiments, positive chemotaxis and thus higher growth in sector A, relative to sector B were observed at all times of the experiment, except for t_{21} where cells showed almost equal distribution on both sides of the Petri plate (sector A and B). Furthermore, the presence of AC appeared to reduce bacterial growth, relative to the experiments where AC was excluded from the agar, as only slight increase in cell numbers was observed (from $\approx 1 \times 10^8$ to 8×10^8 in sector A, and from $\approx 1 \times 10^8$ to 3×10^8 in sector B). Nevertheless, *P.putida* G7 cells responded to vapor-phase NAPH

by developing growth and exhibiting positive chemotaxis, with ca. 76% of the bacteria being present close to the spot source after t_{95}.

Discussion

The role of NAPH consumption on the spatio-temporal distribution of P.putida G7. As it has been previously demonstrated the bacteria were repelled by the vapor-phase gradients of NAPH (chapter 3, section 3.1). It was further assumed that the efficient gas-phase diffusion was the reason for observed negative chemotaxis and resulted in possible toxic NAPH flux to the cells. In the present study we tested whether substrate consumption could be a detoxification mechanism reducing its high and potentially inhibitory concentrations in the headspace, allowing for growth and dispersal along vapor-phase gradients of naphthalene. NAPH crystals were placed in the headspace above swimming agar, allowing cells to swim and develop growth. Figure 3.2 shows that *P.putida* G7 exhibit negative chemotaxis and growth after t_7 and t_{21} when exposed to NAPH gradients via the gas-phase. However, this trend was reversed after t_{50}, where cells change their location of initial settlement and moved towards the substrate, showing positive chemotaxis and significant growth close to its crystals after t_{95}.

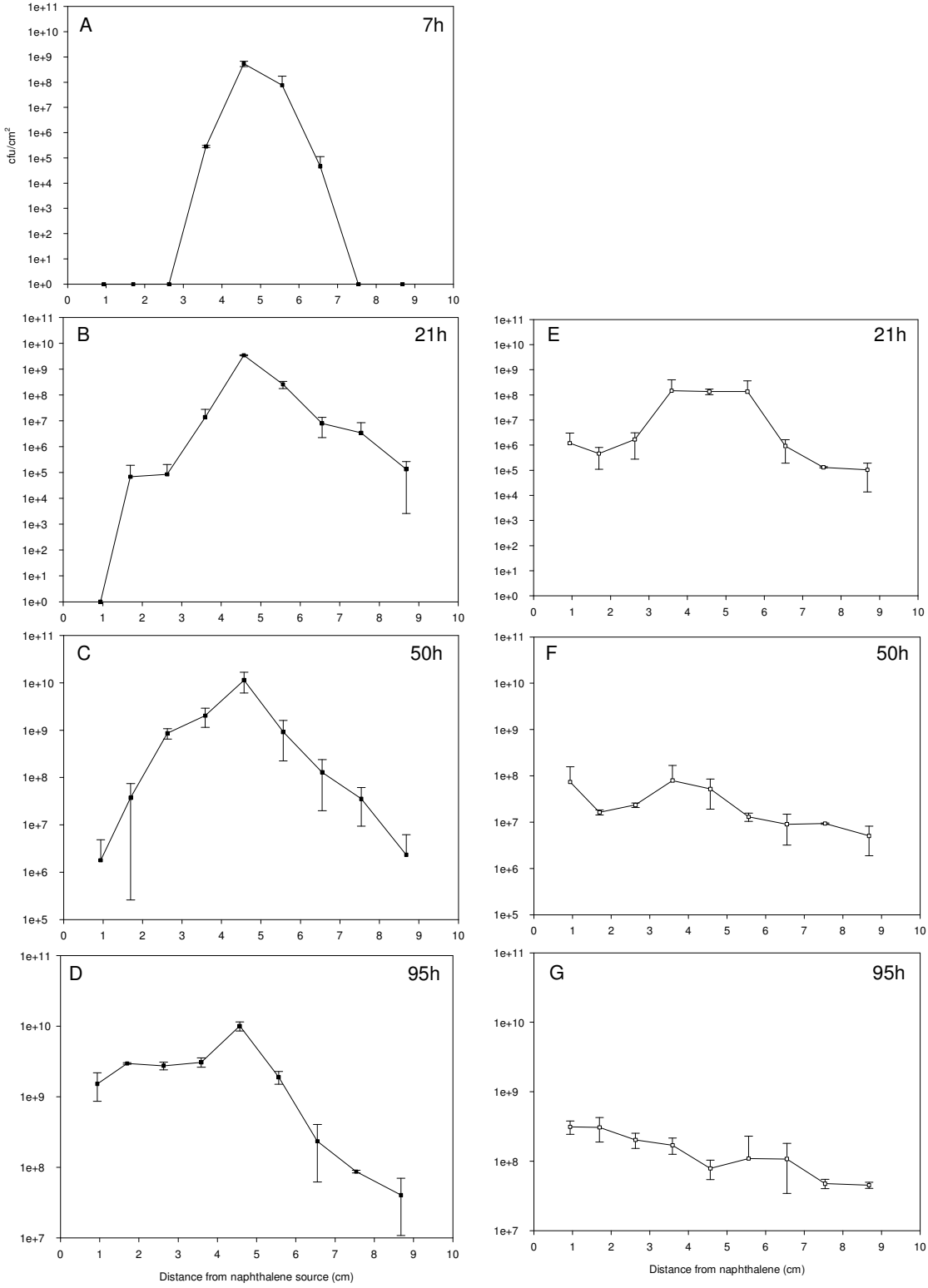

Figure 3.3. Spatial distribution of *P.putida* G7 along vapor-phase gradients of NAPH in the absence (filled symbols) and presence (opened symbols) of AC after t_7, t_{21}, t_{50} and t_{95}.

Similar to earlier findings, the bacteria were most likely repelled by vapor-phase NAPH gradients (t_7-t_{21}), and after partitioning of NAPH into the agar and by the development of subsequent concentration gradient in the agar, the cells were attracted by its aqueous gradients (t_{50}-t_{95}) (section 3.1). However, since in the present study the bacteria were allowed to grow on vapor-phase NAPH, thus observed results are most likely caused by both effects, its aqueous concentration gradients developing in the agar, and growth on NAPH vapors, as indicated by increased numbers of the bacteria in vicinity to the source from $\approx 3 \times 10^5$ after t_7 to 1×10^{10}cells after t_{95}. Such results indicate that via substrate consumption the headspace concentrations might be reduced to levels allowing for growth and positive chemotaxis towards the source. This is further supported by the results obtained from the experiments where AC-agar was used to minimize dissolved NAPH concentrations in the agar. As AC was shown to be an efficient sink for aqueous NAPH, reducing its water–dissolved concentration to tiny fractions, one can assume that in the presence of AC vapor-phase NAPH was the principle chemoeffector for chemotactic bacteria. Thus, observed positive chemotaxis and growth in regions where headspace substrate concentrations were the highest (sector A) show that by providing sufficient biomass the impact of vapor-phase NAPH gradients on growth and chemotactic response of *P.putida* G7 could be reduced. Hence, our results unambiguously point out at the detoxifying role of naphthalene consumption. Contaminants degradation as an efficient detoxification mechanism has been already described in literature, with chemicals dissolved in a liquid medium (47, 82). Microbial degradation has been approximated by the decrease in final contaminants concentrations, whereas contaminants detoxification was related to decrease in mutagenic potential and was measured by using so-mutagenicity test (AmesTest). By coupling the degradation and mutagenic potential of tested chemicals it has been demonstrated that contaminant-degrading bacteria could be used for detoxification of contaminated environments (47).

Conclusions

Our data reveal that substrate consumption changes the location of initial settlement of chemotactic bacteria and hence allows closer approach of NAPH source. Substrate utilization reduces the headspace concentrations to levels which gives privilege to the degrading microorganisms, and thus reduces the impact of vapor-phase contaminants gradients on bacterial behavior. By sensing gas-phase NAPH gradients chemotactic bacteria could avoid potentially inhibitory headspace concentrations and thus position themselves at a distant representing a compromise of acceptable toxicity and sufficient substrate supply, as shown for instance when testing chemotactic response of *Pseudomonas aeruginosa* strain PAO1 towards chlorinated ethenes (80). By seeking suitable conditions for further growth and increasing cell biomass, bacteria could reduce headspace naphthalene concentrations to levels allowing for closer chemical approach. Thus, bacterial chemotaxis is an excellent adaptation strategy allowing immediate response towards environmental conditions (53). Thus, obtained results point out at the importance of bacterial chemotaxis in detoxification of polluted environments (83).

Chapter 4
Final remarks

The main objective of this thesis was to investigate the interplay between the diffusive gas-phase transport of naphthalene and the activity of the naphthalene-degrading bacteria, and its repercussion on the vapor-phase substrate degradation.

4.1 The significance and practical implications of obtained results

Literature normally suggests that bacterial chemotaxis requires at least some solubility of the target chemical, i.e. sufficient to generate an aqueous-phase concentration gradient (68). However, based on the obtained results it seems to be possible that also poorly water soluble contaminants give rise to bacterial chemotaxis via their gas-phase distribution at concentrations as low as 10^{-9} mol L^{-1}, when present in the unsaturated porous media (for more details please refer to section 3.1). Thus, in principle, one may speculate that chemotactic bacteria are capable of 'olfactory' swimming. Olfaction, defined as sensing and following volatile compounds present in the environment, is well documented in higher eukaryotes, i.e. animals, plants, yeasts, and it plays an important role in searching for food resources, as well as in sensing predators or other organisms (71). Hence, bacteria exhibiting olfactory swimming by 'smelling' vapor-phase contaminants and following their concentration gradients could be of a great importance in the degradation of volatile compounds present in the vadose zone and aquifers. In order to theoretically evaluate whether and to which extent bacterial chemotaxis along vapor-phase contaminants' gradients is relevant for their biodegradation, 22 compounds which vary in their vapor pressures (*Vp*), Henry's law constants (*H*) and aqueous solubilities (*Caq*) were chosen. Based on the ideal gas formula, expressed by:

$$Cg = \frac{Po}{RT},$$

where *Po* is the contaminant vapor pressure (atm), *R* is the gas constant for volatile compounds (*R*=8,206x10^{-2} (dimensionless)), and T is the temperature (K) (26), the gaseous

concentrations (*Cg*) for each individual contaminant were calculated (assuming room temperature) (Table 4.1).

Table 4.1. Some examples of volatile compounds and their physico-chemical characteristics.

	Vapor pressure Vp (atm)	Henry's constant H (L atm mol^{-1})	Gaseous concentration Cg (mol L^{-1})	Aqueous solubility Caq (mol L^{-1})
Methane	2.75×10^{2}	6.61×10^{2}	1.13×10^{1}	1.51×10^{-3}
Ethane	3.98×10^{1}	4.90×10^{2}	1.63×10^{0}	2.04×10^{-3}
Propane	9.33×10^{0}	7.08×10^{2}	3.81×10^{-1}	9.07×10^{-4}
Chloromethane	5.75×10^{0}	9.55×10^{0}	2.35×10^{-1}	1.10×10^{-1}
Chloroethane (Vinyl chloride)	3.89×10^{0}	2.24×10^{1}	1.59×10^{-1}	9.30×10^{-2}
Dichloromethane	5.89×10^{-1}	2.57×10^{0}	2.41×10^{-2}	1.50×10^{-1}
Trichloromethane	2.57×10^{-1}	3.98×10^{0}	1.05×10^{-2}	6.70×10^{-2}
n-hexane	2.04×10^{-1}	1.38×10^{3}	8.34×10^{-3}	1.51×10^{-4}
Benzene	1.26×10^{-1}	5.50×10^{0}	5.14×10^{-3}	2.30×10^{-2}
1,2-dichloroethane	9.12×10^{-2}	1.07×10^{0}	3.73×10^{-3}	8.80×10^{-2}
Toluene	3.80×10^{-2}	6.67×10^{0}	1.55×10^{-3}	5.62×10^{-3}
Chlorobenzene	1.58×10^{-2}	3.55×10^{0}	6.48×10^{-4}	4.35×10^{-3}
Ethylbenzene	1.26×10^{-2}	$7.94\times10^{0}7$	5.14×10^{-4}	1.58×10^{-3}
1,4-dichlorobenzene	9.12×10^{-4}	2.24×10^{0}	3.73×10^{-5}	7.14×10^{-1}
Phenol	2.57×10^{-4}	4.00×10^{-4}	1.05×10^{-5}	8.80×10^{-1}
Hexadecane	1.86×10^{-6}	1.17×10^{2}	4.61×10^{-8}	1.58×10^{-8}
Naphthalene	1.05×10^{-4}	4.30×10^{-2}	4.28×10^{-6}	2.45×10^{-4}
Pentachlorobenzene	8.91×10^{-5}	7.94×10^{0}	3.64×10^{-6}	2.72×10^{-6}
Biphenyl	1.00×10^{-5}	---	4.09×10^{-7}	1.32×10^{-4}
Phenanthrene	1.62×10^{-7}	3.00×10^{-2}	6.63×10^{-9}	6.31×10^{-6}
Anthracene	7.94×10^{-9}	2.30×10^{-3}	3.25×10^{-10}	3.47×10^{-7}
Pyrene	6.03×10^{-9}	9.00×10^{-3}	2.46×10^{-10}	6.76×10^{-7}

Calculated values of the gaseous concentrations were compared with the *Cg* value for naphthalene, which was obtained from the study where the influence of vapor-phase gradients of naphthalene on the chemotactic response of the bacteria was tested (for more details please refer to chapter 3, section 3.1). As the value of 10^{-9} mol L^{-1} was the minimal measured gas-

phase naphthalene concentration that provoked chemotactic response of *P.putida* G7, it was used as the threshold (reference) value to distinguish between compounds which, theoretically, could cause chemotactic movement of the bacteria along their vapor-phase concentration gradients (*Cg* values higher than the threshold), and those which would not influence such behavior (*Cg* values lower than the threshold). Similarly, Henry's constant for naphthalene ($H = 4.30\times10^{-2}$ atm) was also used as the reference and was compared with the other values. Interestingly, obtained results were not the same for the both parameters tested (*Cg* and *H*), as shown on Figure 4.1. On this scheme gaseous concentrations (*Cg*) and Henry's constants (*H*) of the target compounds are plotted according to their decreasing *Cg* and *H* values, and chemicals above the threshold value are shown as black squares (A), whereas those below the reference value - as grey triangles (B).

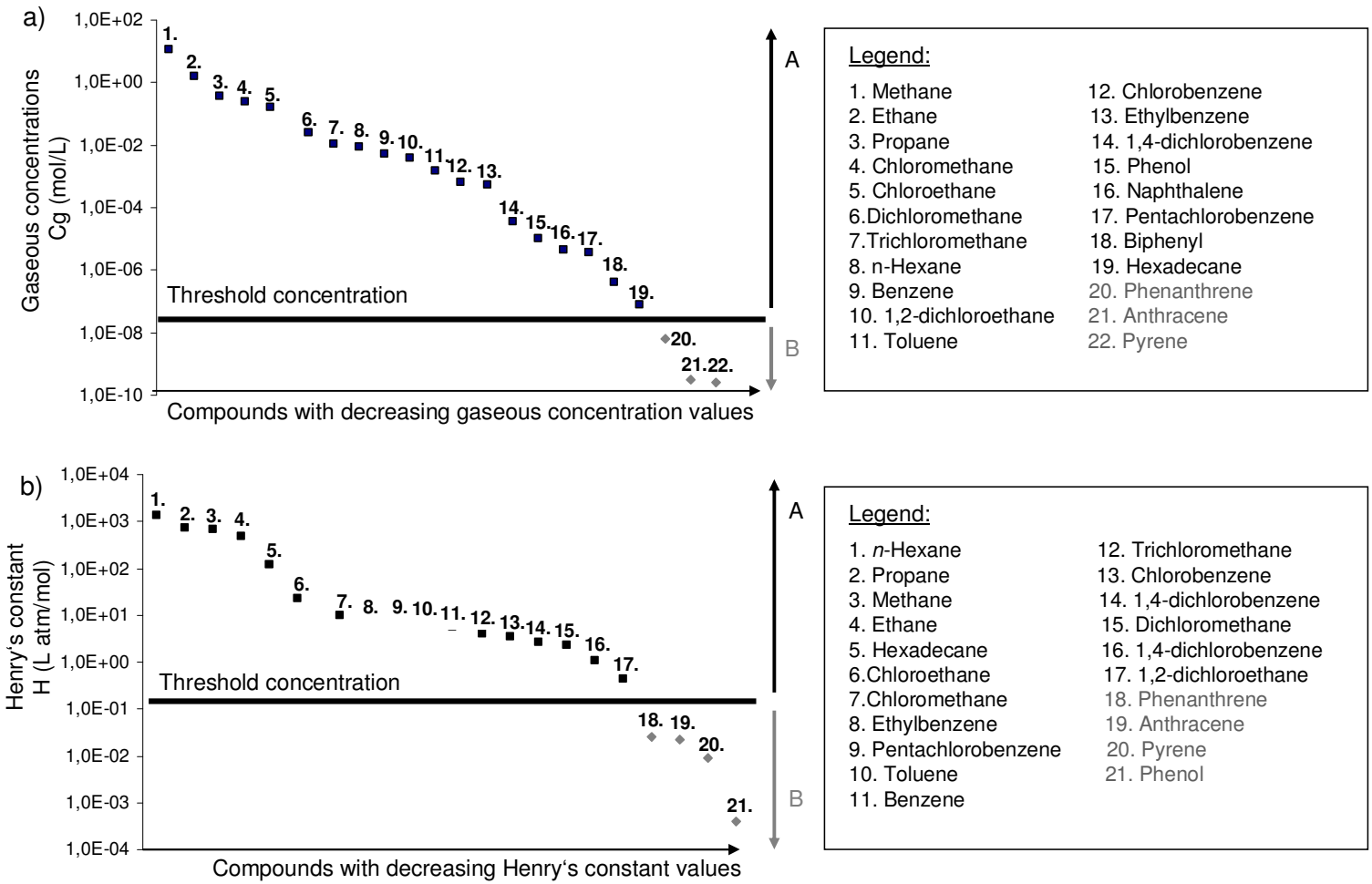

Figure 4.1. Theoretical assumption of the relevance of bacterial chemotaxis in the degradation of volatile compounds.

Different results obtained when testing two distinct parameters demonstrate that, when applying appropriate remediation techniques one should be careful with the data interpretation, not to underestimate the observed trend. Although based on the above mentioned assumptions one could speculate that bacterial chemotaxis could be of a great relevance in the degradation of various volatile and semi-volatile chemicals, it would be still necessary to perform further laboratory studies. It is because bacteria do not exhibit the same tolerance to all environmental contaminants and, hence, different gaseous concentrations are expected to result in distinct chemotactic responses. In addition, as so far bacterial chemotaxis was mostly tested towards aqueous concentration gradients of soil contaminants (55, 75, 80, 81), the information about the swimming along vapor-phase contaminant gradients is scarce. Despite some attempts to test bacterial chemotaxis towards various volatile compounds (i.e. ethylene, benzene and chlorinated ethenes (67, 82)), these studies used plug agarose assays (62) where water-bound bacteria were exposed to agarose-embedded contaminants. They thus tended to neglect situations likely to be found in the unsaturated soils, where bacteria may be under the influence of vapor-phase chemicals, e.g., emanating from contaminated aquifers.

Furthermore, the results obtained in this thesis demonstrated that vapor-phase gradients of naphthalene significantly influenced the spatio-temporal growth of the bacteria. Microbial activity was strongly dependent on the location of initial settlement of naphthalene-degrading bacteria (air-agar interface versus water-phase), and on the amount of biomass (low cell density versus high bacterial biomass). The latter findings suggest that active naphthalene consumption was an efficient detoxification mechanism reducing the headspace substrate concentrations to levels allowing for further cell development and for positive chemotaxis. Thus, the results show that given the right conditions for microbial activity contaminant-degrading bacteria present in the vadose zone may be an excellent natural bio-filter for gas-phase volatile contaminants emanating from contaminated groundwater or soil. Such findings contribute to better understanding of, so-called vertical soil systems (or vertical soil filters),

which currently are being tested at the Helmholtz-Center for Environmental Research – UFZ, in Leipzig (Germany), within the SAFIRA II project. Due to long-term industrial activities and, hence, highly contaminated groundwater the city Leuna (Germany) was chosen as a study area. The main objective of this project is to understand which processes are responsible for the removal of volatile contaminants, and to study their distribution within the unsaturated subsurface soils and groundwaters. The investigated vertical soil system consists of approximately 25 cm thick upper layer (composed of expanded clay material of diameter 8 – 16 mm), and ca. 120 cm thick lower layer (containing expanded clay pellets of diameter 3 - 6 mm). The latter is to mimic the vadose zone conditions. Water contaminated with various volatile chemicals (i.e. BTEX compounds, MTBE, ammonia, toluene, chlorinated benzenes, phenols, chlorinated phenols, xylenes and pesticides) is injected within the upper part of the filter, and after passing through the unsaturated zone, it is re-collected on the bottom of lower layer. Based on measured concentrations at the in- and out-let it is possible to quantify the mass of eliminated volatile contaminants. By a combination of mathematical description models, contaminants properties and physicochemical soil characteristics, microbial degradation was shown to be the major processes being responsible for the highest removal mass of the tested contaminants. On the contrary, volatilization or sorption to solid soil materials contributed only to minor or negligible amounts to overall removal rate (83). By coupling mathematical description models together with laboratory studies (please refer to chapter 2, section 2.1) one can better understand microbial role in the degradation of contaminant vapors present in the vadose zone and aquifers.

Furthermore, the obtained results suggest that perhaps it could be possible to use the vadose zone bacteria as natural sink for contaminants vapors present in the air. As by means of biodegradation the diffusive transport of volatile contaminants would be directed towards the subsurface, it may be possible to create steeper concentration gradients along vertical soil systems. As already suggested by Pernthaler et al (2008) bacteria possessing capacities to

degrade volatile contaminants could be used as a natural tools reducing, e.g., the concentrations of greenhouse gases present in the atmosphere (84). By providing proper soil conditions promoting growth of such microbes one could use i.e. methane-oxidizing bacteria to alleviate global warming.

4.2 Further research needs

By testing chemotactic responses of the various contaminant-degrading bacteria towards a numbers of volatile compounds it may be possible to create microbial landscapes. This is of a great significance as it would allow to test how the bacteria behave under real soil conditions. As volatile contaminants 'travel' over long distances within soil they are also most likely to create, so-called 'odor landscapes', with different spatial odorant concentrations. Thus, under such conditions bacterial chemotaxis possibly could influence the spatio-temporal contaminant degradation, leading to changes in soil microbial ecology (70). In addition, by observing dynamics of such soil microbial communities it could be interesting to retrieve bacteria showing peculiar reactions and analyze them based on their morphology, physico-chemistry, biochemistry or behavioral characteristics. Such analyses would provide new information needed to better understand which of the specific characteristics are responsible for distinct interactions with the environment, e.g., which cell properties are involved in microbial resistance to potentially toxic compounds, or which properties allow soil microbial populations to develop suitable strategies modifying exposure to contaminant bioavailability.

In this thesis it has been demonstrated that soil bacteria present in the vadose zone may be used as natural bio-filters for volatile contaminants emanating from contaminated groundwaters, as well as could be an excellent tool to reduce air-contamination by capturing chemical vapors present in the atmosphere.

References

1. Stolp H. 1988. Microbial ecology. Cambridge, University Press.

2. Lavelle P. 2005. Soil ecology. Dordrecht Boston, Kluwer Academic Publishers.

3. Rossello-Mora, R., Amann, R. 2001. The species concept for prokaryotes. FEMS Microbiology Reviews 25, 39-67.

4. Atlas, R. 1993. Microbial ecology: fundamentals and applications. 3rd Edition. Redwood City California, Benjamin/Cummings Pub. Co.

5. Federle, T.W., Dobbins, D.C., Thornton-Manning, J.R., Jones, D.D. 1986. Microbial biomass, activity, and community structure in subsurface soils. Ground Water 24, 365-374.

6. Torsvik, V., Ovreas, L. 2002. Microbial diversity and function in soil: from genes to ecosystems. Current Opinion in Microbiology 5, 240-245.

7. Alexander, M. 1999. Biodegradation and bioremediation. 2nd Edition. San Diego, Academic Press.

8. Anderson, T. 1994. Bioremediation through rhizosphere technology: developed from a symposium sponsored by the Division of Agrochemicals and the Division of Environmental Chemistry at the 206th national meeting of the. Washington DC, American Chemical Society.

9. Peng, R.H., Xiong, A.S., Xue, Y., Fu, X.Y, Gao, F., Zhao, W., Tian, Y.S., Yao, Q.H. 2008. Microbial biodegradation of polyaromatic hydrocarbons. FEMS Microbiology Reviews 32, 927-955.

10. Maier R. 2009. Environmental microbiology. 2nd Edition. Burlington MA, Academic Press.

11. Berkowitz, B., Silliman, S.E., Dunn, A.M. 2004. Impact of the capillary fringe on local flow, chemical migration, and microbiology. Vadose Zone Journal 3, 534-548.

12. Holden, P.A., Fierer, N. 2005. Microbial processes in the vadose zone. Vadose Zone Journal 4, 1-21.

13. Or, D., Smets, B.F., Wraith, J.M., Dechesne, A., Friedman, S.P. 2007. Physical constraints affecting bacterial habitats and activity in unsaturated porous media – a review. Advances in Water Resources 30, 1505-1527.

14. Kieft, T.L. 1999. Microbial ecology of the vadose zone. Atlantic Canada Society for Microbial Ecology, Halifax, Canada.

15. Marr, L.C., Booth, E.C., Andersen, R.G., Widdowson, M.A., Novak, J.T. 2006. Direct volatilization of naphthalene to the atmosphere at a phytoremediation site. Environmental Science and Technology 40, 5560-5566.

16. Schäfer, A., Ustohal, P., Harms, H., Stauffer, F., Themistoceles, D., Zehnder, A.J.B. 1998. Transport of bacteria in unsaturated porous media. Journal of Contaminant Hydrology 33, 149-169.

17. Wan, J., Wilson, J.L., Kieft, T.L. 1994. Influence of the gas-water interface on transport of microorganisms through unsaturated porous media. Applied and Environmental Microbiology 60, 509-515.

18. Hohener, P., Dakhel, N., Christophersen, M., Broholm, M., Kjeldsen, P. 2006. Biodegradation of hydrocarbons vapors: Comparison of laboratory studies and field investigations in the vadose zone at the emplaced fuel source experiment, Airbase Vaerlose, Denmark. Journal of Contaminant Hydrology 88, 337-358.

19. Dechesne, A., Owsianiak, M., Bazire, A., Grundmann, G.L., Binning, P.J., Smets, B.F. 2010. Biodegradation in a partially saturated sand matrix: compounding effects of water content, bacterial spatial distribution, and motility. Environmental Science and Technology 44, 2386-2392.

20. Chapelle, F.H. 1999. Bioremediation of petroleum hydrocarbon-contaminated ground water: The perspectives of history and hydrology. Ground Water 37, 122-132.

21. Gerba, C.P., McNabb, J.F. 1981. Microbial aspects of groundwater pollution. ASM News 47, 326-329.

22. Crowe, J.H., Crowe, L.M., Chapman, D. 1984. Preservation of membranes in anhydrobiotic organisms: The role of trehalose. Science 223, 701-703.

23. Alvarez, H., Silva, R.A., Cesari, A.C., Zamit, A.L., Peressutti, S.R., Reichelt, R., Keller, U., Malkus, U., Rasch, C., Maskow, T., Mayer, F., Steinbüchel, A. 2004. Physiological and morphological responses of the soil bacterium *Rhodococcus opacus* strain PD630 to water stress. FEMS Microbiology Ecology 50, 75-86.

24. Pasteris, G., Werner, D., Kaufmann, K., Höhener, P. 2002. Vapor phase transport and biodegradation of volatile fuel compounds in the unsaturated zone: a large scale lysimeter experiment. Environmental Science and Technology 36, 30-39.

25. Brown, T. 2008. Chemistry: the central science. 11th Edition. Harlow Prentice Hall.

26. Schwarzenbach, R. 2003. Environmental organic chemistry. 2nd Edition. Hoboken N.J., John Wiley & Sons.

27. Lewis, T.E., Crockett, A.B., Siegrist, R.L. 1994. Soil sampling and analysis for volatile organic compounds. Environmental Monitoring and Assessment 30, 213-246.

28. Kaufmann, K., Christophersen, M., Buttler, A., Harms, H., Höhener, P. 2004. Microbial community response to petroleum hydrocarbon contamination in the unsaturated zone at the experimental field site Vaerlose, Denmark. FEMS Microbiology Ecology 48, 387-399.

29. Hunt, J.R., Holden, P.A., Firestone, M.K. 1995. Coupling transport and biodegradation of VOCs in surface and subsurface soils. Environmental Health Perspectives 103, 75-78.

30. Leff, J.W., Fierer, N. 2008. Volatile organic compound (VOC) emissions from soil and litter samples. Soil Biology and Biochemistry 40, 1629-1636.

31. McNeal, K.S., Herbert, B.E. 2009. Volatile organic metabolites as indicators of soil microbial activity and community composition shifts. Soil Science Society of America Journal 73, 579-588.

32. Samanta, S.K., Singh, O.V., Jain, R.K. 2002. Polycyclic aromatic hydrocarbons: environmental pollution and bioremediation. Trends in Biotechnology 20, 243-248.

33. Wild, E., Dent, J., Thomas, G.O., Jones, K.C. 2006. Visualizing the air-to-leaf transfer and within-leaf movement and distribution of phenanthrene: Further studies utilizing two-photon excitation microscopy. Environmental Science and Technology 40, 907-916.

34. Moldrup, P., Olesen, T., Komatsu, T., Schjonning, P., Rolston, D.E. 2001. Tortuosity, diffusivity, and permeability in the soil liquid and gaseous phases. Soil Science Society of America Journal 65, 613-623.

35. Christophersen, M., Broholm, M.M., Mosbaek, H., Karapanagioti, H.K., Burganos, V.N., Kjeldsen, P. 2005. Transport of hydrocarbons from an emplaced fuel source experiment in the vadose zone at Airbase Vaerløse, Denmark. Journal of Contaminant Hydrology 81, 1-33.

36. Matsumura, F. 1989. Biotic degradation of pollutants. Ecotoxicology and climate 1989;79-89.

37. Providenti, M.A., Lee, H., Trevors, J.T. 1993. Selected factors limiting the microbial degradation of recalcitrant compounds. Journal of Industrial Microbiology 12, 379-395.

38. Bosma, T.N.P., Middeldorp, P.J.M., Schraa, G., Zehnder, A.J.B. 1997. Mass transfer limitation of biotransformation: Quantifying bioavailability. Environmental Science and Technology 31, 248-252.

39. Semple, K.T., Doick, K.J., Wick, L.Y., Harms, H. 2007. Microbial interactions with organic contaminants in soil: Definitions, processes and measurement. Environmental Pollution 150, 166-176.

40. Johnsen, A.R., Wick, L.Y., Harms, H. 2005. Principles of microbial PAH-degradation in soil. Environmental Pollution 133, 71-84.

41. Cerniglia, C.E. 1992. Biodegradation of polycyclic aromatic hydrocarbons. Biodegradation 3, 351-368.

42. Best, J.B. 1995. The interference of intracellular enzymatic properties from kinetic data obtained on living cells. I. Some kinetic considerations regarding an enzyme enclosed by a diffusion barrier. Journal of Cellular and Comparative Physiology 46, 1-27.

43. Simoni, S.F., Schäfer, A., Harms, H., Zehnder, A.J.B. 2001. Factors affecting mass transfer limited biodegradation in saturated porous media. Journal of Contaminant Hydrology 50, 99-120.

44. Han, K., Levenspiel, O. 1998. Extended monod kinetics for substrate, product, and cell inhibition. Biotechnology and Bioengineering 32, 430-447.

45. Mulchandani, A., Luong, J. 1989. Microbial inhibition kinetics revisited. Enzyme and Microbial Technology 11, 66-73.

46. Kristensen, A.H., Henriksen, K., Mortensen, L., Scow, K.M., Moldrup, P. 2010. Soil physical constraints on intrinsic biodegradation of petroleum vapors in a layered subsurface. Vadose Zone Journal 9, 137-147.

47. Juhasz, A.L., Stanley, G.A., Britz, M.L. 2000. Microbial degradation and detoxification of high molecular weight polycyclic aromatic hydrocarbons by *Stenotrophomonas maltophilia* strain VUN 10,003. Letters in Applied Microbiology 30, 396-401.

48. Parales, R.E., Ditty, J.L., Harwood, C.S. 2000. Toluene-degrading bacteria are chemotactic towards the environmental pollutants benzene, toluene, and trichloroethylene. Applied and Environmental Microbiology 66, 4098-4104.

49. Kohlmeier, S., Smits, T.H.M., Ford, R.M., Keel, C., Harms, H., Wick, L.Y. 2005. Taking the fungal highway: Mobilization of pollutant-degrading bacteria by fungi. Environmental Science and Technology 39, 4640-4646.

50. Furuno, S., Päzolt, K., Rabe, C., Neu, T.R., Harms, H., Wick, L.Y. 2009. Fungal mycelia allow chemotactic dispersal of polycyclic aromatic hydrocarbon-degrading bacteria in water-unsaturated systems. Environmental Microbiology 12, 1391-1398.

51. Harshey, R.M. 2003. Bacterial motility on a surface: many ways to a common goal. Annual Review of Microbiology 57, 249-273.

52. Strauss, I., Frymier, P.D., Hahn, C.M., Ford, R.M. 1995. Analysis of bacterial migration: II. Studies with multiple attractant gradients. AIChE Journal 41, 402-414.

53. Alexandre, G., Greer-Phillips, S., Zhulin, I.B. 2004. Ecological role of energy taxis in microorganisms. FEMS Microbiology Reviews 28, 113-126.

54. Pandey, G., Jain, R.K. 2001. Bacterial chemotaxis toward environmental pollutants: Role in bioremediation. Applied and Environmental Microbiology 68, 5789-5795.

55. Law AMJ, Aitken MD. 2005. Continuous-flow capillary assay for measuring bacterial chemotaxis. Applied and Environmental Microbiology 71, 3137-3143.

56. Alexandre, G., Zhulin, I.B. 2001. More than one way to sense chemicals. Journal of Bacteriology 183, 4681-4686.

57. Pedit, J.A., Marx, R.B., Miller, C.T., Aitken, M.D. 2001. Quantitative analysis of experiments on bacterial chemotaxis to naphthalene. Biotechnology and Bioengineering 78, 626-634.

58. Widman, M.T., Emerson, D., Chiu, C.C., Worden, R.M. 1997. Modeling microbial chemotaxis in a diffusion gradient chamber. Biotechnology and Bioengineering 55, 191-205.

59. Harwood, C.S., Fosnaugh, K., Dispensa, M. 1989. Flagellation of *Pseudomonas putida* and analysis of its motile behavior. Journal of Bacteriology 171, 4063-4066.

60. Adler, J. 1973. A method for measuring chemotaxis and use of the method to determine optimum conditions for chemotaxis by *Escherichia coli*. Microbiology 74, 77-91.

61. Grimm, A.C., Harwood, C.S. 1997. Chemotaxis of *Pseudomonas* spp. to the polyaromatic hydrocarbon naphthalene. Applied and Environmental Microbiology 63, 4111-4115.

62. Yu, H.S., Alam, M. 1997. An agarose-in-plug bridge method to study chemotaxis in the archaeon *Halobacterium salinarum*. FEMS Microbiology Letters 156, 265-269.

63. Harms, H., Wick, L.Y. 2006. Dispersing pollutant-degrading bacteria in contaminated soil without touching it. Engineering in Life Sciences 6, 252-260.

64. Marx, R.B., Aitken, M.D. 2000. Bacterial chemotaxis enhances naphthalene degradation in a heterogeneous aqueous system. Environmental Science and Technology 34, 3379-3383.

65. Ford, R., Harvey, R. 2007. Role of chemotaxis in the transport of bacteria through saturated porous media. Advances in Water Resources 30, 1608-1617.

66. Nichols, N.N., Harwood, C.S. 1997. PcaK, a high-affinity permease for the aromatic compounds 4-hydroxybenzoate and protocatechuate from *Pseudomonas putida*. Journal of Bacteriology 179, 5056-5061.

67. Vardar, G., Barbieri, P., Wood, T.K. 2005. Chemotaxis of *Pseudomonas stutzeri* OX1 and *Burkholderia cepacia* G4 toward chlorinated ethenes. Applied Microbiology and Biotechnology 66, 696-701.

68. Ortega-Calvo, J.J., Marchenko, A.I., Vorobyov, A.V., Borovick, R.V. 2003. Chemotaxis in polycyclic aromatic hydrocarbon-degrading bacteria isolated from coal-tar- and oil-polluted rhizospheres. FEMS Microbiology Ecology 44, 373-381.

69. Lanfranconi, M.P., Alvarez, H.M., Studdert, C.A. 2003. A strain isolated from gas oil-contaminated soil displays chemotaxis towards gas oil and hexadecane. Environmental Microbiology 5, 1002-1008.

70. Moore, P., Crimaldi, J. 2004. Odor landscapes and animal behavior: tracking odor plumes in different physical worlds. Journal of Marine Systems 49, 55-64.

71. Nijland, R., Burgess, J.G. 2010. Bacterial olfaction. Biotechnology Journal 5, 974-977.

72. Welsh, D.T. 2000. Ecological significance of compatible solute accumulation by micro-organisms: from single cells to global climate. FEMS Microbiology Reviews 24, 263-290.

73. Schäfer, A., Harms, H., Zehnder, A.J.B. 1998. Bacterial accumulation at the air-water interface. Environmental Science and Technology 32, 3704-3712.

74. Hanzel, J., Harms, H., Wick, L.Y. 2010. Bacterial chemotaxis along vapor-phase gradients of naphthalene. Environmental Science and Technology 44, 9304-9310.

75. Marx, R.B., Aitken, M.D. 1999. Quantification of chemotaxis to naphthalene by *Pseudomonas putida* G7. Applied and Environmental Microbiology 65, 2847-2852.

76. Shitashiro, M., Kato, J., Fukumura, T., Kuroda, A., Ikeda, T., Takiguchi, N., Ohtake, H. 2003. Evaluation of bacterial aerotaxis for its potential use in detecting the toxicity of chemicals to microorganisms. Journal of Biotechnology 101, 11-18.

77. Paul, D., Singh, R., Jain, R.K. 2006. Chemotaxis of *Ralstonia* sp. SJ98 towards *p*-nitrophenol in soil. Environmental Microbiology 8, 1797-1804.

78. Aprill, W., Sims, R., Sims, J., Matthews, J. 1990. Assessing detoxification and degradation of wood preserving and petroleum wastes in contaminated soil. Waste Management & Research 8, 45-65.

79. Harwood, C.S., Rivelli, M., Ornston, L.N. 1984. Aromatic acids are chemoattractants for *Pseudomonas putida.* Journal of Bacteriology 160, 622-628.

80. Law, A.M.J., Aitken, M.D. 2003. Bacterial chemotaxis to naphthalene desorbing from a nonaqueous liquid. Applied and Environmental Microbiology 69, 5968-5973.

81. Grimm, A.C., Harwood, C.S. 1997. Chemotaxis of *Pseudomonas* spp. to the polyaromatic hydrocarbon naphthalene. Applied and Environmental Microbiology 63, 4111-4115.

82. Liu, X., Wood, P.L., Parales, J.V., Parales, R.E. 2009. Chemotaxis to pyrimidines and identification of a cytosine chemoreceptor in *Pseudomonas putida*. Journal of Bacteriology 191, 2909-2916.

83. De Biase, C., Reger, D., Schmidt, A., Jechalke, S., Reiche, N., Martínez-Lavanchy, P.M., Rosell, M., Van Afferden, M., Maier, U., Oswald, S.E., Thullner, M. 2011. Treatment of volatile organic contaminants in a vertical flow filter: Relevance of different removal processes. Ecological Engineering 37, 1292-1303.

84. Pernthaler, A., Dekas, A.E., Brown, T., Goffredi, S.K., Embaye, T., Orphan, V.J. 2008. Diverse syntrophic partnerships from deep-sea methane vents revealed by direct cell capture and metagenomics. PNAS - Proceedings of the National Academy of Sciences of the United States of America 105, 7052-7057.

Acknowledgments

First, I would like to thank Lukas Wick and Hauke Harms for giving me the opportunity to work at the UFZ and within the RASEBIO project. I also appreciate their good supervision of the thesis.

Martin Thullner I thank for his input into my work and, especially, for his help and always constructive comments concerning the mathematical part of my thesis.

Members of the RASEBIO project are acknowledged for fruitful scientific exchange during our internal meetings and various conferences.

I wish thank Jana Reichenbach, Rita Remer and Birgit Wurtz for their great technical assistance in the lab, and creating very pleasant working atmosphere. In particular, I would like to stress my appreciation to Jana for her priceless help and endurance while working on my experiments. Also help from all students who were working with me in the lab is greatly acknowledged.

Many deep thanks go to my friends for their company, engagement and motivation, especially during the last months. I also wish to thank my family for their companionship and an infinite support.

Publication list

Publications

1. **J. Hanzel**, H. Harms, L.Y. Wick. 2010. Bacterial chemotaxis along vapor-phase gradients of naphthalene. *Environmental Science and Technology* 44 (24): 9304-9310.
2. **J. Hanzel**, M. Thullner, H. Harms, L.Y. Wick. 2011. Microbial growth with vapor-phase substrate. *Environmental Pollution* 159 (4): 858-864.
3. **J. Hanzel**, M. Thullner, H. Harms, L.Y. Wick. 2011. Walking the tightrope of bioavilability: Growth dynamics of PAH degraders on vapour-phase PAH. *Microbial Biotechnology.* submitted.

Oral presentations

1. Rasebio International Symposium - Microbial contaminant degradation at biochemical interphases. Leipzig, Germany, 2 – 4 March 2010.
   Bacterial chemotaxis along vapor-phase gradients of naphthalene.
   J.Hanzel, H.Harms, L.Y. Wick

2. Annual PhD Student Conference. Leipzig, Germany, 28 April 2010.
   Do chemotactic bacteria smell airborne chemicals?
   J.Hanzel, H.Harms, L.Y. Wick
   Winner of the 3rd Oral Presentation Prize

Posters

1. CITE – Chemicals in the Environment. Leipzig, Germany, 23 March 2010.
   Chemotaxis of P. putida cells towards vapor-phase naphthalene gradients.
   J.Hanzel, M.Thullner, H.Harms, L.Y. Wick

2. Rasebio Summer School - Chemicals in Soil: Interactions, Availability and Residue Formation. Leipzig, Germany, 22 – 25 September 2008.
   Poster and Oral Flash presentation: Chemotactic response of *Pseudomonas putida* to airborne naphthalene.
   J.Hanzel, M.Thullner, H.Harms, L.Y. Wick
   Winner of the 2nd Scientific Poster Prize

3. Rasebio Summer School - Chemicals in Soil: Interactions, Availability and Residue Formation. Leipzig, Germany, 24 - 27 September 2007.
   Influence of naphthalene diffusion on bacterial growth and motility.
   J.Hanzel, M.Thullner, H.Harms, L.Y. Wick

4. Annual Conference of the Association for General and Applied Microbiology

(VAAM). Frankfurt am Main, Germany, 9 – 11 March 2008.
The influence of naphthalene diffusion on bacterial growth and dispersal.
J.Hanzel, M.Thullner, H.Harms, L.Y. Wick

5. Annual Conference of the Association for General and Applied Microbiology (VAAM). Bochum, Germany, 8 – 11 March 2009.
Chemotactic response of *Pseudomonas putida* to airborne naphthalene.
J.Hanzel, M.Thullner, H.Harms, L.Y. Wick

Curriculum Vitae

CONTACT

Joanna Hanzel
Erich-Zeigner-Allee 34
04229 Leipzig, Germany

Email: hanzeljoanna@googlemail.com
Phone: +49 17668053602

PERSONAL DATA

Nationality: Polish
Date of Birth: 25. Mai 1982
Place of Birth: Cieszyn, Poland

EDUCATION

2006 – 2009	PhD Student Faulty Biology, Pharmacy and Psychology Leipzig University, Germany Marie-Curie Fellow, Early Stage Training (EST) PhD accomplished at the Helmholtz-Center for Environmental Research - UFZ, Leipzig, Germany Project: RASEBIO - Risk Assment and Environmental Saftey Affected by Compound Bioavailability in Multiphase Environments
2004 – 2006	Master of Science Faculty of Biotechnology of Plants and Microorganisms University of Silesia, Katowice, Poland Department of Microbiology Topic of Master thesis: Bacteria in lead-contaminated forest soils – bioavilability as factor explaining high prevalance of lead sensitive bacteria
2005 – 2006	Socrtaes/Erasmus Programme Faculty of Biological and Environmental Sciences Helisnki University, Finland Master thesis perfromed at Department of Environmental Sciences, Lahti, Finalnd
2001 – 2004	Bachelor of Science Faculty of Biotechnology of Plants and Microorganisms University of Silesia, Katowice, Poland

Certificate of authorship

Ich erkläre dass ich die vorliegende Doktorarbeit selbständig und nur unter Verwendung der angegebenen Quellen und Hilfsmittel angefertigt habe.

Leipzig, den 20. Juli 2011

Joanna Hanzel